Renzo Vitale

Renzo Vitale

**Perceptual Aspects Of Sound Scattering
In Concert Halls**

$\lambda o \gamma o \varsigma$

Perceptual Aspects Of Sound Scattering

In Concert Halls

Von der Fakultät für Elektrotechnik und Informationstechnik der
Rheinisch-Westfälischen Technischen Hochschule Aachen
zur Erlangung des akademischen Grades eines

Doktors Der Ingenieurwissenschaften

genehmigte Dissertation

vorgelegt von

Ingegnere Maestro

Renzo Vitale

aus Sora, Italien

Berichter

Universitätsprofessor Dr. rer. nat. Michael Vorländer
Universitätsprofessorin Dr. -Ing. Dorit Merhof

Tag der mündlichen Prüfung: 18. Juni 2014

Diese Dissertation ist auf den Internetseiten der Hochschulbibliothek online verfügbar

Renzo Vitale

Perceptual Aspects Of Sound Scattering In Concert Halls

Aachener Beiträge zur Technischen Akustik

To my Music

faithful lover, soul nourishment,

ecstatic communion between transcendence and silence

Abstract

This work aims to expand the understanding of sound scattering in architectural spaces and the comprehension of its influence on the auditory perception in concert halls. The notion of scattering coefficient, which numerically represents the physical phenomenon of sound scattering, constitutes the main paradigm for the entire work.

In a first part, the scattering coefficient is presented in its meaning and implications, providing both the mathematical formulation and the empirical evaluation. Scattering coefficients of new objects, such as pieces of furniture, have been for the first time determined, hence the foundations for a new scattering coefficient open database is laid. A new solution for avoiding recurrent measurement inaccuracies is presented by means of an improved measurement setup, which consists of a revised scale model reverberation chamber. The benefit of having more accurate acoustic computer simulations by using a wider set of experimental data for scattering coefficient is proved by a case study of classroom acoustics. The implementation of scattering coefficient in different room acoustic computer software is shown and discussed by using a concert hall as a case study.

In a second part, the relationship between scattering coefficient and auditory perception is explored. Binaural impulse responses have been determined for three different scenarios, such as two virtual enclosed spaces and one real concert hall, and convolved with music samples to be used in listening tests. Results from listening tests show how changes in scattering coefficient of diffusing surfaces affect the perception of music among the audience in concert halls. A difference limen for scattering coefficient is determined by means of auralized binaural room impulse responses, which have been obtained under different scattering conditions. Results from listening tests are shown and discussed.

Keywords: scattering coefficient, sound scattering, room acoustic computer simulation, architectural acoustics, auditory perception, difference limen.

Contents

1   Introduction

A concert hall has often been compared to a musical instrument: an enclosed physical space (*body*) with acoustical properties that mainly depend on dimensions, volume, shape and materials. As much as this comparison is attractive and in many ways appropriate, there is a main distinction between a concert hall and a musical instrument: the former incorporates both performers and listeners within its dimensional boundaries, whereas the latter always remains external to them. A concert hall molds the sound field generated by instruments, which propagates through multiple reflections over the architectural surfaces and ultimately reaches the ears of listeners. Hence, a physical room and its acoustical design, which can be described in terms of objective parameters, have a direct influence over the way an audience perceive the music produced by musical instruments therein.

The subjective impression of a listener in concert halls has recently become a focal point in room acoustics. It is not surprising that the interest of researchers strongly moved towards the understanding of relations between objective and subjective parameters. A common reason for that is the need to support architects and engineers during the planning stages of new concert halls, where a clear statement between acoustic measurements and human perception is necessary. Physical variations of acoustical quantities might be neglected if they are not perceivable by the auditory system, thus facilitating the solution of structural choices, such as geometric texture or materials typology, as well as favoring new architectural approaches. Therefore, a psychoacoustic validation becomes a priority in architectural acoustics and concert halls design.

The investigation of the objective-vs-subjective domains is not straightforward: it was already shown, in fact, that it is very difficult to find a direct connection between architectural planning criteria, objective acoustical descriptors and subjective response from listeners (Bradley, 2010). Even the conclusions from the most recent international standards in room acoustics, such as the ISO 3382-1, have been proved to be lacking when the details of subjective perception and preferences of the listeners have to be explained (Lokki, 2013). It was also proved that no existing acoustic parameter is well correlated with overall acoustic impression for musicians for halls with suitable level of acoustic response from the auditorium (Dammerud et al., 2008).

Although many recent findings in psychoacoustics and room acoustics are favoring the comprehension of the objective and subjective relationships of acoustical quantities, there is still need to further investigate certain aspects that remained so far unclear. The sensitivity of human hearing to variations of the scattering coefficient (s) is one of them and it will be the main topic of this thesis.

1.1 Background

In recent years, the scattering coefficient has been more and more integrated in room acoustics computer simulation as it significantly improves the precision and accuracy of simulation results (Bork, 2000; Lam, 1996). The scattering coefficient offers a handy description of diffuse reflections of the sound field: it is defined as the ratio of the non-specularly reflected sound energy to the totally reflected energy (Vorländer, 2000). This coefficient depends on the surface structure (corrugations and finite size) while a pure specular reflection occurs at a smooth large plane surface. The measurement method for determining this coefficient has already been developed and standardized by ISO-17497.
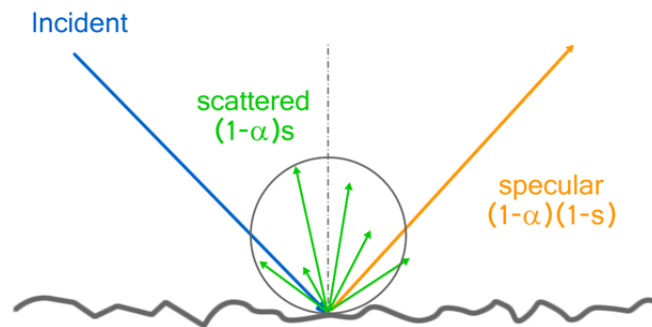
Figure 1.1 – Energy components of scattered sound.

Nowadays, the available scattering coefficient data are mainly related to architectural surfaces with different patterns and structures (Jeon et al., 2004). A lot of effort has been put on the determination of numerical methods for calculating this coefficient beforehand (Kosaka et al., 2005; Embrechts et al., 2006; Sakuma et al., 2009). However, a diffuse trend of acoustic consultants is to determine scattering coefficients by best guess, which is usually done by choosing an arbitrary value for all the frequency bands. Scattering coefficients for some materials or surfaces have been given by (Vorländer, 2007). Other suggested data are available after (Xianyang, 2006), though they represent mid-frequency values (expanded into octave band values using interpolation or extrapolation) and not effective measurements. Therefore, there is indeed a lack of data due to unperformed investigations on common objects (Lokki et al., 2008), especially for items that are normally present in closed spaces, such as chairs, desks, and bookshelves.

On the other hand, prediction tools for room acoustics are becoming more and more used for studying the acoustical behavior of new designed rooms. This is also the case of smaller enclosed spaces such as classrooms, where room acoustics simulations have already been proposed (Bistafa et al., 2001; Christiansen et al., 2005; Fels et al., 2007). In order to noticeably improve the precision of computer simulations, several aspects must be considered, not least the use of a proper scattering coefficient, which was shown to be responsible of a significant improvement in simulation results (Vorländer, 1995).

Even though there have been several proofs that scattering from surfaces enhances the quality of concert halls (Beranek, 1996; Cox et al., 2004), not enough effort has been put to investigate the influence of scattering on auditory perception. A first study in this direction was conducted by (Torres et al., 2000), who evaluated the time-frequency perception of scattering in the binaural room impulse response; they showed that the perceived differences were dependent on the input signals and that diffusion was affecting mainly coloration and spaciousness. A few other studies have contributed to fill the gap between objective and subjective assessment of scattering. The influence of the early sound field on the perception of diffuse reflections was investigated by (Cox et al., 1996), who showed that the early components of the sound field act as a masking effect over the spatial aspects of diffusion, thus reducing the relevance of diffusion itself.

More recently, thresholds and different limens of scattering coefficient were assessed in auralized concert halls for the first time by (Vitale et al., 2010; Vitale et al., 2011), who determined the *Just Noticeable Difference* (JND) for a shoebox-like concert hall by means of three different kinds of prediction software. They also found that the perception of scattering coefficient variations in a small environment affects spaciousness more than coloration, whereas coloration is affected more in larger environments. Further contributions in the same direction have recently been provided by (Shtrepi et al., 2013; Shtrepi et al., 2014), who also investigated the relationship with acoustical objective parameters, as well as by (Jeong et al., 2013), who investigated the effect of changes in the scattering coefficient of wall diffusers on listener perception in a physical scale model. They found out that the presence of sidewall diffusers influenced the perception in terms of reverberance, loudness and spaciousness.

1.2   Aim and Methodology

Aim of this thesis is to contribute to the understanding of the relations between human perception and objective parameters in room acoustics by investigating the perception of scattering coefficient, *s*. In particular, the following questions will be addressed and discussed:

- If the scattering properties of a wall surface within a concert hall change, would a listener be able to perceive any difference in the music performed therein?
- Is it possible to detect a differential threshold of perception for scattering coefficient?
- How precise must be a measurement of the scattering coefficient?

In order to answer to these questions, a methodology has been developed that consists of the following stages:

1. **Measurements of scattering coefficient**
   The lack of scattering coefficient data has limited the practical application of room acoustic computer simulation. Thus, the scattering coefficient of several objects has been evaluated through measurements in a scaled reverberation chamber. Considering the limitations of the common scaled reverberation chamber, a revised model of the chamber has been introduced that relocates the turntable directly outside of the room.

2. **Computer simulations with measured values of scattering coefficient**
   The acoustical influence of typical objects within rooms has been investigated; the specific case of an ordinary classroom with common pieces of furniture, such as chairs and desks, is shown. Results of computer simulations of the sound field reflections for this environment in terms of scattering coefficient are presented.

3. **Perception of scattering coefficient in auralized concert halls**
   Two different enclosed spaces, namely a shoebox-shaped room and the Dortmund music hall, have been acoustically simulated. Binaural impulse responses in two locations under different scattering conditions have been auralized with music samples. Listening tests have been performed in the form of 3-Alternative Forced Choice, thus allowing the determination of a difference limen.

4. **Perception of scattering coefficient in real concert halls**
   Acoustical measurements have been conducted at the *Espace de Projection* (ESPRO) at the *Institut de Recherche et Coordination Acoustique/Musique* (IRCAM) in Paris. Binaural impulse responses in two locations under different room configurations (hence scattering conditions) have been auralized with music and noise samples. Listening tests have been performed in the form of a triangular test, thus allowing the determination of difference and similarity thresholds.

1.3   Outline of the Dissertation

This thesis is structured as follows. Chapter 2 summarizes a few aspects required for the comprehension of this work, such as the basics of acoustics in terms of sound waves and sound propagation. A chapter about the description of measurement techniques for determining scattering coefficient follows, which also include measurements of several common objects as well as the description of a revised model of scaled reverberation chamber. Chapter 4 introduces concepts of room acoustic computer simulations with specific reference to three types of software, which are RAVEN, CATT-Acoustic and ODEON. The influence of measured data for scattering coefficient over the simulation performance is investigated for a lecture hall. The focus is then put on perceptual aspects. Chapter 5 introduces concepts of sensory evaluation techniques that are essential for understanding how humans react to different stimuli. The problem of detecting difference, similarity and threshold of scattering is discussed together with the introduction of appropriate statistical models. The perception of scattering in auralized spaces is investigated in chapter 6 by means of two case studies: a shoebox-shaped room and a concert hall respectively. Auralized samples, as obtained through room acoustical simulations for several scattering coefficient values, have been used as stimuli for listening tests in order to determine difference limens for scattering coefficient. Chapter 7 explores the perception of scattering by means of in-situ acoustical measurements performed in a real concert hall. Auralized samples, as obtained through in-situ measurements for some wall configurations, have been used as stimuli for listening tests in order to determine difference and similarity for scattering coefficient. The last chapter summarizes the results as well as the contributions presented in this thesis. Possible orientations and scenarios for future research are eventually outlined.

2   Sound Field in Enclosed Spaces

Every enclosed space speaks with its own timbre, which is revealed whenever a sound is therein produced. The way humans perceive this timbre mainly depends on the type of sound generated, the position where it is produced and, most of all, the position where a listener is located. In order to capture and decode the sound stimuli, humans developed a specific cognitive process of aural awareness, which can be described, from the manifestation of a sound to its interpretation, by means of a simple functional model as follows (Blesser et al., 2007):

- *Raw sensation*: pressure variations are detected by the hearing system;

- *Perception*: cognitive processes (including listener's history and experience) transform a raw sensation into an awareness that has a meaning (such as languages);

- *Affective interaction*: a specific emotional condition can be induced, hence captured and decoded by an individual.

Acoustics and psychoacoustics are only interested to the first two components, the raw sensation and the perception, which can be more empirically characterized and decomposed into measurable entities. In pure acoustical terms, the main source of information regarding the audible properties of the sound field in a room is the impulse response, which allows the acoustical characterization of an environment (whether it is a small room or an auditorium) by means of objective and subjective parameters. Hence, the impulse response extends the knowledge of the factors that control the acoustical qualities, which are subjectively perceptible. Moreover, it is also an essential tool for an acoustical objective description, for prediction and validation of the expected performances of a location, and ultimately for supporting the designing stage of engineers and architects.

2.1   Characterization of an Acoustical System

The characterization of an enclosed environment can be entirely performed through room acoustic measurements of the room impulse response (RIR), which has been defined as the temporal pressure functions of the room resulting from its excitation by a Dirac delta function (Vorländer et al., 1994). This assumption arises from the consideration that the transmission of a sound within a room, as well as the transmission of sounds between rooms, may normally be considered as

a close approximation to a linear and time-invariant (LTI) system (ISO 18233). A principle of LTI systems theory states that the knowledge of the impulse response of a (transmission) system allows to verify its properties as well as to completely characterize the behavior of the system itself (Oppenheim et al., 1983). In acoustics, if the information about the direction of incidence is preserved, the impulse response contains all information about the acoustics of a room between two specific source and receiver positions.

Given a LTI time continuous system and its impulse response *h(t)*, every output *y(t)* of the system can be described by the convolution between the input *x(t)* and *h(t)*, as follows:

$$y(t) = x(t) \otimes h(t) = \int_{-\infty}^{+\infty} x(\tau) h(t-\tau) d\tau \qquad (1.1)$$

If the properties of the Fourier transform are applied to the previous equation, a description of a LTI system can also be obtained in the frequency domain as follows (Oran Brigham, 1988):

$$y(t) = x(t) \otimes h(t) \Leftrightarrow Y(f) = X(f) H(f) \qquad (1.2)$$

where *X(f)* and *Y(f)* denote the Fourier transform of the input and output signal respectively, and *H(f)* represents the so called frequency response of the system, that is the Fourier transform of the impulse response.

The measurement chain for determining the impulse response in an acoustical domain is generally a quite complex system that starts with an excitation signal (generally a sweep) and ends with the determination of the impulse response. Before of being diffused in a room, the excitation signal is processed by a digital-to-analog converter and suitably amplified in order to properly feed the environment. The excitation signal is spread in the hall by an omnidirectional source and then is captured by a microphone. After an inverse signal processing, a deconvolution is performed, allowing the determination of the impulse response. The methods for the correct choice of the technical equipment as well as the application of the proper measurement procedures are extensively described in the standard ISO 3382 and ISO 18233.

2.2   Binaural Room Impulse Response

Let us consider a generic enclosed space containing a sound source and a listener, which are located in two different positions. If a short sound impulse is emitted by the source on a certain position, a spherical wave propagates away from the source in all directions and eventually reaches the listener through different paths (Fig.2.1).
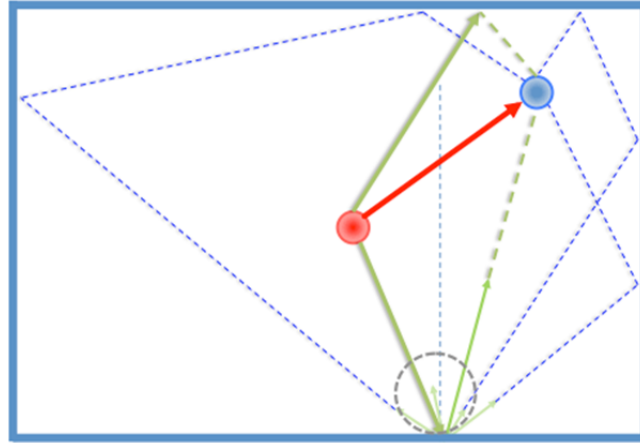
Figure 2.1 - A sound source (red) emits a short impulse, which propagates as a spherical wave through the room, thus generating several reflections that reach a listener (blue) at a different time and with a different energy.

The raw sensation of the listener is related to the total sound field perceived, which can be decomposed into three components, namely the *direct sound*, the *early reflections* and the *late reverberation* (see Par.4.1.4).

The direct sound runs the shortest path between the source and the listener; hence, is the first element to be heard in the listener position (this component is represented by the red line in the illustration). For this reason, the direct sound is also processed by the human brain for localizing the sound source according to the so-called precedence effect (Blauert, 1996).

This component is soon followed by the early reflections, which are other parts of the sound wave that have been reflected one or more times by the room boundaries or by objects in the room before reaching the receiver. These reflections are added to the initial direct sound by the human brain and interpreted as an overall component. It has been shown, in fact, that reflections occurring within 2 ms and about 50 ms later than the first wave front are perceived as a single fused auditory image. The early reflections are the most important part in relation to the perceived quality of an enclosed space, because they enhance the loudness, support the intelligibility of speech, the clarity of music and the impression of the auditory source width.

The reflections arriving to the listener position with a delay of more than 50-80 ms with respect to the direct sound constitutes the late reverberation. The density of these later reflections increases with time (proportional to t^2), but their intensity decreases because of the attenuation due to air and surface absorption at the room boundaries. This component is also related to the diffuse part of the sound field, since it forms a late reverberation which is nearly independent of the listener's position, because of the energetic integration over time angle that human brains performs. Reverberation is a very important acoustic attribute of an enclosed space; in fact, it is widely accepted in room acoustics as the predominant indicator of the acoustical properties of a room.

2.3   Room Acoustic Parameters

A wide amount of objective and subjective information can be extracted from the room impulse response. This situation has been accomplished by the definition of several acoustical parameters that can be directly derived from the impulse response, a list of which is included in the standard ISO 3382. For each parameter, which is objective in nature, an association with subjective aspects has been defined. Five groups of quantities have been determined (see Tab.1.1). All parameters are referred to energetic quantities, because they are determined starting from sound pressure square. A description of the previous parameter as well as the way of determining them is hereafter given.

Subjective listener aspect	Acoustic quantity
Loudness	*Sound Strength*, **G** [dB]
Reverberance	*Early Decay Time*, **EDT** [s]
Clarity of Sound	*Clarity*, **C₈₀** [dB]
	Definition, **D₅₀** [-]
	Centre Time, **Tₛ** [ms]
Apparent Source Width	*Early Lateral Energy Fraction*, **LF** [-] or **LFC** [-]
Listener Envelopment	*Late Lateral Sound Level*, **LG** [dB]

Table 1.1 - Acoustic quantities grouped according to listener aspect (after ISO 3382)

Sound Strength (G) – Improperly called sound intensity, sound strength is defined as the logarithmic ratio of the sound pressure exposure of the measured impulse response to that of the response measured at a distance of 10 m from the same sound source in a free field. This quantity can be also easily obtained, in case of impulsive technique, as the difference between the single event level of the signal in a measuring point ($L_{p,E}$), and the same value detected at 10 m from the omnidirectional source ($Lp_{E,10}$):

$$G = 10\log_{10}\frac{\int_0^\infty p^2(t)dt}{\int_0^\infty p_{10}^2(t)dt} = L_{pE} - L_{pE,10}[dB] \qquad (1.3)$$

where *p(t)* is the instantaneous pressure measured at the measurement point and $p_{10}(t)$ is that measured at a distance of 10 m.

Early Decay Time (EDT) – It is defined as the time interval in which the sound energy level decreases of 10 dB. It can be measured starting from the maximum level of the impulse response up to -10 dB below it. EDT is conceptually different from reverberation time (T) since it considers the first 10 dB of the curve obtained with backward integration of the squared impulse response.

In a highly diffusing environment, EDT and T are usually similar, while they can differ for irregular hall (coupled rooms, delayed reflections). EDT seems to be better related to a subjective listening judgment than T, because it takes more

into account the influence of the first reflections that are closer to a subjective spatiality impression of the audience. However, there are also studies that showed a high level of mutual correlation between EDT and T, to a level that it is retained indifferent the choice of one of the two in relation to subjective aspects (Nishi, 1992; Jordan 1981).

Clarity (C50, C80) – This index considers the balance between early and late arriving energy, and can be evaluated as:

$$C_{t_e} = 10\log\left(\frac{\int_0^{t_e} p^2(t)dt}{\int_{t_e}^{\infty} p^2(t)dt}\right)[dB] \tag{1.4}$$

where t_e is the early limit time of either 50 ms or 80 ms. This parameter links the perceived clarity and T and it is highly significant for delicate music periods, where the understanding of fast and legato sections respect to notes with longer duration and stronger intensity is significant. The energy in the first 80 ms includes direct and early reflections components, thus C80 is also an index directly correlated with the comprehension of speech.

Definition (D) – This index is very similar to clarity, and can be calculated as:

$$D_{50} = 10\log\left(\frac{\int_0^{50} p^2(t)dt}{\int_0^{\infty} p^2(t)dt}\right)[dB] \tag{1.5}$$

Differently from C80, here a smaller time interval is imposed in order to consider only the effect of early reflections. The time interval of 50 ms appears to be more indicated for speech, while 80 ms is more adequate for music.

2.4   Sound Field and Boundary Surfaces

The radiation of a sound field in enclosed spaces can be described by means of a *point source*, a concept that does not exist in the real world, but which helps to understand the propagation of sound for simple and more complicated sources. Whenever a sound field is generated, energy of wave motion is created, which propagates outward from the center of the source. The corresponding air particles are carrying sound by moving backward and forward, parallel to the wave motion's direction: in this way, an alternating increase and decrease of air pressure exists. Spherical waves propagate in the air until they encounter an obstacle, such as a boundary surface. When this happens, four different phenomena take place (Fig.2.2), which are *reflection*, *scattering* (or *diffusion*), *absorption* and *transmission*.

A reflection occurs whenever an incidence wave impinges on some wall, and it can be defined as the abrupt direction change of the wave front at an interface between two dissimilar media, most likely with a change of both amplitude and phase. Absorption converts sound energy into heat energy. The most common measurement of that is the absorption coefficient (α), which is a ratio of not reflected to incident sound energy. If a material does not absorb any sound incident upon it, its absorption coefficient is 0, whereas if a material absorbs all sound incident upon it, its absorption coefficient is 1. These limits are theoretical, since every material reflects and absorbs some sound. Anyway, absorption coefficients range between 0 and 1. Methods and principles for measuring the absorption coefficient are described in the norm ISO 354.
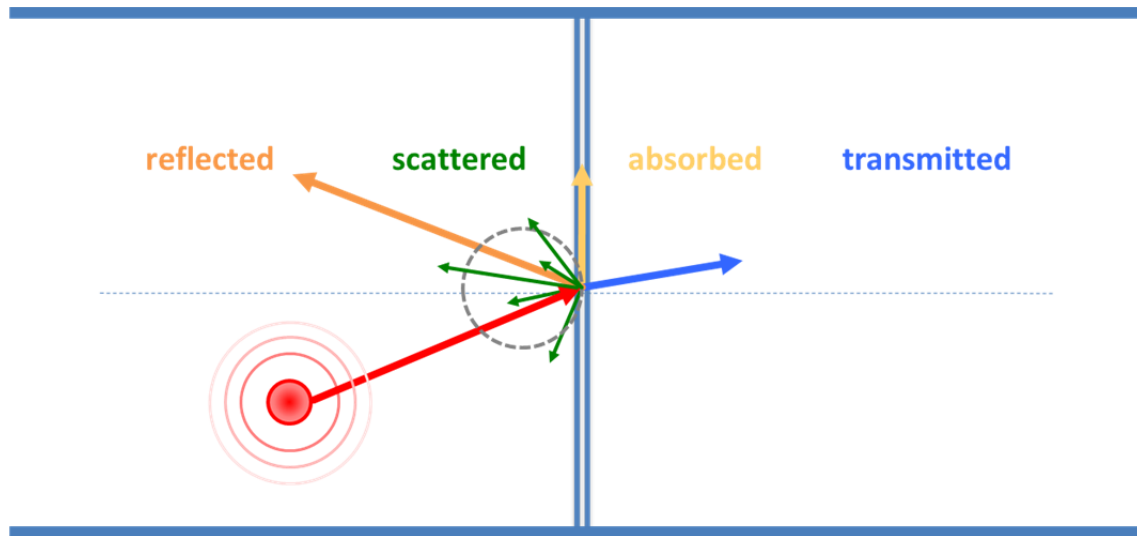
Figure 2.2 – The possible interactions of a sound field with a boundar surface.

Each material with which a sound wave interacts absorbs some sound. A boundary condition where the surface is not necessarily rigid or impenetrable is described by the *specific acoustic impedance*, which is the relation between sound pressure and particle velocity.

Almost every surface is uneven or presents some kind or roughness. If the wavelength of the incident sound field is comparable with the dimension of the surface corrugations, a scattered wave will occur in addition to the specular reflection, whereby a distinct portion of the sound energy is scattered in all directions resulting in *diffuse* reflections. A useful way to describe the sound field in this case is by means of *scattering* and *diffusion* coefficients, which have been standardized by ISO 17497 and will be extensively introduced in the next chapter.

The remaining part of the sound that is hitting a wall (in particular the low frequency components) is transmitted through the separating surface into the adjacent room. This effect of sound *transmission* can be expressed by the *sound reduction index R*, which describes the ratio of the incident sound intensity on this element in relation to the transmitted intensity.

3   Measurements of Surface Diffusion

The sound perceived by a listener during a concert in an auditorium is a combination of the direct sound coming from a source, generally represented by the musicians on the stage, and the indirect reflections from surfaces and other objects. These two elements, direct sound and reflection, are the main responsible for the quality of the acoustic in a room. One of the central topics in acoustics is how to manipulate these reflections that affect the way the sound propagates and is ultimately perceived. As a consequence, knowledge of the acoustical reflection properties of surfaces within concert halls is of major importance in the room acoustical design process. Besides the room shape and dimensions, as well as the materials properties in terms of absorption coefficient, the diffusion properties of the surfaces play a key role for enclosed spaces devoted to music, such as recording studios, auditoria, concert and opera halls, theaters and recording studios.

A lot of effort has been put in the past for the investigation and assessment of the absorption coefficient, thus many information are nowadays available about several kind of materials in terms of measurement techniques and prediction models. Besides the standardized methods of determining the reflection factor or the absorption coefficient of a material (ISO10534-2; ISO354-2), given the need to quantify acoustic surfaces in situ (also in concert halls) there has been very much interest in new in-situ measurement methods. The development of a *Microflown* sensor based on a *pu*-probe (De Bree et al., 1996), which allows a direct measurement of the acoustic particle velocity, has introduced new approaches to in-situ measurements for sound absorption (Müller-Trapet et al., 2013).

The interest toward an in-depth knowledge about scattering surfaces emerged only later with respect to the absorption of surfaces. Nevertheless, in recent decades there have been several studies and contributions to develop methods for measuring and characterizing surface scattering. Outcomes showed that, as opposite to absorption coefficient, there does not appear to be one ideal coefficient for describing scattering surfaces (Cox et al., 2006). Hence, two different coefficients have been defined, namely the *diffusion coefficient* and the *scattering coefficient* (see Par.2.4). The latter turned out to be the most appropriate for using in room acoustical computer simulation that involve high frequency modelling and scattering techniques, as it provides a simplified and physically correct way to quantify surface scattering (see Ch.4). The scattering coefficient

offers a handy description of the ratio between specular and diffuse reflected energy on surfaces and structures.

One of the problems related to the use of scattering coefficient in room acoustics is that there is indeed a lack of scattering coefficient data due to unperformed investigations on common objects (Lokki et al., 2008), especially for items that are normally present in closed spaces. For this reason, this chapter aims at giving substantial contributions to this aspect by measuring scattering coefficient of common objects, such as desks, chairs, tables and bookshelves. This data will later be used in a specific case study that shows how room acoustic simulation can be bee improved by using proper values of scattering coefficient (see par.4.4).

The measurement process, which has been performed within a scale model reverberation chamber, has highlighted several critical aspects of the chamber itself, some of them already known. In order to improve the quality of measurements, a revised model for the reverberation chamber has been developed and thereafter proposed. Finally, a real-scale measurement of angle-dependent scattering coefficient (namely diffusion coefficient) has been performed as a comparison, which showed that directional information about the sound field is lost by using the scattering coefficient. At the same time, they show that real scale measurements of directional diffusion coefficient are very complex and are worth to consider only in special situations.

3.1 Measurement Techniques

Several measurement methods have been proposed during the past three decades for measuring both scattering and diffusion coefficient. They can be either classified according to the supposed incident field (free field or diffuse field method) or to the measurement conditions (in situ or laboratory methods). A description of the measurement methods effectively used within this thesis will be hereafter presented, namely the measurement of the random-incidence scattering coefficient in a reverberation room and the measurement of the directional diffusion coefficient in a free field random-incidence. Both of them have been standardized in ISO-17497-1 and ISO-17497-2 respectively. For a more detailed information about measurement methods for sound absorption and surface diffusion, it should be referred to (Cox et al., 2009) and (De Geetere, 2004).

3.1.1 Measurement of Scattering Coefficient

The measurement method for determining scattering coefficient in the reverberation chamber has been first introduced and described by (Mommertz et al., 1995; Vorländer et al., 2000). This method was later adopted and standardized by the ISO-17497-1, which is why it is also known as the ISO method.

The idea behind this method can be easily explained by looking at band-filtered pulses, as resulting from reflections over a corrugated surface for different sample orientations in time domain, as in Fig.3.1.
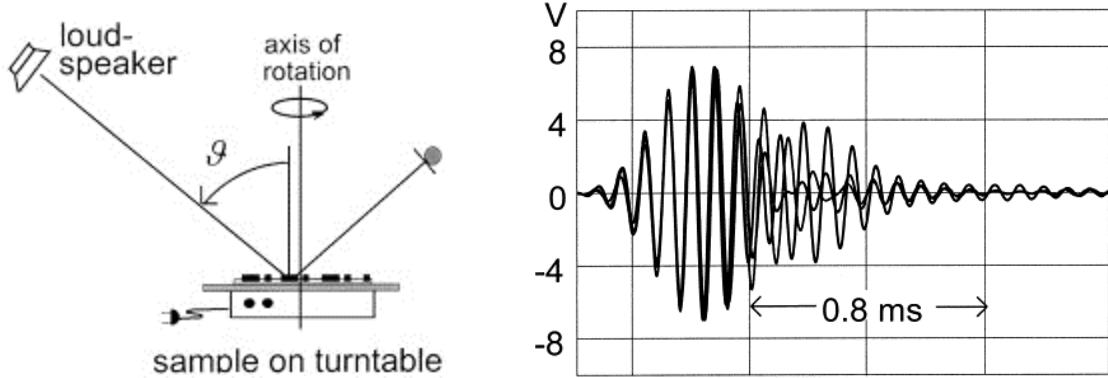
Figure 3.3 - (left) Measurement set-up; (right) detection of reflected pulses for different sample orientations at 10 kHz (after Vorländer et al., 2000).

Those pulses consist of two parts: the initial parts of the reflections are highly correlated, because they represent the specular components of the reflections, which remain unaltered during the sample rotation as they follow the shortest path; the later parts are not in phase, instead they strongly depend on the specific orientation, thus representing the scattering part. Hence, the principle of the measurement method is to extract the specular energy from the reflected pulses, which is done by synchronized (phase-locked) averaging of the impulse responses obtained for different sample orientations.

The method can be directly applied to measurements in the reverberation room as follows. A circular test sample is placed on a turntable and rotated. The impulse response is repeatedly measured as the turntable is rotated. According to Fig.3.1, the latter parts of the impulse response will cancel out due to the scattering from the surface, so that the averaged impulse response will only contain the specular reflection component. The reverberation time due to the specular component can be obtained by a backward integration of the impulse response. This procedure is iterated for four times with slight differences as shown in Fig.3.2, so that a total of four reverberation times will be obtained. Once these reverberation times are collected, the scattering coefficient s can be obtained according to the following expression (Vorländer et al., 2000):

$$s = 1 - \frac{E_{spec}}{E_{total}} = \frac{\alpha_{spec} - \alpha_s}{1 - \alpha_s} \tag{3.1}$$

where the random incidence absorption coefficient α_s of the sample is obtained as:

$$\alpha_s = 55.3 \frac{V}{S} \left(\frac{1}{c_2 T_2} - \frac{1}{c_1 T_1} \right) - \frac{4V}{S} (m_2 - m_1) \tag{3.2}$$

and the specular absorption coefficient α_{spec} of the sample is calculated as:

$$\alpha_{spec} = 55.3 \frac{V}{S} \left(\frac{1}{c_4 T_4} - \frac{1}{c_3 T_3} \right) - \frac{4V}{S} (m_2 - m_1) \tag{3.3}$$

with V the volume of the reverberation room, S the sample surface, c the speed of sound, T the reverberation time and m the energy attenuation coefficient of air.
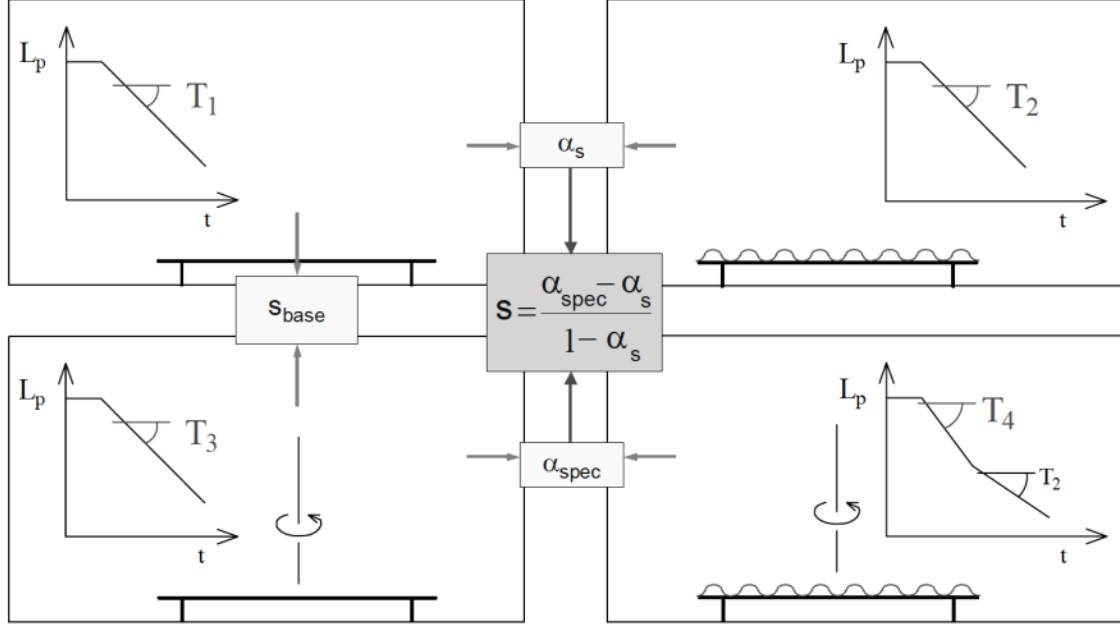
Figure 3.4 – The ISO method for measuring the random incidence scattering coefficient in a reverberation room (after De Geetere, 2004). Impulse responses are measured without and with the test sample following ISO 354 and giving the reverberation times T_1 and T_2, respectively. The result of the measurement with a stepwise or continuously rotating turntable, including the base plate but without the test sample, is the reverberation time T_3. The result with the rotating test sample is the reverberation time T_4.

One of the main advantages of this method is that it refers to the physical meaning of the scattering coefficient, hence is closely related to the definition and measurement of the absorption coefficient according to ISO 354. Moreover, this method can also be performed in scale model reverberation chambers, which makes it particularly attractive, since it allows samples of different types of structures to be constructed and measured more easily. At full scale, in fact, the measurement is rather slow and laborious.

However, there are several aspects that need to be considered when performing this measurement, such as the sample layout (dimension, texture, structure and position), the reverberation chamber preparation, the number of measurements and the influence of external parameters, such as time variances as well as humidity and temperature change. Further details have been provided by (Vorländer et al., 2004), who compared real scale and scale model set-ups and provided precious suggestions about sample periods, edge effects, turntable control, average numbers and so on.

3.1.2 Measurement of Directional Diffusion Coefficient

A free-field method for measuring the directional diffusion coefficient of surfaces has been standardized by ISO-17497-2, which allows to obtain magnitude polar responses that assess the spatial distribution of energy as scattered from a diffusing surface. This is achieved by measuring all reflected pressures (or intensities) on a hemisphere with its center coinciding with the center of the surface.

Measurements are performed in an anechoic room, which basically consist of impulse response detection with/without the test sample for several source and receiver positions. If more than one microphone or source is used, the impulse response without the test surface present and with the source centered on the reference point, facing the receiver position, will be measured as well.

A source is used to irradiate the test surface, and microphones should be placed in a radial position (semicircle or hemi-sphere) in front of the surface, so that the pressure impulse response is recorded using transfer-function techniques (i.e. impulse response measurements, Fast Fourier Transform, Time-Delay Spectrometry, or Maximum Sequence-Length).

This method can be performed in a single plane using a 2D goniometer on a semicircle, or over a hemisphere using a 3D goniometer. The latter approach delivers much more information as it provides three dimensional polar balloons as an outcome; moreover, it is particularly appropriate for surfaces that produce scattering in multiple plans, which otherwise would not be detected by a 2D approach. However, the 3D method is very difficult and expensive to construct. Scale model measurements are a potential alternative for samples that can be easily scaled. A few experimental setups have been described in detail by (Cox et al., 2009).
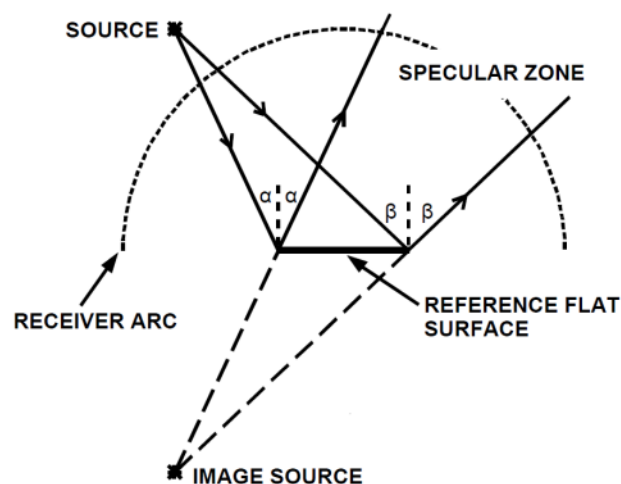
Figure 3.5 - The specular zone is the area contained by imaginary lines that are constructed from the image source, which is created about the plane of the reference flat surface via the edges of the reference flat surface to the receiver arc (from ISO 17497-2).

Since the relative levels detected by the microphones are dependent on distances from the source and receiver to surface, two spatial loci have been defined: the *far field* is the region where the scattered pressure falls by 6 dB per distance doubling for 3D geometries, whereas the *near field* is the region closer to the surface where interferences effects produce undulating reflected sound pressure, thus the angular field distribution is dependent on the distance from the radiator. Approximate far-field conditions can be achieved if at least 80 % of the receiver positions are outside the so called *specular zone*, defined as the region (or solid reflection angle) over which a geometric reflection occurs (Fig.3.3). In situation where some or all sources and receivers are in the near field, measurements to determine the diffusion coefficient should take place both at application-realistic near-field positions and in the far field.

An important aspect of the measurement is the extraction of the scattered impulse response from a test sample at a given observation angle, which can be accomplished through a five steps by determining: the loudspeaker/microphone response (h_3), the background response without sample (h_2), response with sample (h_1) response of sample without background response ($h_1 - h_2$), deconvolved sample response (h_4) windowed sample response (Fig.3.4-left).
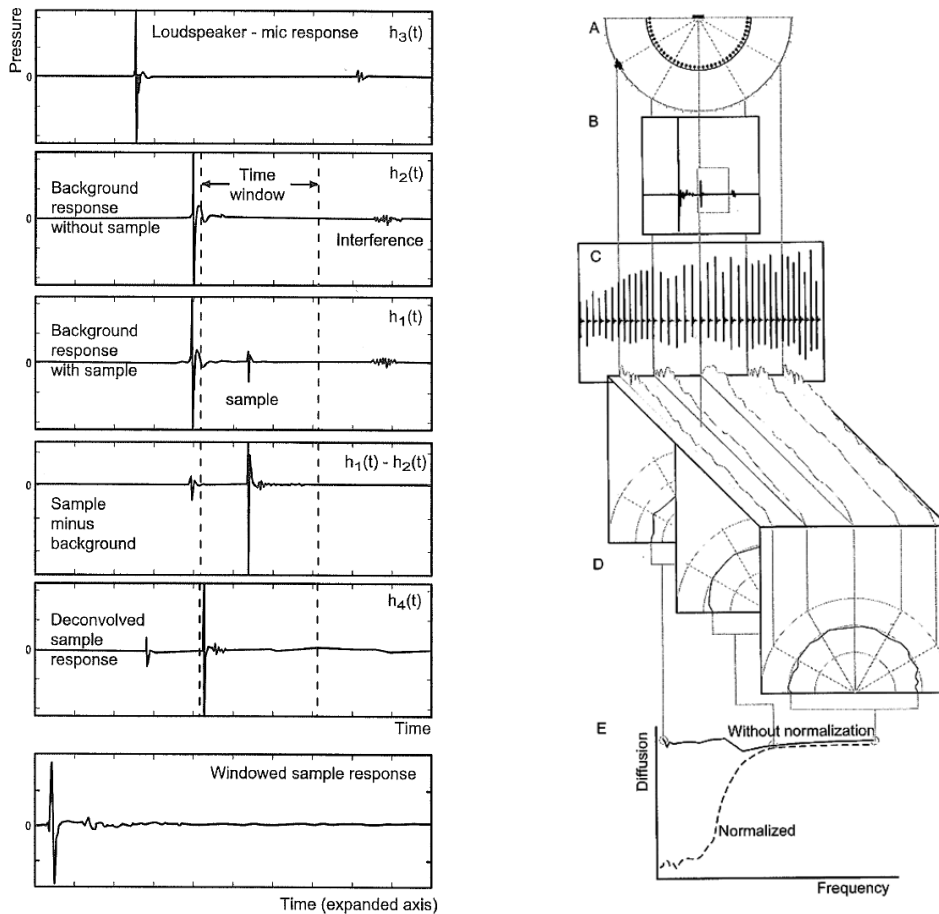
Figure 3.6 - Data processing for: (left) extracting the scattered impulse response from a sample; (right) extracting the diffusion coefficient from impulse responses (after Cox et al., 2009).

Once the scattered impulse response has been calculated, the data are further post-processed to provide frequency responses, polar responses and eventually diffusion coefficients as illustrated in Fig.3.4-right. In particular, the scattered data for different angles of observation (h_4) are concatenated together to form a temporal angular impulse response, which then is Fourier-transformed to get the frequency responses. Finally, the energy from each one-third octave band is summed to obtain polar responses that are further processed to calculate the *directional diffusion coefficient* as follows:

$$d_\psi = \frac{\left(\sum_{i=1}^{n} 10^{L_i/10} \right)^2 - \sum_{i=1}^{n} \left(10^{L_i * 10} \right)^2}{(n-1) \sum_{i=1}^{n} \left(10^{L_i * 10} \right)^2} \tag{3.4}$$

Where L_i are a set of sound pressure levels in dB in a polar response, n is the number of receivers and ψ is the angle of incidence. This equation is only valid when each receiver position samples the same measurement area. This equation corresponds to an averaged circular autocorrelation function of the scattered energy from n different receivers.

The procedure for determining the directional diffusion coefficient is more laborious than the one for the determining the scattering coefficient, particularly at real scale. At the end, the massive data obtained by polar responses are reduced to a frequency dependent singular figure of merit by means of autocorrelation. However, even though a single value for each frequency and receiver is obtained, it is in the analysis of the polar responses that precious information about the sample can be deduced.

The diffusion coefficient cannot be blindly used as an input to current diffusion algorithms in geometric room acoustic models. The diffusion coefficient characterizes the sound reflected from a surface in terms of the uniformity of the scattered polar distribution. The scattering coefficient, as will be shown in details in Ch.4, is much more appropriate for computer simulation.

A case study of 3D measurements over a hemisphere of a scattering surface in real scale is presented in par.3.4.

3.2   Beyond Ordinary Samples: Measuring Scattering of Rows of Objects

The measurements of scattering coefficient performed to date have always addressed different types of surface roughness or textures. Although the scattering coefficient has been more and more integrated in room acoustics computer simulation, the lack of scattering coefficient data remains an open issue, especially

for commonly used furniture that are present in closed spaces such as rows chairs, desks, bookshelves. This aspect is of primary interest, particularly for environments where furniture constitutes a large part of the total scattering surface (classrooms, churches or concert halls).

Therefore, a case study for quantifying the influence of typical furniture in ordinary classrooms on the sound field reflections in terms of scattering is hereby presented. In a first stage, furniture of interest are properly designed and built in a scaled-down version (Fig.3.5). The scattering coefficient is then evaluated through measurements in a scaled reverberation chamber. The collected data will be used in a second phase for performing room acoustic simulations of a classroom, which will be compared with in situ measurements (see Par.4.4). Results will show how proper data enhance the quality of the computer simulation. The measured scattering coefficients have been available online as well. The set-up used for measurements of the random-incidence scattering coefficient in a scaled reverberation chamber will be hereafter presented.

Figure 3.7 - Scaled pieces of furniture made up of balsa wood (scale 1:10).

3.2.1 Scale Model Measurements

Measurements of different objects have been performed in the old scale model reverberation chamber at the Institute of Technical Acoustics (ITA), RWTH Aachen (Germany). This chamber has later been replaced with a revised model, which is described in detail in par.3.5. The old scale model has a volume of approximately 1 m³ and a surface area of 6.07 m², with dimensions of 0.82m x 1.26m x 0.96m (Fig. 3.6).
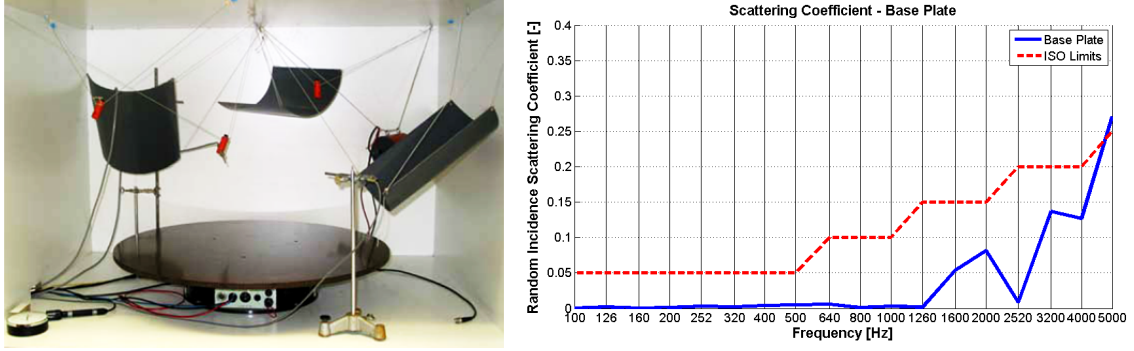
Figure 3.8 - (left) Old scale model reverberation chamber at ITA; (right) measured scattering coefficient of the base plate compared to the upper limit suggested in ISO 17497-1.

The dimensions of the scale model reverberation chamber are in relation 1:5 with respect to the full-scale reverberation chamber at ITA, which makes this chamber smaller than what is recommended by ISO 354 and ISO 17497-1. According to the Schroeder frequency (Schroeder, 1954), the sound field in this chamber can be considered to be diffuse around 1100 Hz. To improve the sound diffusion in the chamber and bring this frequency downwards, three sound diffusers made of PVC have been hanged in the room. Former studies made in this room indicated that the use of three diffusers should be enough to give a diffuse sound field from 600 Hz on (Kreutner, 1995).

For measurements performed in scale models, the similarity relations (Makrinenko, 1994) must always be considered and the results in frequency have to be corrected by the following relation, if results in full scale are needed:

$$f_{real} = f_{model} / N \tag{3.5}$$

where N is the physical scale factor of the model.

The chamber is provided with a turntable (B&K, height 0.128 m, diameter 0.35 m) and a flat base plate (height 0.015 m, diameter 0.8 m). The original period of the turntable was 80 s, however it has been expanded with an external microcontroller, which allowed different settings in terms of speed, acceleration and numbers of steps. The scattering coefficient of the base plate itself has been determined by the measurement of T_1 (reverberation time of the chamber measured without rotation of the turntable) and T_3 (reverberation time obtained from the averaged impulse response after a complete rotation of the turn table), through equation 3.2, where c_2, T_2 and m_2 were replaced with c_3, T_3 and m_3 respectively. The turntable can be turned on and off by means of a switcher, which is controlled from outside the reverberation chamber. A humidity sensor has been placed inside the chamber, so that the relative humidity of the air in the reverberation chamber could be read from the outside.

Measurement devices included also two types of sound sources: a small piezoelectric dodecahedron loudspeaker, suitable for measurements up to 60 kHz,

and a conventional loudspeaker, with a frequency response up to 12.5 kHz (Fig.3.7).
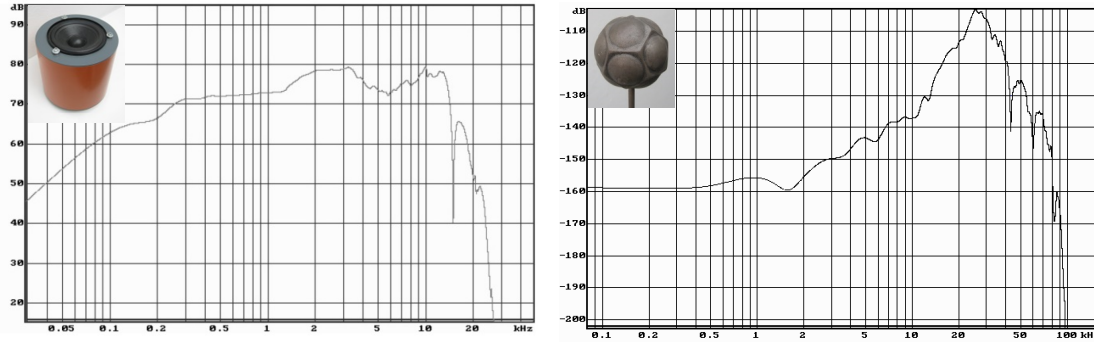
Figure 3.9 – Frequency responses of the loudspakers used within the old reverberation schamber at ITA.

The impulse responses have been detected by two ¼" precision microphones and an audio interface with 192 kHz sampling frequency. A sweep was used as test signal and 72 measurements (with 5° turntable angular steps) for three different source-receiver positions were performed.

In order to validate the measurement setup, a reference measurement of a sinusoidal surface has been performed before the measurements of common objects begin. Results are in accordance to those previously published in literature (Fig.3.8).
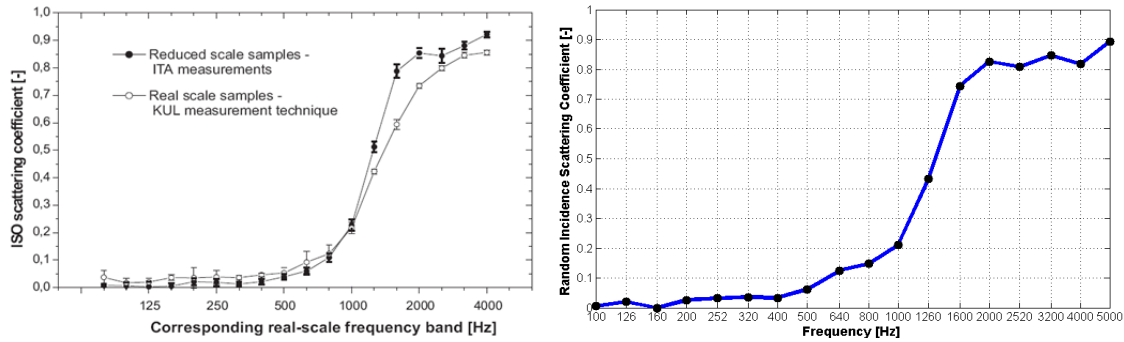
Figure 3.10 – (left) Comparison of the scattering coefficients of a sinusoidal surface measured by using the K.U.Leuven technique for the real-scale sample and in Aachen for the reduced-scale samples (Vorländer et al., 2004); (right) reference measurement performed to validate the setup before the measurement of common objects begins.

3.2.2 Sample Objects and Configurations

Several pieces of furniture have been built in a scaled version model with ratio 1:10 (Fig.3.9). Samples are made up of balsa wood and reflect the design of common real objects. In this first study results associated with chairs and desks will be presented. Four different spatial configurations have been investigated (Fig. 4.11), with a particular focus on a typical classroom configuration.
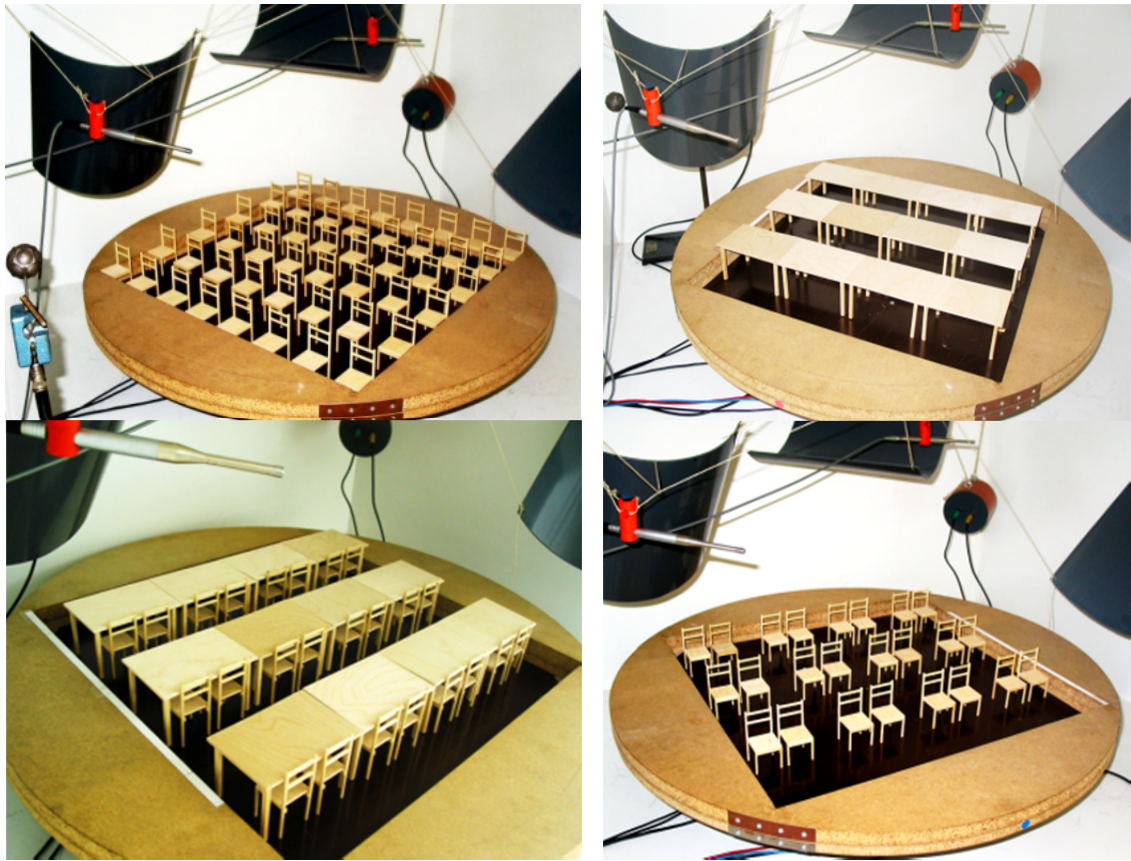
Figure 3.11 - Furniture configurations under investigation

In a first layout, a matrix of 48 chairs equally spaced has been placed in a squared recess. The sitting height of the chairs has been mounted flush with the height of the recess, in order to avoid border effects (De Avelar et al., 2002). A metal grid has been used for realizing a faster and precise spacing between samples. In a second configuration, 12 desks have been placed in a three rows matrix inside a squared recess in order to reproduce the exact layout of a real lecture room. No spacing has been left between the desks. The factors determining the minimum number of periods required to represent a periodic sample remain to be investigated. However, twelve elements can be considered a sufficient amount, since it has been shown that the presence of at least 11 periods (elements in this case) is enough to measure a representative scattering coefficient (Vorländer et al., 2004).

In a third configuration, 24 chairs have been added to the desks configuration, determining in this way a common classroom layout. In a fourth configuration, desks have been removed and only 24 chairs, in a paired placing, have been measured. In this way it is possible to evaluate effects of different elements. Results of scattering coefficients are presented in Fig.3.10.

Ff	1	2	3	4
200	0.19	0.22	0.28	0.28
250	0.2	0.23	0.35	0.38
320	0.2	0.28	0.33	0.36
400	0.19	0.28	0.32	0.35
500	0.22	0.24	0.33	0.36
640	0.31	0.38	0.42	0.44
800	0.34	0.41	0.48	0.5
1000	0.38	0.44	0.52	0.51
1250	0.44	0.49	0.61	0.63
1600	0.46	0.5	0.57	0.7
2000	0.5	0.55	0.5	0.69
2500	0.65	0.66	0.7	0.77
3200	0.52	0.41	0.63	0.77
4000	0.41	0.53	0.61	0.69
5000	0.49	0.59	0.55	0.8
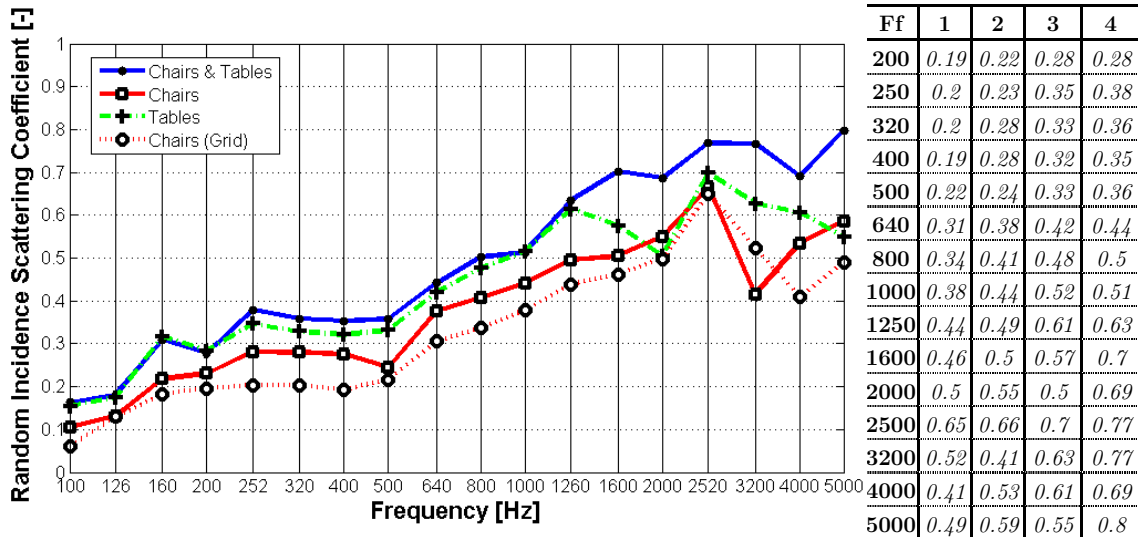
Figure 3.12 - Measured scattering coefficients. Curves (left) and values (right) of four different configurations: 48 chairs in a grid (1), 24 chairs in pairs (2), 12 tables (3), 12 tables and 24 chairs (4).

They show that the typical configuration for a classroom (tables and chairs) is responsible for the highest scattering behavior. Moreover, the placement of chairs in a paired configuration instead of a grid displacement produces a higher scattering. Finally, it seems that since tables have a wider surface, they contribute to a higher scattering at the low-mid frequencies, whereas the chairs, which have a finer structure, introduce more scattering at higher frequencies (from 1.6 kHz on).

3.2.3 Measurements Limitations

Several known problems were experienced while doing scale model measurements of scattering coefficient (Vorländer et al., 2004). In particular, because of strong air absorption, the measured reverberation times at high frequencies became very similar (Fig.3.11). Moreover, time variance effects, such as small changes in air temperature or humidity, resulted in a severe decrease of the measured reverberation time, especially at high frequencies (Chu, 1995). Because of air absorption, T_2 and T_4 may become similar, thus making it more difficult to distinguish between decay slopes. In this case, the transition from one curve decay to another takes place at lower decay levels and some difficulties arise when this level reaches the measurement noise floor. Therefore, for the sake of accuracy, only results up to 50 kHz (5 kHz for the real scaled frequency) have been shown, since the data in the range 50-80 kHz are affected by a significant error.
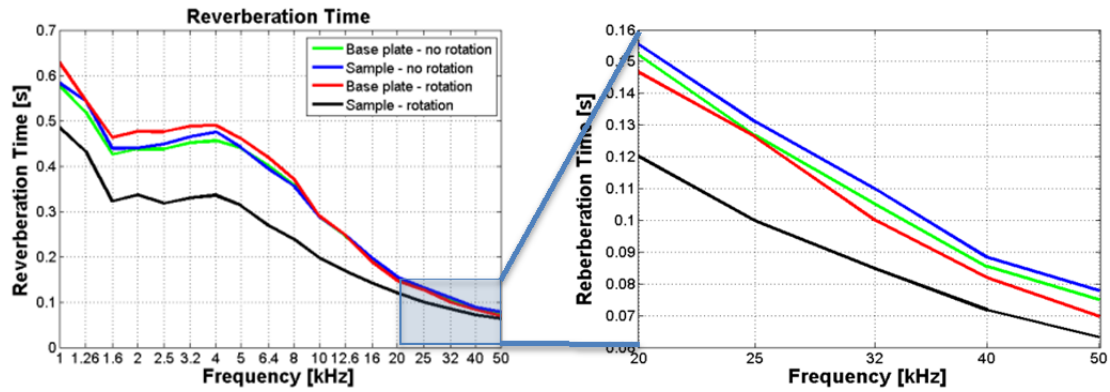
Figure 3.13 – Air absorption and time variance effects at high frequencies are responsible for more similar reverberation times.

3.3   A Revised Scale Model Reverberation Chamber

For measurements of random-incidence scattering coefficients according to ISO 17497-1, scale models have proven to yield results with reasonable time and effort. Especially handling the samples becomes much easier so that several measurements, which may be difficult or even unfeasible in a full-scale reverberation chamber, turn out to be possible. Despite these advantages, using a scale model environment poses other difficulties that are related to the extended frequency range.

Besides the inherent and unavoidable problems associated to scale model measurements, there are a few issues that could be addressed and resolved. For instance, the baseplate scattering should be zero, but in practice it is not, due to baseplate imperfections and measurement uncertainties. Hence, the turntable inside the room acts has an additional scattering object, which is not correct. Moreover, since the time variance is a known problem, a constant monitoring of temperature and humidity should be obtained, so that the speed of sound can be evaluated accordingly. Furthermore, an inadequate thickness of the chamber walls does not provide a proper sound insulation from the outside; hence, measurements are much more exposed to external noise.

Another critical aspect is related to the frequency range. Data of interest ranges between 100 Hz and 8 kHz that means, in a 1:10 scale, a frequency range of 1-80 kHz. In order to include the side band, the frequency range of measurement should eventually be extended up to 90 kHz. This limit can be achieved with proper audio interfaces and devices. However, this creates a major problem with the sound sources. A better sound source would be required, as the actual piezoelectric loudspeaker provides an inhomogeneous frequency response, which decreases rapidly starting from 60 kHz. A stable and linear sound source, possibly omnidirectional, is necessary, but this is hardly achievable because, at those frequencies, the radiation pattern presents very strong spikes that are difficult (if

not impossible) to smooth. This circumstance affects diffusivity as well, which is an essential condition for the ISO method. The hanging system of microphones should also be reconsidered for obtaining more precision and efficiency.

In order to achieve a better repeatability and stability of the measurements, a revised scale model room, which complies with ISO354 and ISO17497 for scale factors $\geq$ 5, has been developed (Müller-Trapet et al., 2010), which presents several improvements with respect to the ordinary scale model rooms. The new chamber is constructed of six 2.8 cm thick wooden panels that are finished with a two-component coating lacquer, ensuring high acoustic reflectivity and appropriate sound insulation. The interior dimensions of the chamber are 1.2 m x 1.5 m x 0.95 m.

The first target to get accomplished has been the extraction of the turntable outside of the chamber, which has been achieved by means of a circular opening (diameter of 90 cm) on the base plate (Fig.3.12). This opening hosts a double scissor lift table, on top of which the turntable is placed. In this way, the turntable can be lowered so that the rotating base plate is mounted flush with the floor. This solution drastically reduces edge effects of the sample. In case of non-circular samples, a circular frame with an inner recess can be built and placed directly over the rotating plate (an experimental configuration of this type is shown in par.7.3). Thanks to the variable height, samples with different depths can be equally measured.
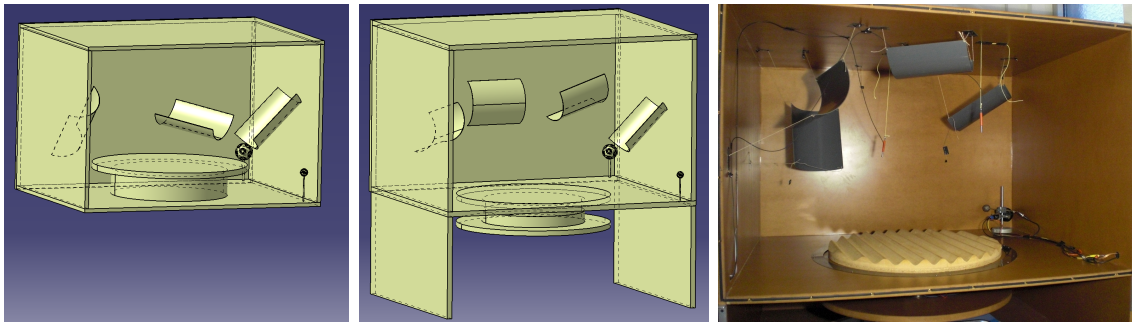
Figure 3.14 - Main concept behind the revised scaled model reverberation chamber: (left) the old reverberation chamber setup; (middle) the new solution with a lifting turntable; (right) measurement layout for a sinusoidal surface where the turntable has been lowerd down by the double scissor lift table.

The new chamber includes temperature and humidity sensors that constantly detect variations in order to enable correction for air absorption.

Measurements in the new model room have been performed to evaluate the repeatability of the measurements and the quality of the results compared with reference data from calculation. Results from measurements of the mean scattering coefficient of the baseplate and sinusoidal sample in the old and new chamber are shown in Fig.3.13. A relevant reduction in terms of standard deviation has been obtained in both cases specifically at high frequencies. This is

an important result because, as described in par.3.2.3, the high frequencies values are the most sensitive to errors, so an error reduction in that range improves the quality of results.
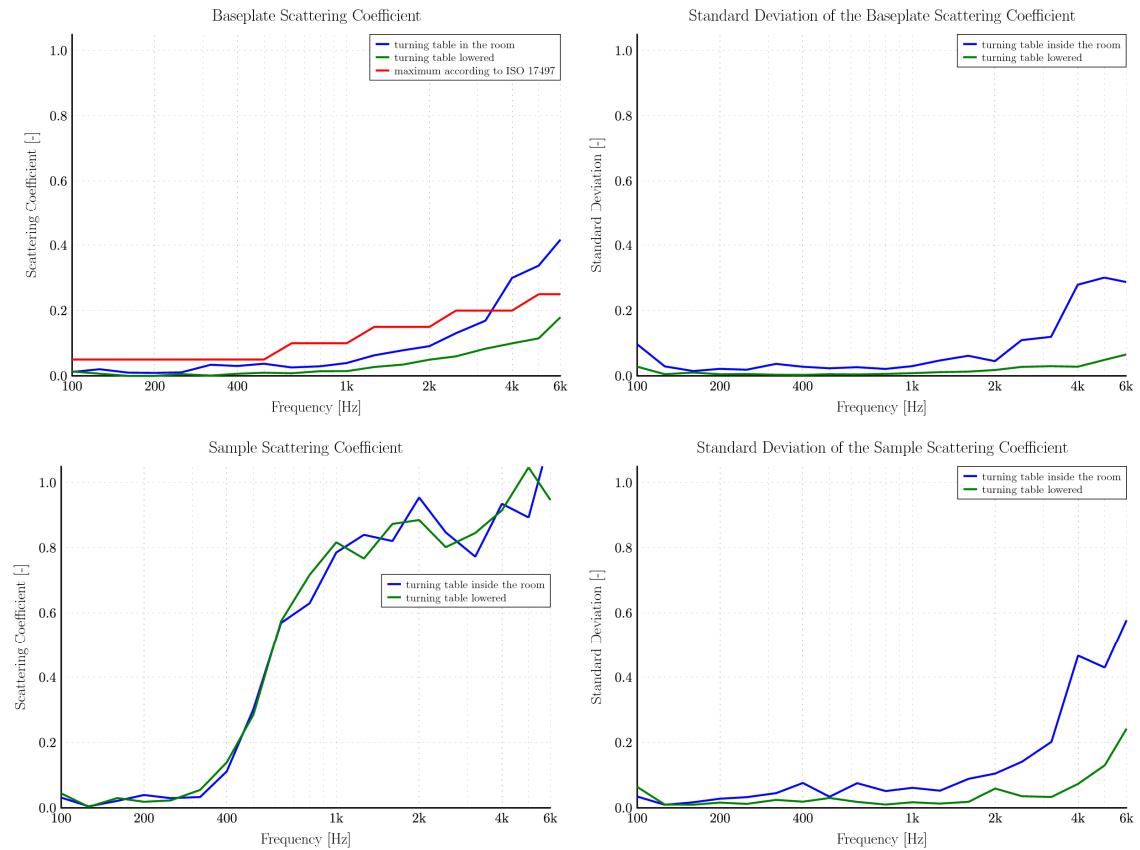
Figure 3.15 - (left) Comparison between old and revised reverberation chamber in relation to the turntable location; (right) the standard deviaiton is improved if the turntable is extracted from the room and the rotating plate is mounted flush with the chamber base plate.

Other improvements have also been developed, such as the implementation of a robotic system to autonomously measure multiple microphone positions, which allows the displacement of microphones in up to twelve different positions without the need of opening the room, thus avoiding time variance issues.

A new solution for the hanging diffusers has been introduced by replacing them with wall-panel diffusers, also referred to as a boundary diffuser. In order to evaluate the effects of this change, an investigation on the effect of different diffuser types on sound field diffusivity has recently been carried out (Bradley et al., 2014). The sound field diffusivity has been analyzed in terms of maximum absorption coefficient, standard deviation of decay rate, and total confidence interval. Results revealed that boundary diffusers and hanging diffusers produce roughly equivalent diffusion in the sound field, so the configurations are interchangeable.

The measurement chain has been improved respect to the old chamber by the introduction of 192 kHz sound interfaces, which potentially fulfill the requirement of measuring up to 80 kHz. However, even though a new dodecahedron sound

source has been introduced, this does not provided a suitable signal above 50 kHz; therefore, a better sound source for high frequencies needs to be developed in the future.

3.4   Angle Dependent Scattering: Measurements of Random Incidence Diffusion Coefficient

A case study for assessing the surface scattering of a concert hall diffuser is hereafter presented. The sample under investigation consists of a wall panel made up of a light metal grid, upon which several wooden laths with triangular sections are nailed and laid in parallel alignment. This type of panel was used to entirely cover the left and right sidewalls of a concert hall. The dimensions of the original panel were 2.68 m x 2.68 m, out of which a 90 cm x 85 cm sample was extracted, which contained 12 wooden laths (Fig.3.14).

In order to satisfy the far field conditions (at least 80% of the receiver positions are outside the specular zone), only a smaller part of the original test sample was used. This was possible because the test sample presented a periodic structure, so that at least four complete sequences have been included and the lobing effect of repetitions approaches reality with high accuracy.
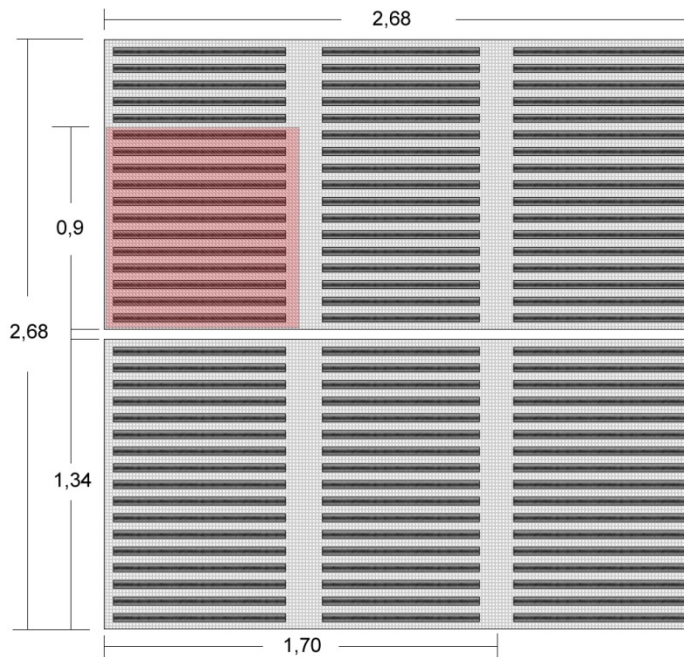
Figure 3.16 – Plane view of the original sample (grey) and the extracted smaller sample (red).

The measurements were taken according to the standard ISO 17497-2. A turntable with a diameter of 3.80 m built on purpose, which was electromechanically controlled. The test sample was placed in the middle of the turntable and mounted flush with the base plate.

A microphone arm, made up of 19 KE-4 Sennheiser microphones, was hanging from the room ceiling and suspended 5 cm over the turntable surface (Fig.3.15). A loudspeaker was supported by a thin metal bar, which was locked in the middle of the turning table, so that both of them could turn at the same time (Fig.3.16).
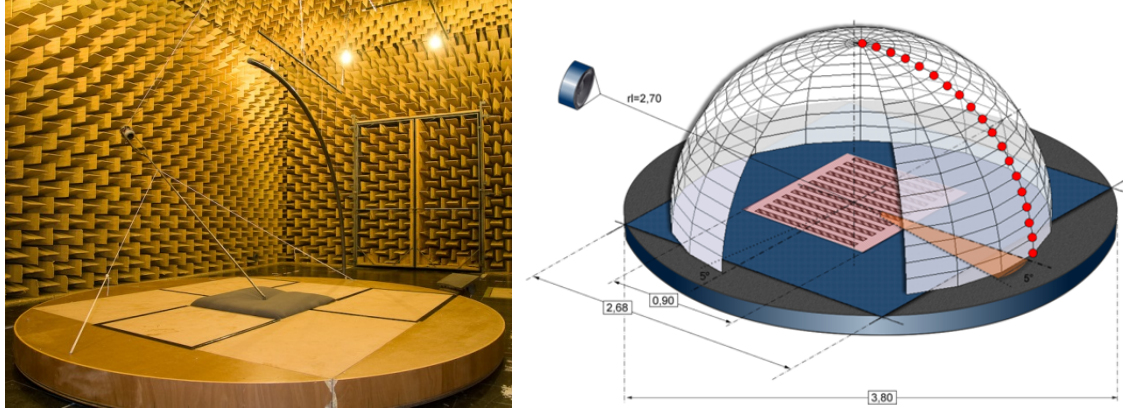
Figure 3.17 - (left) Measurement setup for detecting the background response without sample (h_2); (right) sampling scheme: red dots represents the position of microphones (dimesions are in meters).

Measurements were made with a receiver angular resolution of *5°*, from *5°* to *360°* (horizontal resolution of 72 points). In order to obtain the random incidence diffusion coefficient, source positions over a hemisphere were selected with the azimuth and elevation angles as given in Fig.3.17. The azimuth angle is intended as the reciprocal position between the loudspeaker and the sample. Azimuth angle equal to *0°* corresponds to the measurement point "P1 – 90", whereas azimuth angle equal to *30°* corresponds to the measurement point "P2 – 120" and so on.
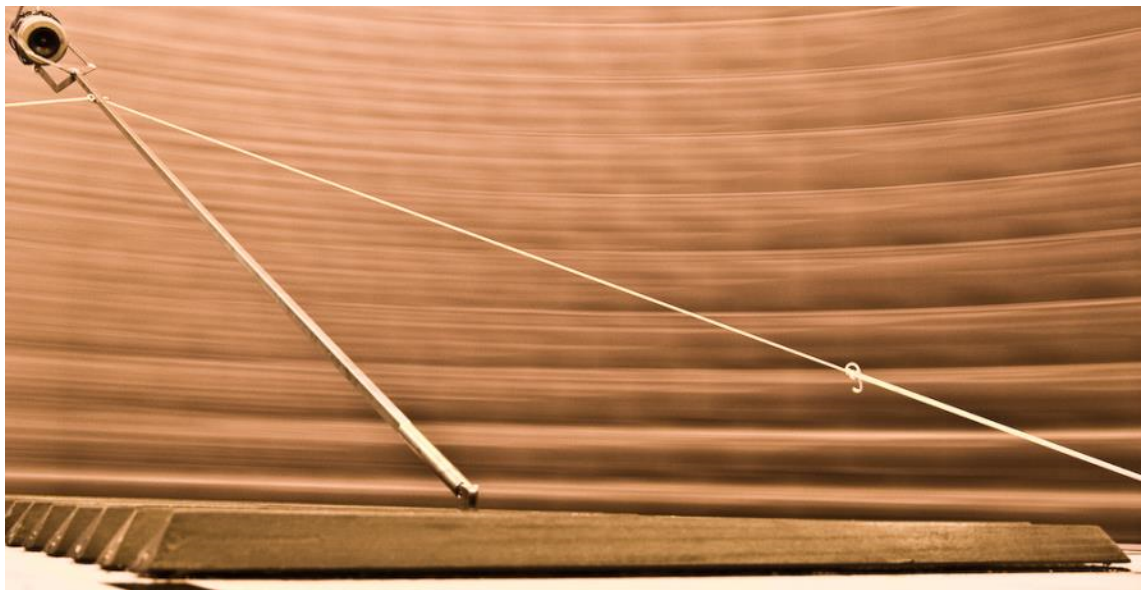
Figure 3.18 - Detail of the loudspeaker mounting system, which consists of a thin metal bar locked in the middle of the turning table and hold with two side thread. The wooden laths of the sample can be seen in the bottom.

Position	Elevation θ	Azimut φ
1	*35*	*0*
2	*35*	*30*
3	*35*	*60*
4	*35*	*90*
5	*60*	*0*
6	*60*	*30*
7	*60*	*60*
8	*60*	*90*
9	*80*	*0*
10	*80*	*30*
11	*80*	*60*
12	*80*	*90*
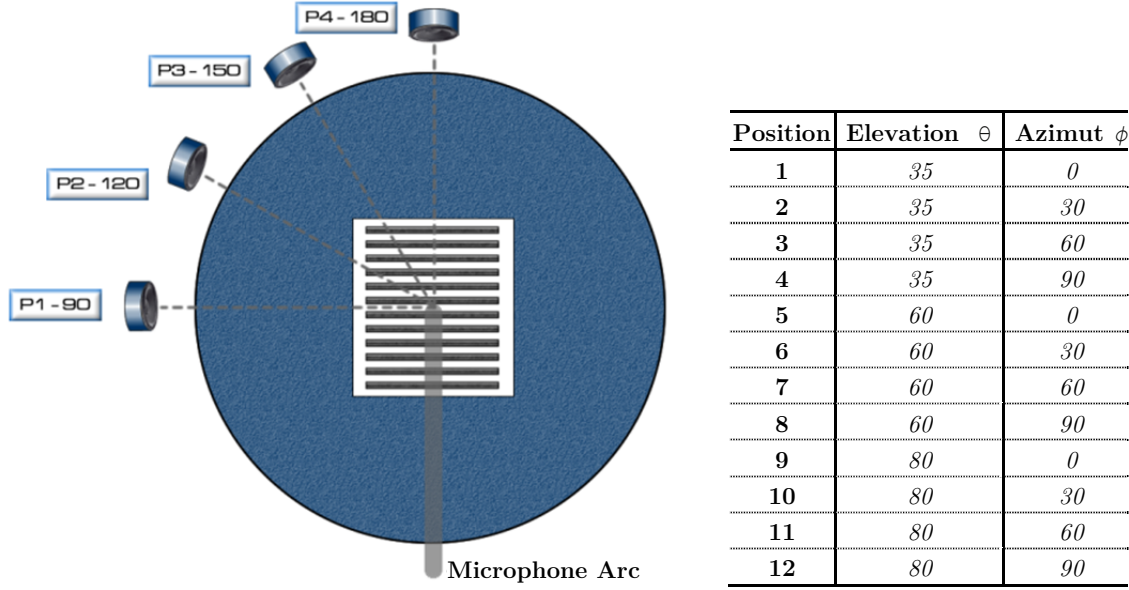
Figure 3.19 - (left) reciprocal measurement positions between loudspeaker and test sample; (right) azimuth and elevation angles for the source positions over a hemisphere.

The collected impulse responses were processed according to the method described in par.3.1.2., and the random incidence diffusion coefficient was calculated applying Eq.3.4. Results are given in terms of random incidence diffusion coefficient, which represents a measure of the uniformity of diffusion for a representative sample of sources over a complete hemisphere. Values and plots are showed in Fig.3.18.

Frequency [Hz]	Angle of incidence		
	35°	60°	80°
250	*0.89*	*0.79*	*0.86*
320	*0.87*	*0.77*	*0.75*
400	*0.87*	*0.77*	*0.79*
500	*0.84*	*0.78*	*0.76*
640	*0.88*	*0.85*	*0.72*
800	*0.89*	*0.84*	*0.62*
1000	*0.89*	*0.69*	*0.54*
1250	*0.85*	*0.65*	*0.58*
1600	*0.87*	*0.71*	*0.63*
2000	*0.85*	*0.72*	*0.58*
2500	*0.85*	*0.68*	*0.59*
3200	*0.88*	*0.75*	*0.65*
4000	*0.75*	*0.80*	*0.68*
5000	*0.75*	*0.75*	*0.71*
5000	*0.77*	*0.62*	*0.66*
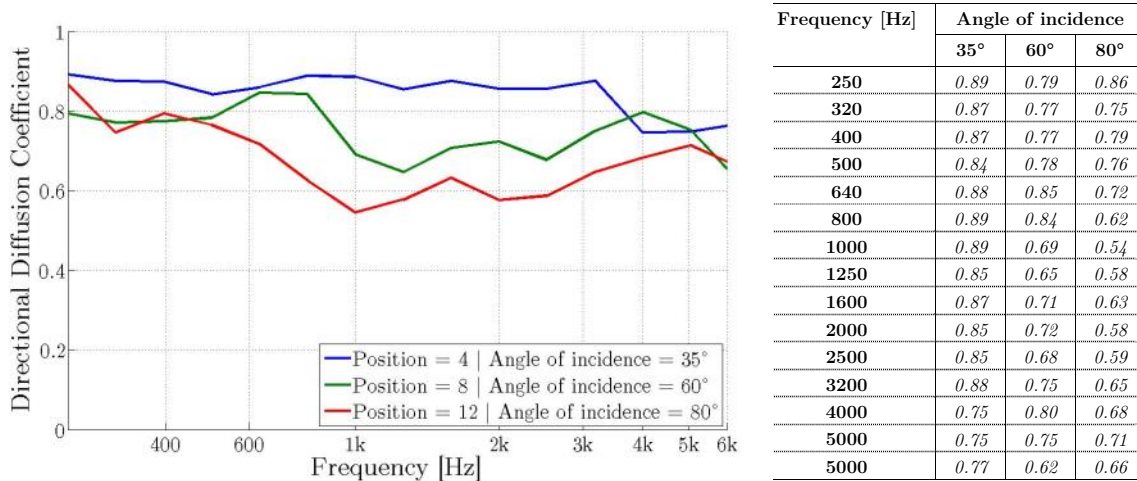
Figure 3.20 - Diffusion coefficient values for three different angle positions.

The plots of the diffusion coefficient show that, for the frequency band considered, the sample under test presents a good diffusion capacity for low incidence angles of the sound field (i.e. *35°*). The diffusing properties decrease with the increase of the incidence angle. For an angle of incidence of *80°*, the diffusion coefficient decrease up to 35% (for 1kHz) respect to the case of *35°*, that is to say there is directional inhomogeneity in the scattered energy.

The three-dimensional polar balloons for a frequency of 1 kHz and an angle of incidence of *35°* are shown in Fig. 3.19. The remaining plots for other frequency values and angles of incidence are shown in the Appendix A.
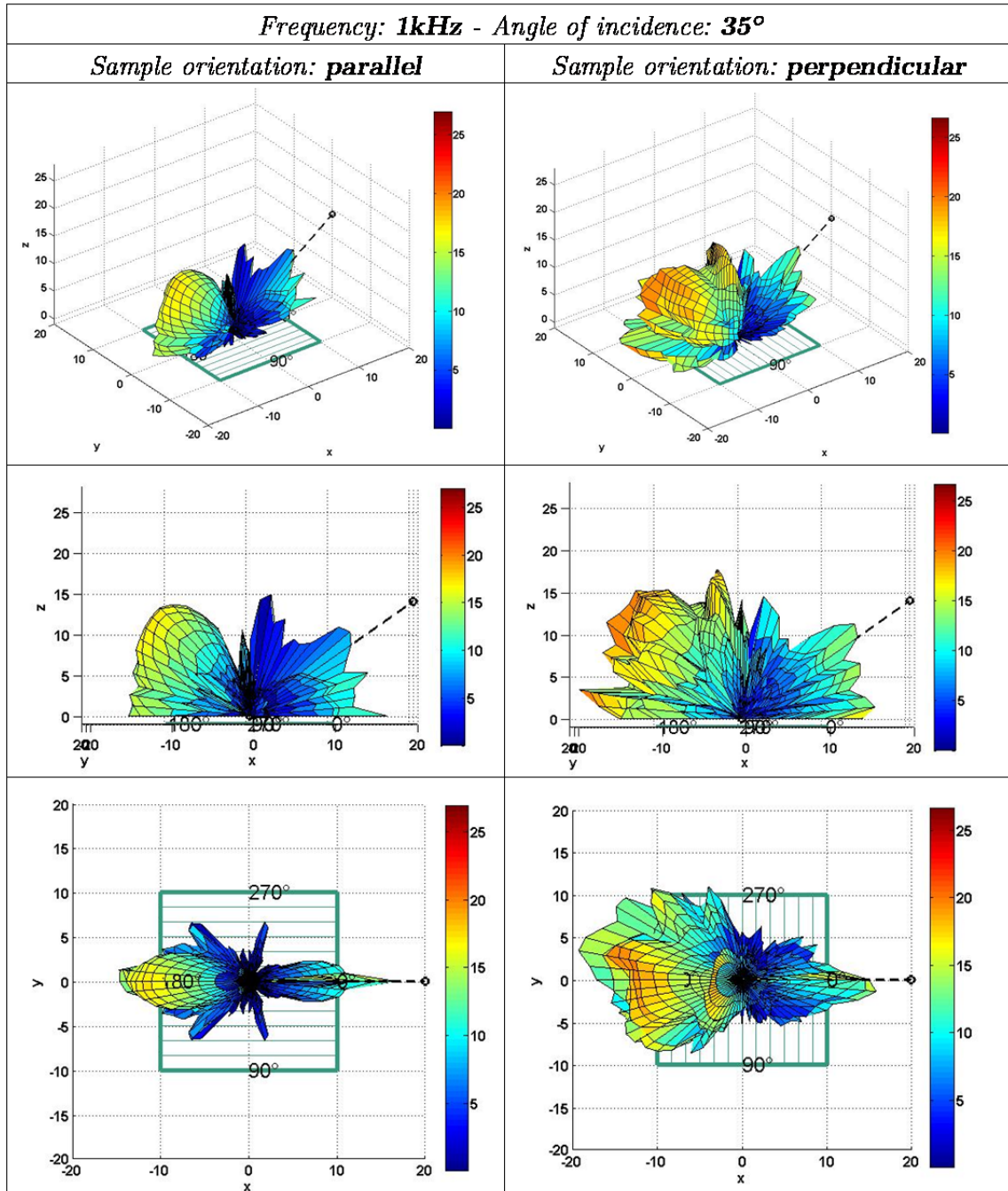
Figure 3.21 - Three dimensional polar balloon plots measured from the diffusing surface, which is shown below the polar responses as a geometrical sketch (green). On the left side, the sound field angle direction is parallel to the wooden laths, whereas on the right side the incident field is perpendicular to it. Measurements are shown for a frequency of 1kHz and an angle of incidence of 35°.

Comments about results will be given hereafter for each angle of incidence:

- **35°**: In the parallel case, the diffusion along the specular direction is limited, whereas in the perpendicular, the diffusion is much wider. In this latter case, a plurality of lobes with a higher intensity can be observed. In

both cases, the scattering becomes stronger as the frequency increases. In the parallel case, the radiation is wider for 2 and 4 kHz than at 1 kHz. The influence of the test pattern is evident at higher frequencies, especially in the parallel case. Noise emerges with higher intensity components, which are radiated out in many directions. The *90° - 270°* axis remain almost without tangential components.

- **60°**: In contrast to the *35°* configuration, this case presents much larger energy components along the mirror direction, already at low frequencies. The polar pattern is wider in the semicircle between *90°* - (*180°*) - *270°* for low frequencies. In the cross-oriented case, there are both a main lobe along the reflecting direction and a plurality of side-lobes, particularly along *135°* and *225°*. The same thing happens also in the parallel case, where the lobes are even more evident. In both cases, the sound scattering is stronger and wider as the frequency increases. The main lobe is particularly prominent and focused. The sample pattern plays an important role for higher frequencies, i.e. 4 kHz. The sound is scattered everywhere, particularly along the *90° - 270°* direction. A relevant part of the sound is reflected back from the sample laths in the direction of the source.

- **80°**: The sound is strongly reflected already from 1 kHz, where about 10 dB more respect to the 35° case can be observed. In both cases, the scattering is stronger and wider with increasing frequency. The radiation pattern is closely connected with the orientation of the pattern subdivision. The components along the specular direction are much stronger than the others. The main lobe is quite focused. Similarly to the *60°* case, the entire radiation from the sample is very strong at higher frequency. The influence of the sample pattern here is extremely clear and evident.

This case study showed that measurements of a diffuser by means of 3D polar balloons give more information and insights that cannot be deduced from measurement of scattering coefficient. It has been already explained, how the two coefficients are different and how they are related to other purposes. The concern with diffusion measurement is to measure the ability of diffusers to uniformly scatter in all directions, rather than the ability of a surface to move energy away from the specular angles, as the scattering coefficient does. In other words, the scattering coefficient is a measure of the amount of sound scattered away from the specular reflection direction, the diffusion coefficient measures the quality (in terms of spatial uniformity) of reflections produced by a surface. However, there are situations were sidewall patterns are differently oriented (a peculiar case is the ESPRO at IRCAM presented in Ch.7), thus angle-dependent information. In those cases, measurements of random incidence diffusion coefficient should be performed.

4   Room Acoustic Computer Simulation

The analysis of acoustic fields can be carried out according to different levels of accuracy, without affecting the target or the results of the investigation. Many complex phenomena related to the wave nature of sound, such as interference or diffraction, might not condition results in a significant way; this means that it is possible to study the acoustic field by means of simplified geometric laws. This is the case of spacious environments (concert halls, theatres) where few and well localized sound sources are present and the resulting sound field mainly depends on the multi path reflection phenomena of the sound against the walls: these are generally smooth and dimensionally wider than the wavelengths involved, so that it is reasonable to affirm that the reflections take place in a specular way, without the border diffraction (or diffusion) effect due to surface harshness.

Geometrical room acoustics allows to simplify the physical description of sound fields (see par. 4.1), which is the reason why it has been implemented in the first approaches of room acoustic computer simulation (Schroeder, 1962; Krokstad et al., 1968). Similarly to the geometrical optics approach, the main idea is to treat sound waves in the same way as light rays are treated in optics. However, aspects like diffusion are not always negligible, in which case additional aspects have to be considered, thus resulting in a higher degree of complexity (Garai, 2001).

Depending on the specific applications as well as on the physical approach of sound phenomena (wave or rays), several alternative models have been developed in the past. To describe sound using the wave model approach, solutions to the wave equation are found analytically (when possible) or are approximated using methods such as the Finite Element Method (FEM) or the Boundary Element Method (BEM). The first executes spatial domain approximation, while the second performs approximations on the border of the spatial domain. These methods are often not practical for architectural acoustics because the number of modes in a room increases rapidly to an unwieldy value as frequency increases. As a result, these methods are generally restricted to small rooms and low frequencies.

The most used domain in room acoustics undoubtedly refers to the geometric treatment of the sound field. Several models have been developed in this area, among which Ray Tracing Method (RTM), Radiosity and Mirror Image Sources (MSM), are the most significant. They differ between each other in terms of the theoretical hypothesis as well as the fields of applications. The ray model approach describes sound as a small segment of a spherically diverging wave,

which originates from a point and propagates in a specified direction. This description has led to more practical methods for architectural acoustics, namely ray-tracing and image source methods. These methods fall under the general realm of geometric acoustics. They involve a simplification based on a special solution to the wave equation that is valid when the wavelength of sound is small compared to overall reflecting surface dimensions and large compared to surface irregularities and curvature. Geometric acoustics does not account for diffraction but assumes that rays propagate in straight lines. It also assumes that absorption at surfaces is independent of the angle of incidence. Interference is not taken into account, meaning that when several sound field components are superposed, their phase relationships are not considered. This simplification is valid when the different components are incoherent with respect to each other, which is usually true when the components have broad frequency spectra. In spite of these limitations associated with geometric acoustics, this framework provides significant and useful information about the sound characteristics of a room.

In conclusion, there are two main room acoustics simulation methods: *wave-based* methods are used for frequencies below the Schroeder frequency (above which room modes are statistically overlapping), whereas *hybrid* methods, based on geometrical acoustics, are used for simulations above that frequency. Hybrid methods combine image sources with stochastic models for the simulation of the room's reverberant sound, hence they account for both specular and diffuse reflections. They might even account for sound diffraction if adequate model extensions are used.

In this chapter, an introduction of geometrical room acoustics will be given together with a brief review of a few modelling approaches such as the RTM, the Radiosity method and the MSM. Their usage within three types of room acoustic simulation software will be described. As a specific case study, an ordinary classroom with common pieces of furniture, such as chairs and desks, is shown. Results of computer simulations of the sound field reflections for this environment in terms of scattering coefficient are presented.

4.1   Geometrical Room Acoustics

The geometrical approximation holds when the wavelength of sound has negligible dimensions respect to the environment, as it happens in particular with higher frequencies. As in geometrical optics, a sound ray is intended as a small portion of a spherical wave with vanishing aperture, which originates from a certain point (Kuttruff, 2000). Its direction of propagation is well defined and it is subject to the same laws of propagation as light rays (apart from the speed). Thus, neglecting the medium attenuation, the total energy conveyed by a ray remains constant, while its intensity falls as $1/r^2$, as in every spherical wave

(where r denotes the distance from its origin). Refraction, interference and diffraction are generally not considered in geometrical room acoustics, although an extension of the MSM for edge diffraction was presented by (Svensson et al., 1999). With reference to interference, if several sound field components are superimposed their mutual phase relations are not taken into account: simply their energy densities or intensities are added. This procedure is possible if the different components are incoherent with respect to each other. It is by now clear that the rays approach it is only an approximation of the sound field, and it is valid only under certain conditions.

A possible solution to the wave equation is represented by:

$$p(r,t) = A(r) \cdot e^{i\omega[t - \Gamma(r)/c_0]} \tag{4.1}$$

where c_0 is a reference constant value for the phase speed and Γ is the so called *iconal function*. For $\Gamma(r) = k$ (being k a constant) we obtain the locus of constant phase surfaces, so that $\nabla\Gamma(r)$, perpendicular to those surfaces, is the direction of wave propagation. By substituting eq. 3.1 in the wave equation, we obtain:

$$\nabla\Gamma \cdot \nabla\Gamma = n^2 \tag{4.2}$$

where, similarly to geometric optics, n is given by

$$n(r) = \frac{c_0}{c(r)} \tag{4.3}$$

where $c(r)$ is the phase speed as function of position. As a consequence, the sound waves solutions of (Eq.3.2) propagate almost like plane waves. Sufficient conditions for the validity of (Eq.3.2) are that both the amplitude $A(r)$ and the phase speed $c(r)$ do not change notably on distances comparable to the wave length. With regard to the amplitude, it follows that one can identify sound rays with sound energy bundles, in the middle of which the wave amplitude remains almost constant. As for the phase speed, it follows that the concept of sound rays holds only when the trajectory of elementary bundles of sound energy is locally almost rectilinear, that is when refraction occurs in a small amount. This condition is generally satisfied at high frequencies. Originally, geometric room acoustics models did not include the effects of scattering generated by edges and surface roughness. However, since it has been shown that such a simplification affect negatively the prediction accuracy, several treatments for describing the diffuse sound field have been proposed (Cox et al., 2006).

Although both RTM and MSM belongs to the geometrical room acoustics approach, they are elicited from two diverse physical approaches. The main difference between lies in implementation of the energy detection and the internal nature of physical energy propagation: in RTM the energy detectors are volumes and the energy spreading is stochastic by counting, whereas in MSM the energy

detectors are points and the energy spreading is deterministic by distance (Vorländer, 2010).

Given that a pure MSM would not be capable to simulate a complex room with enough accuracy, combinations of the models have been introduced and are widely accepted. All the recent room acoustics simulation software implement hybrid models; in this way they are able to handle specular and diffuse reflections in order to evaluate room impulse responses that are closer to real measurements.

4.1.1 Stochastic Ray Tracing Method (RTM)

This model considers a particular schematization for the sound energy propagation: instead of being scattered on spherical wave front (as it happens in MSM), ray tracing method admits that the sound energy is split along sound rays or rectilinear trajectories (Schroeder, 1970; Kulowksi, 1985). Ray tracing methods find reverberation paths between a source and receiver by generating rays emanating from the source position and following them through the environment until an appropriate set of rays has been found that reach a representation of the receiver position. At this position, the respective energy envelope of the RIR is eventually calculated and sound particles associated with rays can be summed.

The generation of rays can be realized with a deterministic or statistic approach. Rays propagates in all directions according to acoustic geometry laws and they have, ideally, infinitesimal and constant section. Geometrical divergence of emitted sound energy is represented by the geometric divergence of the sound rays. The sound energy of the source is quantized by a finite number of elements, called *sound particles* (or *phonons*), associated with sound rays. Each particle loses energy while propagating because of air absorption, occurring reflections, material-dependent absorption and scattering of sound.

Along the border surfaces, the sound can be reflected either with specular (the angle of incidence and reflection coincide) or diffuse (in random direction) reflections. This is usually decided by an algorithm that compares a random number between zero and one with the scattering coefficient of the hit object. The distribution of the scattered energy usually follows the Radiosity model and the Lambert's law (see 4.1.2).

In presence of specific surfaces that scatter in a preferred direction, an angle-dependent energy distribution should be used instead. Besides the absorption coefficient, the scattering coefficient has to be taken into account for the energy attenuation of each particle. Hence, the energy of each particle is weighted with s in case the reflection is diffuse; otherwise with $(1 - s)$ if the reflection is specular. Each particle expires when a predefined termination condition is fulfilled.

Ray tracing is computational intensive, although the time to compute an impulse response in a complex environment has decreased with the increasing of processor power. The precision of such a model grows with the growth of the number of released sound particles.

4.1.2 Radiosity Model

Differently from RTM and MSM methods, Radiosity model has been specifically developed for treating the problem of diffusion. It assumes, in fact, to deal with enclosures with rough boundaries, which scatter the reflected sound energy in an ideally diffuse way (Kuttruff, 1995). This condition (which must not mistakenly be assumed to result in a diffuse sound field) implies the *Lambert's law*, which states that the intensity of the reflected or rather scattered sound, a certain distance from the considered wall element, is proportional to the cosine of the angle between the wall normal and the scattering direction. In particular, by supposing that an area element dS is illuminated by a bundle of parallel or nearly parallel rays which make an angle ϑ_0 to the wall normal (Fig.4.1), whose intensity is I_0, then the intensity of the sound which is scattered in a direction characterized by an angle ϑ (measured at distance r from dS), is given by (Kuttruff, 2000):

$$I(r) = I_0 dS \cdot K = I_0 dS \frac{\cos \vartheta \cos \vartheta_0}{\pi r^2} = B_0 dS \frac{\cos \vartheta}{\pi r^2} \qquad (4.4)$$

where B_0 represents the energy incident on unit area of the wall per second (*irradiation strength*). In case of absorption, the intensity needs to be multiplied by a factor $1 - \alpha(\vartheta)$.
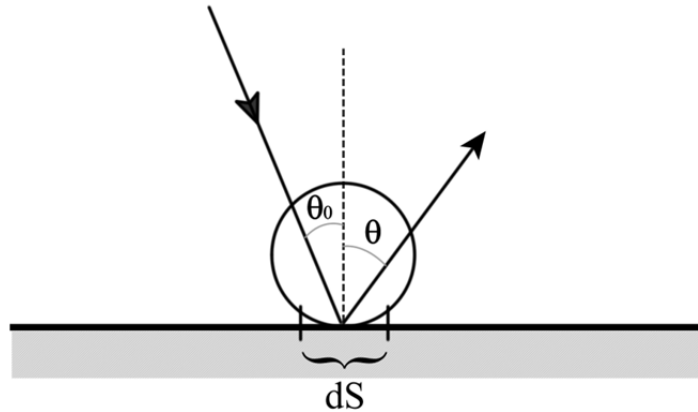
Figure 4.1 - Ideally diffuse sound reflection from an acoustically rough surface

If we indicate with $B(r,t)$ the brightness (or Radiosity if it is time independent) as the sound intensity received by a generic area element dS' at r', it can be shown that (Kuttruff, 1976; Joyce, 1978):

$$B(r,t) = \int_S K(r,r')\rho(r,r')B(r',t-R/c)dS' + B_0(r,t) \qquad (4.5)$$

In this equation, considered the basis for the Radiosity method, the term *B* denotes the irradiation density of the boundary, that is the sound energy arriving at the wall per second and unit area, *R=r-r'* is the distance between two wall points, *c* the sound velocity and *K* is a parameter that describes the kind of wall reflection. The reflection coefficient of the boundary element can be also considered by imposing $\rho = 1 - \alpha$.

4.1.3 Mirror Image Sources Method (MSM)

Mirror Image Sources Method (MSM) computes specular reflection paths by considering virtual sources generated by mirroring the location of the sound source over each polygonal surface of the environment. This method makes it possible to represent a boundary-value problem in terms of an equivalent problem involving multiple sources, but no boundaries (Borish, 1984). In fact, once the image sources have been constructed, the walls can be disregarded altogether, the effect of which is replaced by that of the image source. The key idea is that a direct path from each virtual source has the same directionality and length as a specular reflection path. Thus, specular reflection paths can be modelled up to any order by recursive generation of virtual sources (Fig. 3.2). Even though this model has always wide applications in spacious environment at mid-high frequencies range, recent developments have shown that MSM can be also applied to investigate the prediction of the low-frequency modally dominated part of a room transfer function in rectangular rooms with arbitrary, complex-valued boundary conditions on the room walls (Aretz et al., 2014).
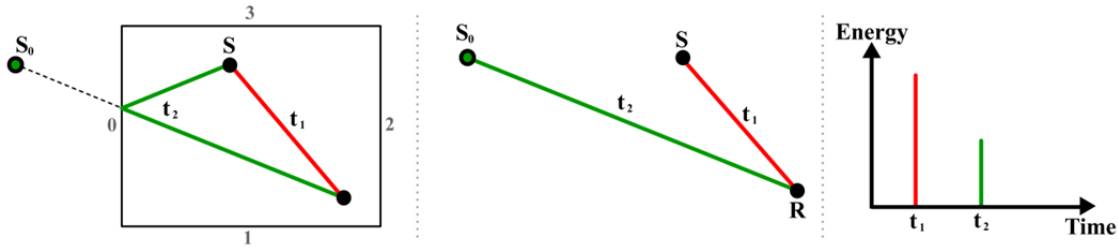
Figure 3.2 - Basic principle of mirror images source model.

The following description of the model is based on the theoretical explanation proposed by (Kuttruff, 2000). The process of reflection follows the (optical) law of specular reflection, which is applied to enclosures the boundaries of which are composed of plane and uniform walls. The fraction of non-reflected sound energy is characterized by the absorption coefficient α of the wall, which can be defined as the ratio between the non-reflected to the incident intensity. Generally, the reflected ray has a different power spectrum and a lower total intensity than the incident one, since the latter depends on the incidence angle and the frequencies contained. This can be taken into account by modifying the spectrum and the directional distribution of the emitted sound. However, such a refinement, is bypassed; instead, a mean value only of the absorption coefficient is account for

by reducing the intensity of the reflected ray by a fraction $1-\alpha$ of the primary intensity. By iterating the mirroring process in rooms bounded with plane surfaces, one obtains images sources of higher order. If an enclosure with N-plane walls is considered, it can be shown that number of images of order i is $N(N\text{-}1)^{i\text{-}1}$ (for $i \geq 1$), while the total number of images of order up to i_0 is obtained by the following expression:

$$N(i_0) = N \frac{(N-1)^{i_0} - 1}{N - 2} \tag{4.6}$$

Some image sources could be neglected because of their invisibility or inaudibility. A specific test called *audibility test* is performed on this purpose as described by (Vorländer, 2010). When all valid image sources have been detected, the original room is no longer needed.

Under the assumption that all sources (including the original) simultaneously emit the same sound signal, the total sound signal received in a single point is then given by the superposition of the contributions of all significant image sources. For each ray in the model, the travel delay as well as the absorptivity of the crossed walls needs to be taken into account. It follows that the received signal can be expressed as:

$$s'(t) = \sum_n A_n s(t - t_n) \tag{4.7}$$

where A_n is the particular strength of each ray and t_n is the travelling time. Accordingly, the impulse response of the room is given by:

$$g(t) = \sum_n A_n \delta(t - t_n) \tag{4.8}$$

In this derivation it was tacitly assumed that contributions of all image sources are mutually incoherent.

4.1.4 The Temporal Distribution of Reflections

Fig. 3.2 shows an elementary example of how an energetic room impulse response can be drawn starting from the mirror image sources model. If one evaluates all the possible reflections within a room up to a certain order, a reflection diagram (named *echogram*) can be eventually traced, where the energy of each reflection is represented together with its time delay. This diagram gives significant information on the temporal structure of the sound field at a certain point in a room. The division into three sections (the *direct sound*, the *early reflections*, and the *late reverberation*) is related to the human's perception of room acoustics, in fact each part affects the auditory sensation in a different way (see par. 6.3).
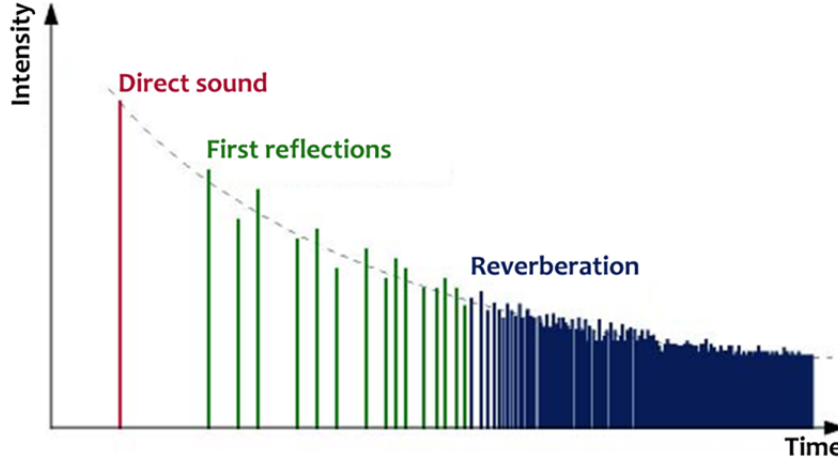
Figure 3.3 - A schematic reflection diagram which shows an energetic room impulse response (echogram).

It is possible to know in detail the displacement of the temporal structure of reflections in a rectangular room by using a system of image rooms and image sources. Let's consider a room (including also floor and ceiling), for which certain image sources of the same order are complementary with respect to their directivity and coincide, as it is the case for rectangular or square room. For such a room, the pattern iterates as shown in Fig.3.4.

Let's suppose that all mirror sources generates impulses of equal strength at *t=0*. In a *dt* time interval all those reflections, which originate from image sources whose distances to the center are between *ct* and *c(t+dt)*, will arrive in the center of the room (*c* is the velocity the sound). These sources are located in a spherical cell with radius *ct*, thickness *cdt* and volume *4πc³t²*. In this shell, the volume *V* of an image room is contained *4πc3t2/V* times, which also coincide with the number of mirror sources contained in the shell volume.

Hence, the average temporal density of the reflections arriving at time *t* is:

$$\frac{dN_r}{dt} = 4\pi \frac{c^3 t^2}{V} \qquad (4.9)$$

from which the number of reflections can be easily obtained through an integration. It follows that:

$$N_r = \frac{4}{3} \frac{(ct)^3}{V} \pi \qquad (4.10)$$

(Kuttruff, 2000) also showed that the total number of wall crossing, i.e. the total number of reflections which a ray with given direction undergoes per second, is:

$$n = \frac{cS}{4V} \qquad (4.11)$$

where *S* is the total wall area of the room and *V* its volume. In the course of wave propagation, the sound intensity amplitude decreases proportionally as *1/r²* according to an exponential law.
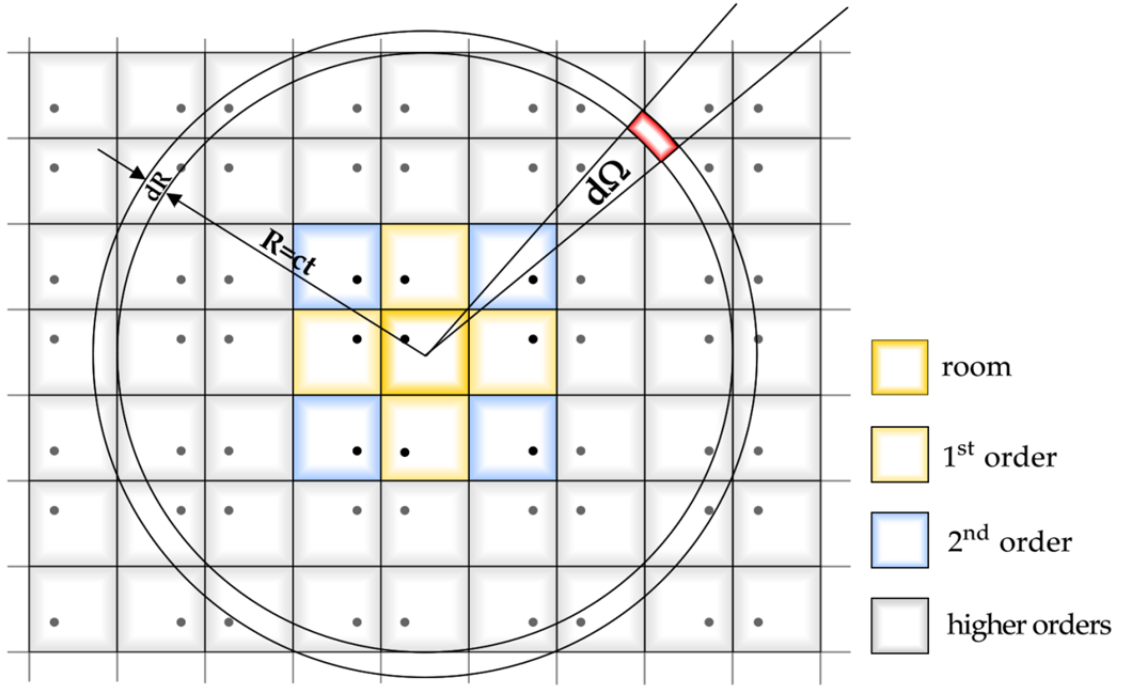
Figure 3.4 - Image sound sources for a square room. The pattern iterates also in the third dimension (perpendicular to the drawing plane).

In particular, being m the medium absorption, n the number of image room crossing, and $r = ct$ (see Fig.3.4) the reduction factor for each wall crossing, the whole energy of all reflections at the point of observation is:

$$E(t) = \frac{1}{(ct)^2} \exp\{[-mc + n\ln(1-\alpha)]t\} \qquad (4.12)$$

4.2   Hybrid Models

The mirror image source model performs particularly well in large rooms with low absorbing or reflecting surfaces (Suh et al., 1999) and produces impulse responses that are easy to evaluate (see 4.1.4). However, MSM assumes that the sound is specularly reflected by plane surfaces, thus neglecting the diffuse aspect of sound field, which was proved to be a major drawback in the simulation results (Vorländer, 1995). On the contrary, the Radiosity and the Ray Tracing models were developed for studying the evolution of diffuse sound fields. Since each method has some weakness, hybrid models have been developed in order to optimize the simulation performance and to give a more accurate acoustical description. This is particularly relevant for the scattering component of the sound field, which becomes a dominant element already from second or third order of reflections. This situation will be hereafter discussed.

The sound field in an enclosed space can be divided into its specular and scattered components. A sound field is said to be totally *diffuse* if the directional distribution of the reflected and scattered energy does not depend on the direction

of the incident sound (Kuttruff, 2000). Differently from optics, in acoustics only partially diffuse reflections can be achieved. In any case, the assumption of totally diffuse reflections comes often closer to the reflecting properties of real walls better than specular reflections. The Radiosity model shows that totally diffuse reflections from a wall take place according to Lambert's law (par.4.1.2). However, in practical situations only a certain fraction *s* will be reflected in a diffuse manner while the remaining fraction 1 – *s* will be specularly reflected (Kuttruff, 1995). Therefore, a mixed specular-diffuse scattering model appears to be a very appropriate solution (Joyce, 1978; Baines, 1983; Kuttruff, 1995).
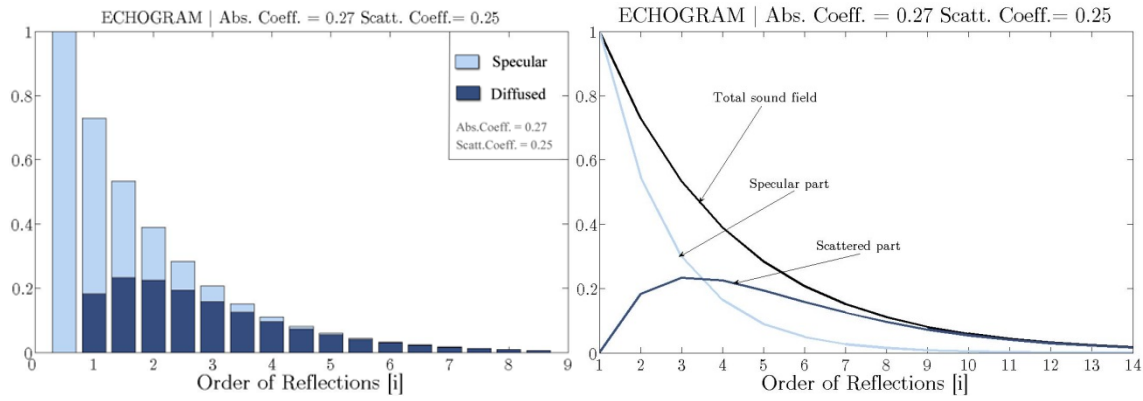
Figure 4.5 - Conversion of specularly into diffusely sound energy during subsequent reflections in equal time interval.

The exponential decay curve can be thought as made up of a specular and a diffuse contribution, which are complementary to each other. The specular part of the reflections, while playing the main role for the first orders of reflection, it rapidly decreases as the orders increase, as shown in Fig.4.5. This happens because after the first reflections, diffuse reflections progressively occur and the conversion of specular sound energy into diffuse sound is irreversible. In other words, in each reflection some of the energy of an incident sound ray is converted into non-specular sound, but reflection of non-specular energy will never result in the formation of a single sound ray.

The plots of Fig.4.5 were obtained by splitting the two components of the sound field according to the following equation (Vorländer et al., 2000):

$$E_{tot}(t) = E_{spec} + E_{refl} = E_0 \left[e^{\bar{n}[\ln(1-\alpha)(1-s)]t} + e^{\bar{n}[\ln(1-\alpha)s]t} \right] \tag{4.13}$$

where $\bar{n}$ is the total average of reflections per second and *s* is the scattering coefficient. The concept of "split" sound field can be easily understood by looking at Fig. 4.6.
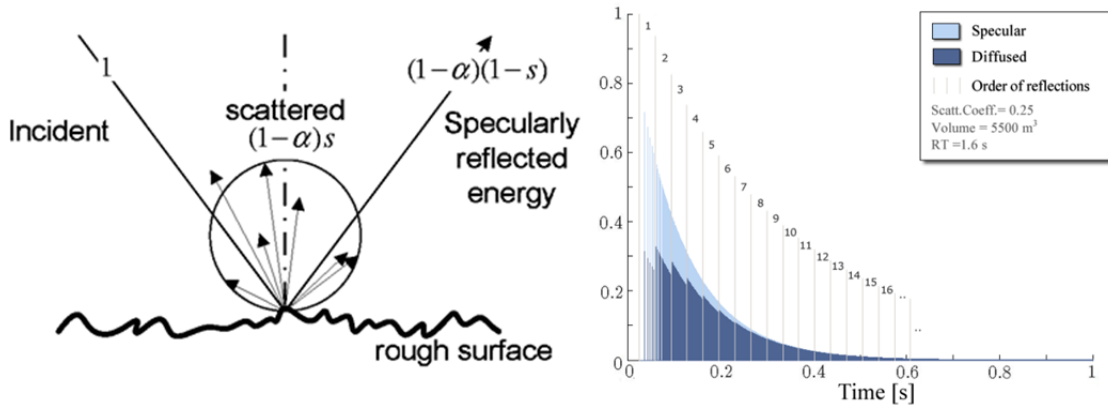
Figure 4.6 - (left) Separation of reflected Energy into scattered and specular components (after Vorländer, 2000); (right) Conversion of specularly into diffusely sound energy for each reflection and each order.

If the incident energy is normalized to 1, the total reflected sound energy would be $1 - \alpha$, where α is the absorption coefficient. The component of the sound energy that is reflected specularly will be $(1 - \alpha)(1 - s)$ and the component that is reflected non-specularly (or scattered) will be $(1 - \alpha)s$. It is useful to visualize the influence of the two different components of the field in relation to the order of reflections, as it is in fig.4.6.

In conclusion, pure image source modeling is allows to precisely determine the direct sound and the early reflections, but it does not produce satisfactory results for the late part of the impulse response. Better results can be obtained by using hybrid methods of geometrical acoustics, which means combining MSM with stochastic models for the simulation of the room's reverberant sound field.

An another approach that is worth mentioning, is the analysis method for estimating diffuseness of sound fields by measuring the time variation in reflected sound energy of impulse responses proposed by (Hanyu, 1993). In this method, a decay-cancelled impulse response is obtained by removing the reverberation decay from the impulse response using a Schroeder decay curve. The degree of diffusion of the sound field is determined by evaluating the time variation in the reflected sound energy of the decay-cancelled impulse response. In this way, the frequency characteristics of diffuseness in sound fields can be analysed from the impulse response measured at a single point, so that the average degree of diffusion in a room can also be evaluated by averaging the analysis results at several points in the room, similar to the analysis of reverberation time.

4.3   Room Acoustic Simulation Software

In recent years, room acoustic computer simulation has become more and more popular in consulting studios, thus replacing in most cases scale model experiments. Reasons for that have to be found in their user-friendly usability,

their increasing performance accuracy and their prices, which are definitely more affordable than physical models. Another benefit of acoustic software is that they optimize the workflow of architects and engineers, whom mostly develop their plans as CAD projects. This means that the transition from the planning process to the acoustic simulation is very smooth. This practice is going to be even further simplified by recent release of a framework that is directly embedded within the CAD software. This tool has been developed to enable immediate acoustic and visual feedback to the user by running interactive room acoustics simulations and auralizations in real-time (Pelzer et al., 2013).

Hereafter, three different type of simulation software will be shortly introduced, that have been used for comparison. Two of them are commercial software, namely ODEON® 10.1 and CATT-Acoustic® v 8.0, whereas the third one is a non-commercial tool called RAVEN. Although all these software involve principles of energy-based geometrical acoustics in terms of MSM and RTM, each software uses a slightly different approach for splitting the specular and diffuse components of the sound field as well as for modeling the propagation of the diffuse part.

4.3.1 RAVEN

RAVEN (Room Acoustics for Virtual Environments) is a room acoustic simulation software which was developed at the Institute of Technical Acoustics, RWTH Aachen by (Schröder, 2011) on the basis of CAESAR (Vorländer, 1989; Heinz, 1994). It provides an open and flexible real-time simulation framework that is fully integrated in the existing Virtual Reality for Scientific Technical Applications framework as a network service and it is pretty unique in the large number of simulation features. RAVEN relies on present-day knowledge of room acoustical simulation techniques and enables a physically accurate auralization of sound propagation in complex environments including important wave effects such as sound scattering, airborne sound insulation between rooms and sound diffraction.

RAVEN is based on a hybrid simulation model, which combines an Image Source method, for the realistic representation of early specular reflections, with a stochastic ray-tracing approach to model the scattered reflections, in the early and late part of the room impulse response. RAVEN can also handle sound diffraction adapting the prediction models by (Svensson, 1999) and (Stephenson, 2007). Moreover, it provides a secondary source model for sound transmission that utilizes room acoustical simulations and filter functions from interpolated spectra of transmission coefficients for rendering auralization filter networks

As for the scattering coefficient, it uses an enhanced method called Diffuse Rain (Heinz, 1993), which combines the principles of ray tracing and Radiosity (Fig.

4.7). Despite the realistic sound field rendering, not only spatially distributed and freely movable sound sources and receivers are supported at runtime but also modifications and manipulations of the environment itself. The input values for the scattering coefficients, as well as for absorption coefficient, can be specified for each one-third octave band.
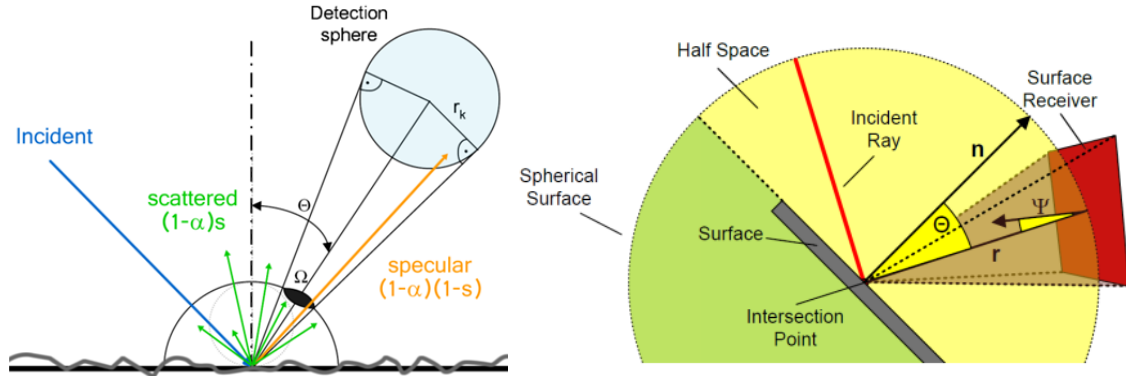
Figure 4.7 - Diffuse rain on a spherical receiver (left) and on a surface receiver (right - picture after Schröder. 2011).

The RAVEN libraries have been recently used for the development of a *SketchUp*-Plug-in, that is a fully operable real-time simulation model has been embedded directly inside an existing CAD modeler (Pelzer et al., 2013). In this way, it is possible for an architect to inspect the room acoustics already at early stages in the design process, which can avoid mistakes in a project phase where major changes are more likely to be done.

4.3.2 CATT-Acoustic

CATT-Acoustic™ is a room acoustic simulation developed by (Dalenbäck, 1995-1996) which employs a prediction method called Randomized Tail-corrected Cone-tracing, hence it combines MSM, cone-tracing and ray-tracing. The early reflection analysis (direct sound and 1st-2nd order) is performed by the MSM whereas the standard Ray-tracing is used for audience area color mapping. The 1st order diffuse reflection is handled by direct reflection from diffusing surfaces. CATT-acoustic involves a frequency-dependent diffusion treatment, which means that walls can be assigned frequency dependent absorption, surface and edge scattering, and transparency coefficients. This is achieved by separately performing ray/cone-tracing for each octave.

The first-order diffuse reflections are handled through the distribution of secondary sources over each diffusing surface, and by randomizing the direction of the reflected rays according to Lambert's distribution law. Higher order diffuse reflections are handled by randomly distributing rays that hit diffusing surfaces. Binaural post-processing with measured and analytical HRTFs as well as source directivity is also supported. The most recent version it also introduces a treatment of early diffraction using a secondary edge-source method based on a

discrete Huygens interpretation of Biot-Tolstoy. As for scattering coefficient, the input values can be specified for each octave band.
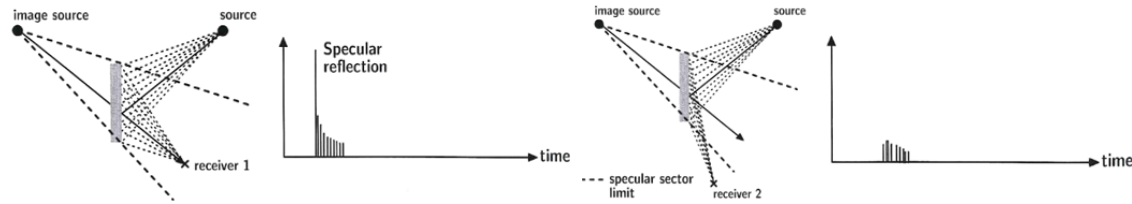
Figure 4.8 - In CATT-Acoustics every surface is divided into patches. This figures show how the first-order diffuse and specular reflections (left) and first order only diffuse reflections are obtained (after Vorländer, 2007).

4.3.3 ODEON

Odeon® 10.1 was introduced by (Naylor, 1993). It is based on a hybrid calculation algorithm, in which early reflections are calculated using a hybrid method which combines the image source method with a ray-radiosity method for reflections that occur before a specified reflection order, while later reflections are calculated using a special ray-tracing/radiosity method (Christensen, 2009). The optimal reflection order at which the model makes a transition from the early to the late method depends on the type of room.

As for scattering, Odeon considers an early and a late scattering. Each time Odeon detects an image source, an inner loop of (scatter) rays is started, taking care of the scattered sound which is reflected from this image source /surface. For instance, if all scattering coefficients in a room is 0.3, then the specular energy of a first order MSM is multiplied (1-0.3) and the specular energy of a second order MSM is multiplied by (1-0.5) x (1-0.5). The scattering rays handle the rest of the energy. During the late ray-tracing phase, small secondary sources, which radiate energy locally from the surfaces according to a frequency-dependent directionality, are generated at the point of incidence. The secondary sources may have a Lambert, Lambert oblique or Uniform directivity, depending on the properties of the reflection and the calculation settings (Fig: 4.9).

Odeon uses also a vector-based scattering: the direction of a reflected ray is calculated by adding the specular vector scaled by a factor (1 - *s*) to a scattered vector, which has been scaled by a factor *s*. Diffraction is accounted through a method called reflection-based scattering, which combines the surface roughness scattering coefficient with the scattering coefficient due to diffraction that is calculated individually for each reflection as calculations take place.

In Odeon, specific measured scattering coefficient frequency functions have been adopted to expand a mid-frequency scattering coefficient input to any frequency band. Once a user specifies one input value for the scattering coefficients for a certain surface at the mid-frequency (707 Hz), which is approximately an average

value of 500-1000 Hz bands, the single input value is expanded into values of the coefficient for each octave band using interpolation or extrapolation.

Figure 4.9 - (left) Vector based scattering as implemented by Odeon: reflecting a surface with a scattering coefficient of 0.5 results in a reflected direction which is the geometrical average of the specular direction and a random scattered direction; (right) Oblique Lambert approach produces a shadow zone (no sound is reflected), which is small for high scattering values (after Christensen, 2009).

4.4   Case Study: RWTH Seminar Room 4G

It has been shown how geometric models, which do not attempt to predict the effects of surface and edge scattering, are liable to produce inaccurate results (Vorländer, 1995). Even though nowadays every software accounts for diffuse reflections, there is a lack of scattering coefficient data, both for ordinary surfaces and for commonly used furniture. This circumstance limits to a certain extent their practical application. In order to bridge this gap, several measurements of typical furniture have been performed in the past (Vitale et al., 2009).

Hereafter a case study will be presented for improving the accuracy of room acoustics computer simulations by quantifying the influence of typical furniture in ordinary classrooms, such as chairs and desks, on the sound field reflections in terms of scattering. The scattering coefficient of several objects has been measured in a scaled reverberation chamber. Afterwards, acoustical measurements in a real furnished classroom have been carried out and compared with room acoustics simulation results. Results will show how the accuracy of the simulation improves as a consequence of measured scattering coefficient data.

4.4.1 Measurement Set-up

Measurements of scattering coefficient have been performed in the old scale model reverberation chamber at the Institute of Technical Acoustics, RWTH Aachen. The diffusion in this room has been improved by using three PVC diffusers hanging on the ceiling. Measurement devices include a turntable with a flat base, two sound sources (a cylindrical loudspeaker for low frequencies and a piezoelectric dodecahedron for high frequencies) covering an overall frequency range of 1-80 kHz, two ¼" precision microphones and an audio interface with 192

kHz sampling frequency. A sweep was used as test signal and 72 measurements (with 5° turntable angular steps) for three different source-receiver positions were performed.

4.4.2 In Situ Measurements

Measurements of a common classroom have been carried out in the seminar room 4G at RWTH Aachen University. This room has an approximate square shaped footprint with a surface area of 510 m² and volume of 520 m³. It contains 60 chairs and 30 desks, which constitute the main scattering area together with the ceiling. Seven microphone positions located in between the last two desks rows have been chosen. A 3-way loudspeaker featuring mid- and high-frequency dodecahedrons, located approximately on the teacher desk position, was used as sound source. The measured reverberation time was 0.8 s.

Figure 4.10 - In-situ measurement location: seminar room 4G at RWTH Aachen University (Germany)

4.4.3 Simulation

An acoustic simulation of the unoccupied lecture room has been executed with the hybrid room acoustics simulation software RAVEN (see par.4.3.1). The simulation model consisted of 147 polygons, 28 planes, a fourth-order image source setup and ray tracing using 30.000 particles for each frequency band. The source-receiver combination reflects the one used in the measurement setup. Fig.4.13 shows a screenshot of the CAD model as well as a view of the running simulation. The yellow area represents the surface occupied by chairs and tables and it has been modeled by applying the scattering coefficient data as measured

in the third scale model configuration (see Fig. 4.11c). In order to evaluate the effects of the scattering coefficient, two different tests were done, once using the measured scattering coefficient values and once using no scattering.
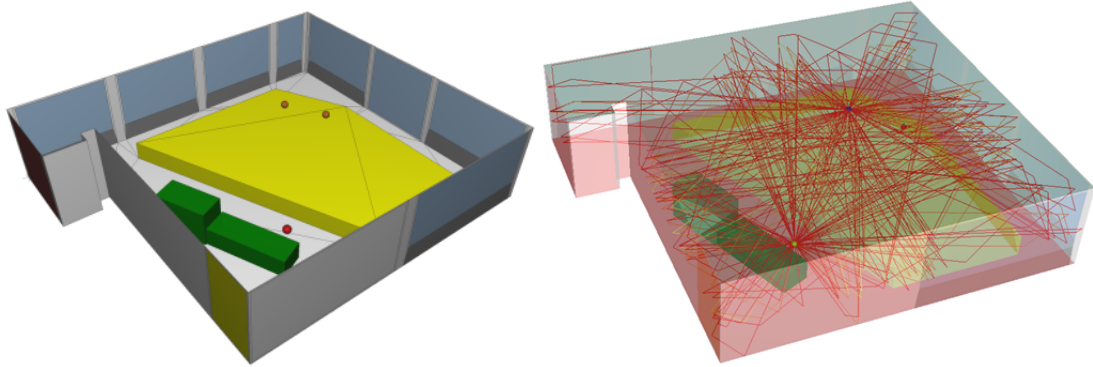
Figure 4.11 - Lecture room plan with one source and two receivers (left) and running simulation (right)

4.4.4 Results and Conclusions

The effect of the scattering coefficient on the simulation precision has been estimated by comparing the decay curves, as obtained from the measured and simulated impulse response. In Fig.4.14 three different set of decay curves are depicted: measured, simulated with measured scattering and simulated with no scattering.
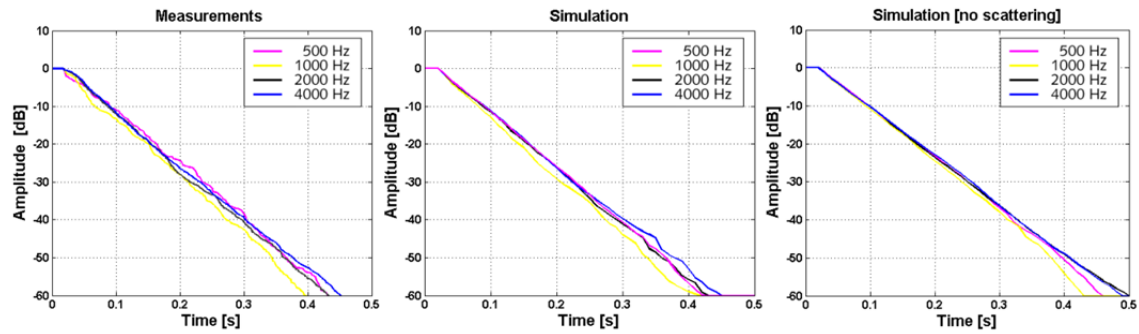
Figure 4.12 - Decay curves obtained from measurements (left), simulation with (middle) and without scattering coefficient (right).

Except for some ripples, decay curves of the first two plots exhibit high similarities in each frequency band. If overlapped, the curves have an almost identical slope. On the contrary, the slope of simulated decay curves without scattering show pronounced divergences with respect to the other plots. Differences are proportional to the scattering coefficient increment.

The improvements achieved by using in-situ measured scattering coefficient in the computer simulation can be better represented by means of error plots of the decay curves (Fig.4.15): they show a major reduction of the error that ranges between $0.5 \div 6$ dB.

It is possible to conclude that the use of measured values of scattered coefficient in the computer simulation improved significantly the precision of the results, thus confirming the importance of using proper values for scattering surfaces. A better prediction of the room behavior, as well as the estimation of relevant acoustic descriptors for room acoustics (i.e. STI in classrooms), may be achieved by extending the use of measured scattering coefficients to all the scattering surfaces present in the simulated room
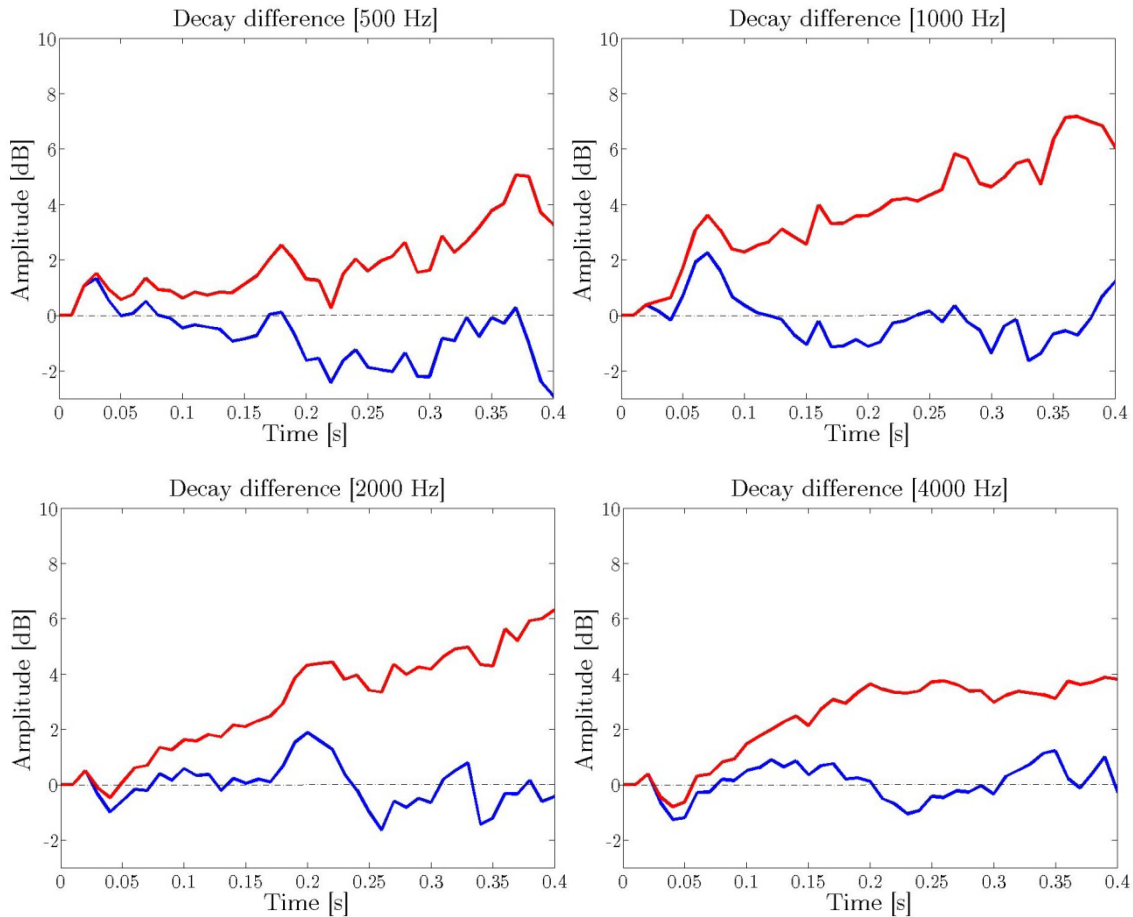
Figure 4.13 - Decay curve error plots: red lines represent the difference between the measured decay curves and the computer simulation without proper values of scattering coefficients, whreas blue curves represent the difference between the measured decay curves and the computer simulation with measured scattering coefficients.

5 Detecting Difference, Similarity and Threshold of Scattering Coefficient

The comprehension of the relationship between physical magnitudes of sound fields and magnitudes of the correlated hearing sensations has become a priority in room and virtual acoustics. There are physical phenomena that present substantial objective differences, which sometimes are not evident in the subjective domain. The knowledge of the human perception related to specific acoustic parameters in room acoustics allows to reduce the degrees of freedom of problems and to optimize the acoustical design of concert halls.

A vocabulary to describe the subjective acoustic impression is an on-going open project in the acoustical community: subjective acoustic parameters are being isolated if they are valid to most people's listening experience; thereafter, an attempt to deduce those properties from the sound fields that are responsible for our experience of each of the subjective aspects is carried out. Eventually, a set of objective and measurable parameters that correlate well with the subjective parameters is defined (Gade, 2007). In this way, an acoustician can be able to guide the architect during his planning process. For this purpose, we shall find out which aspects of the design govern the important objective and in turn the subjective parameters.

The investigation of the influence of scattering coefficient on human perception belongs to this process. We are interested in understanding the auditory sensations related to variations of the scattering coefficient. In particular, given a listener inside a concert hall, there are three specific questions that we want to answer to:

- Is it possible to detect a differential threshold of perception for scattering coefficient?
- If a wall surface with a scattering coefficient s_1 is replaced with another surface with scattering coefficient $s_2 \neq s_1$, would the listener be able to perceive any difference?
- If a difference is perceived, would that be enough for the listener to consider the surfaces as being similar (hence interchangeable) or not?

There are several sensory evaluation methods in psychophysics and psychoacoustics that help answering to these questions (Fastl et al., 2007). In the actual case, each of these questions can be attributed to specific methodological approaches, which are *threshold, difference* and *similarity* testing respectively.

This chapter discusses the concepts behind sensory evaluation techniques with reference to their statistical framework. Methods for determining threshold, difference and similarity of scattering coefficient based on forced choice listening tests (triangle test and 3-Alternative Forced Choice) are illustrated.

5.1   Perception of Scattering Coefficient

In the present work, two acoustical scenarios will be investigated: a *simulated concert hall*, where it is possible to produce multiple artificial stimuli at desired specifications (i.e. assigning any value of scattering coefficient to the surfaces), and a *real concert hall*, where only a limited set of existing surfaces (hence, of scattering coefficient) can be assigned. In the first case, several acoustically simulated BRIR evaluated at various scattering coefficients (0.1, 0.3, 0.5, 0.7, 0.8) with a reference simulated BRIR (anchor value of 0.9) will be compared; afterwards, it will be investigate if listeners can perceive any difference between them. In the second case, a BRIR in a concert hall for each of the three different configurations will be measured (i.e. scattering coefficient of 0.01, 0.25, 0.58) and it will be investigated, whether listeners can perceive any difference between them.

These two scenarios can be translated in psychophysical terms into two kinds of measurements, which we are going to perform: a *sensory discrimination* test (absolute threshold) test and a *difference threshold* test. These tests are very much related, in fact the absolute threshold can be considered as a special case of a difference threshold. The main difference between them is that the absolute discrimination protocol uses a series of controlled stimuli to determine a psychophysical threshold, whereas the discrimination test has only two samples, whose deemed difference is based on a criterion of statistical difference. Both tests will be introduced and analyzed in details in the following sections, whereas their actual execution in the case of a simulated concert hall and a real concert hall will be presented in chapter 6 and 7 respectively.

5.2   Sensory Evaluation Methods

Understanding the psychology and physiology principles of human behaviors has been the main target of the field of sensory evaluation, which observes how senses (vision, hearing, taste, smell and touch) measure and perceive the characteristics of products, materials and quantities. This discipline is mainly focused on the output of these observations: the human responses in terms of appearance, sound, tastes, smells and texture properties. One of the first relevant field of study and application of sensory evaluation techniques has been the budding industries of foods, beverages and cosmetics first in the early 1900s. Statistical methods and

techniques have been developed to serve mainly economic interests, since sensory testing was able to establish the worth of goods and products as well as their very acceptability. Sensory evaluation methods were also found to be properly adequate for other fields, such as medicine (diagnosis of illness or effect of drugs), quality control and product development and more widely in scientific research. Psychoacoustics it is not an exception: most of the techniques and protocols developed in sensory evaluation techniques are suitable to investigate problems related to sound quality and have served as such for many decades so far (Civille et al., 2003).

The open problems discussed in this work refer to the perception of scattering coefficient in concert halls. In a specific attempt to answer to the questions formulated at the beginning of this chapter, two scenarios have been investigated: a few BRIRs obtained through a measurement campaign conducted inside the ESPRO at the IRCAM (Institut de Recherche et Coordination Acoustique/Musique) and multiple simulated BRIRs from Konzerthaus Dortmund. The target is to understand whether audience can perceive differences once the scattering coefficient of the wall has been changed. Given two different audio samples, the empirical question would be: does a sensory difference exist between the samples? Considering the current scenarios, two methodologies will be used: a unified difference-similarity approach for determining difference by means of a triangular testing and a sensory discrimination test for determining a just noticeable difference by means of a 3-Alternative Forced Choice. The following sections will introduce the theory behind these sensory evaluation techniques, as well a specific in-depth analysis of the testing methods.

5.3   Determining Threshold

A sensory threshold is a point of discontinuity, a limit of sensory capacities. This concept has been introduced in psychophysics for describing the condition under which a stimulus, if less intense than sensory threshold, will not elicit any perceivable sensation. Measurements of thresholds are very labor intensive as they usually require several trials with many panelists. Moreover, a threshold represents only one point on a psychometric function, so it will provide very little information about the dynamic characteristics of sensory response respect to the stimulus variation. Nevertheless, there are still many relevant implications related to the assessment of a threshold that largely justify the investigation effort.

Three types of thresholds have been defined: the *absolute threshold* (or detection threshold) is the lowest physical energy level of a stimulus that is perceivable (Lawless et al., 2010); the *recognition threshold* is the minimum level of a stimulus at which the specific stimulus can be recognized and identified; the *difference threshold* is the extent of change in the stimulus necessary to produce a

noticeable difference (Meilgaard et al., 2007). The latter is the type of threshold that we are willing to detect in reference to the scattering coefficient in the simulated concert hall.

The difference threshold is determined by presenting a standard stimulus, which is then compared to a variable stimulus. The standard stimulus is usually selected as a limit value (the lowest or the highest) and is often indicated as *anchor* value. The difference threshold is called *just noticeable difference* (JND) if it is determined by changing the variable stimulus by small amounts above and below the standard until the assessor notices a difference.

5.3.1 The Psychometric Function

The main problem related to the determination of a threshold is that there is variability in the point at which observers change their response, even within a single individual. The probabilistic nature of detection was observed by (Urban, 2010) who called the probability function for detection as *psychometric function.* Among the methods used for threshold determination, the one of constant stimuli will be used for detecting the difference threshold for scattering coefficient in simulated concert halls (see Ch.6). This method involves the presentation of various stimulus levels to the subject in random order, that is the stimuli are not presented in an ascending or descending manner (Gelfand, 2010). The norm ISO-13301 suggests to use the 3-AFC as a sample presentation method for detecting a threshold: a panelist receives three samples simultaneously and is asked to indicate the difference one.

The psychometric function for a 3-AFC test can be obtained as follows. Let's assume two stimuli of a 3-AFC protocol with the following distributions:

$$A \approx N(0,1) \qquad B \approx N(\delta,1) \tag{5.1}$$

In the 3-AFC protocol samples a_1, a_2 and b are presented; a correct answer follows if b is correctly identified, which happens if $a_1 < b$ and $a_2 < b$. The probability of a correct p_c answer can be written as:

$$p_c = P(A_1 < B, \quad A_2 < B) \tag{5.2}$$

By using the identity for marginal probability density functions, it follows that:

$$p_c = \int_{-\infty}^{\infty} P(A < z)P(A_2 < B)P(B = z)dz = \int_{-\infty}^{\infty} \Phi(z)^2 \phi(z - \delta)dz \tag{5.3}$$

where ϕ is the standard normal probability density function, Φ is the standard normal cumulative distribution function and δ is the Thurstonian measure of sensory difference (see Par.5.4). Listening test for determining threshold of scattering coefficient in a simulated concert hall will be presented in Ch.6. Results from listening tests will be used as input for evaluating psychometric functions, so

that the observer's ability to detect a stimulus can be obtained. An example of evaluated psychometric function is given in Fig.5.1.
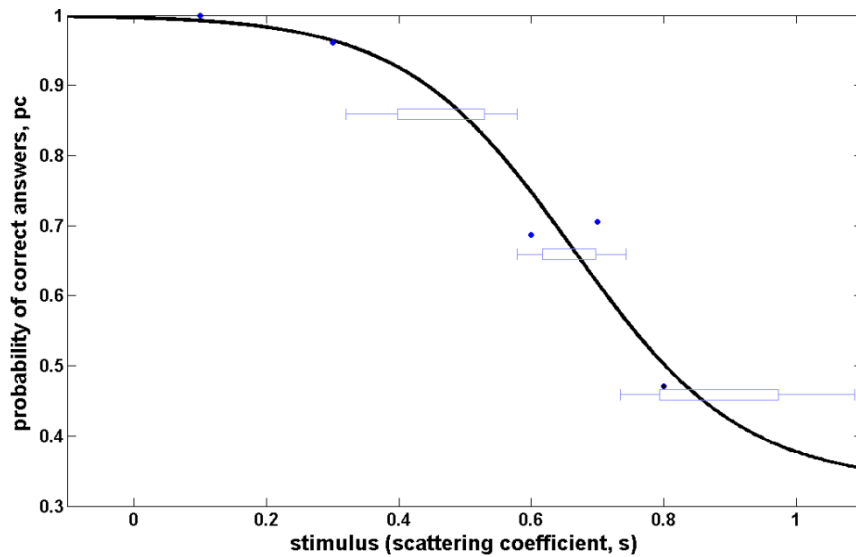
Figure 5.1 - Psychometric function showing the probability of correct responses corresponding to the variation of scattering coefficient in a 3-AFC test.

5.4   Determining Difference and Similarity

A common problem in sensory evaluation technique deals with the detection of differences, that is to find out whether a perceptible sensory difference between samples of two products or entities exists. The bases for sensitivity measurements in psychophysics are discrimination tests because they allow to distinguish between confusable stimuli. It is important to mention that in psychophysics the confusable stimuli can be two similar, yet different intensities of a stimulus or they can be the presence or absence of a lower intensity (O'Mahoney et al., 2002). There are a number of different discrimination tests available, such as the triangle, duo-trio, *n*-AFC (alterative forced choice) or paired comparison tests. Most of these sensory discrimination tests take the form of forced-choice tasks, which means that assessors are forced to respond to only one attribute at a time, they are not allowed to have ties in the ranking: they have to select one single sample.

The triangle test (Peryam et al., 1950; ISO 4120:2004) is a triadic test: three blind stimuli are presented to a panelist, two of which are the same and one slightly different. The panelist is required to select the odd or different sample, even if the selection is based only on a guess. Another triadic test is the 3-AFC, or 3-Alternative Forced Choice test (Green at al., 1966), which is like a triangle test except the instructions specify the nature of the difference. For this reason, this kind of protocol is called directional while the triangle test is not directional. Both protocols are without response bias since no response can be consistently preferred over another without affective the discriminative effect (Christensen,

2013). There are two main models to interpret the results of a triadic test and summarize the sensory distance: a discriminator (or guessing) model or a sensory detection approach based on Thurstonian modelling.

5.4.1 Statistical Hypothesis Testing

Statistical decisions about test outcomes are usually taken by means of hypothesis testing (Meilgaard et al., 2007), which consists in (a) stating the null hypothesis H_0 and the alternative hypothesis H_a, (b) calculating the value of the statistic used to estimate the parameter of interest and (c) computing the probability that the statistic takes on this value, based on the assumed probability distribution of the measurements and H_0.

A statistical hypothesis defines the value of some parameter in a probability distribution (the mean μ or the population proportion p). For discrimination tests, the null hypothesis H_0 states that the two samples do not differ whereas the alternative hypothesis H_a states that they do. In symbols (Schlich, 1993):

$$H_0 : p_c \leq p_g \qquad H_a : p_c > p_g \tag{5.4}$$

where p_g is the guessing probability (or chance percent correct) and p_c the probability of correct answers (alternative hypothesis percent correct). It is assumed that the random variable x follows a binomial distribution $B(n, p_c)$, where n is the total number of responses (or of subjects when no repetitions are considered). The minimum number of correct responses required for rejecting H_0 is usually called the rule of decision.

Figure 5.2 - Overview of risks and cases in a statistical test. Given a null and an alternative hypothesis, an assessor can respond correctly (accept H_0 when is true and reject it when is false) or incorrectly (reject H_0 when is true with α-risk a or accepting H_0 when it is false with a β-risk).

There are two possible conclusions in testing statistical hypothesis: correct or incorrect. Fig.5.2 shows the ways in which each conclusion can be drawn. There are two ways in which an incorrect conclusion may be drawn:

- H_0 is rejected when, in fact, it is true; that is a difference exists when it does not (type I error);
- H_0 is accepted when, in fact, it is false; that is no difference exists when it does (type II error).

The probabilities of making type-I and type-II error are indicated by α and β respectively and are usually specified before the experiment is conducted. Type-I error (sometimes called false alarm) is commonly set low in order to avoid declaring the samples different when actually they are not. Typical values for α are 5% or 1%, thus providing the typical cutoffs in statistical significance testing as 0.05 or 0.01.

The probability of finding a true difference is characterized by the complementary value of type-II error (1- β) and goes under the name of power of the statistical test. In other words, it is the probability to observe a difference that is actually there.

5.5 Guessing Model

This method is based on two main assumptions:

- there are two kinds of participants during a sensory test: discriminators (who perceive the true difference and select the correct odd sample) and non-discriminators, who perceive no difference and guess;
- Non-discriminators include people who guess both correctly and incorrectly. In other words, a given assessor could be both a discriminator and a non-discriminator.

As clearly stated by Lawless, this model "estimates the most likely proportion of people who are momentarily in a discriminating state, thus answer correctly, as opposed to those who might be answering correctly by chance" (Lawless et al., 1998). Based on these assumptions, the sensory distance between samples can be expressed in terms of the proportion of discriminators, p_d, and it can be calculated through an adaptation of Abbott's formula by the following equation (Schlich, 1993):

$$p_d = \frac{p_c - p_g}{1 - p_g} \tag{5.5}$$

where p_c is the probability of correct answers and the guessing probability p_g is 1/3 for the triangle and 3-AFC protocols. Schlich points out that p_d can be also considered as the effect size ($\Delta = p_c - p_g$) and suggests three reference values: 25%

is a small difference (small effect above chance), 37.5% is a medium difference and 50% is a large difference.

If no hypothesis is formulated about the sample that should be preferred, the protocol is considered as two-tailed: this is the case of the triangle test.

Conclusion by (Schlich, 1993), (MacRae, 1995) and (Carr, 1995) led to idea of using a unified approach to detect difference and similarity in discrimination tests. Given two samples, there are two possible targets in a difference test: to determine if two samples are perceptibly different or to determine if they are sufficiently similar to be used interchangeably. Depending on the research objectives, it is possible to use this unified approach for handling both problems by an appropriate selection for the test-sensitivity parameters by α, β and p_d. The basic idea is that in testing for difference the proportion of correct answers p_c is compared with the chance performance level p_g, whereas in testing for similarity the proportion of discriminators p_d is compared to some higher level of expected proportion correct. If p_c is equal or greater than a specific value reported in comparison tables (see Table A1 in ISO 4120:2004) a perceptible difference exits; if p_c is less than or equal to reference values (see Table A2 in ISO 4120:2004), than no meaningful difference exists between the samples.

The unified approach expands the use of Abbott's formula by including equations for calculating the confidence interval on the proportion of the population that can distinguish samples, p_d.

5.5.1 Confidence Intervals

A confidence interval provides an interval in which a parameter lies with a known probability and it can be calculated through the standard error s_d as follows:

$$C_i : p_d \pm z \cdot s_d = [1.5 p_c - 0.5] \pm z \cdot \sqrt{\frac{p_c (1 - p_c)}{n}} \tag{5.6}$$

where the proportion correct is $p_c = c/n$ (c is the number of correct responses, n is the total number of assessors) and z is the normal deviate for a desired level of confidence. In case a difference confidence level for α, β is selected, a critical value of the standard normal distribution for each needs to be considered as follows:

$$C_\alpha^{lower} : p_d - z_\alpha \cdot s_d \quad C_\beta^{upper} : p_d + z_\beta \cdot s_d \tag{5.7}$$

where C_β^{upper} is the upper confidence limit with a z_β confidence interval and C_α^{lower} is the lower confidence limit with a z_α confidence interval on the proportion of distinguishers. The confidence intervals allow determining how strong the evidence of similarity is. If the calculated value is less than the acceptable limits, then a statistically significant similarity can be assessed.

The guessing model presents a few drawbacks, one of most relevant being that the proportion of detectors seems to be not a good indicator of the sensory differences between samples because it is highly dependent on the discrimination protocol through the guessing probability p_g (Ellis, 1993). For example, $p_d = 0.2$ corresponds to a proportion of correct responses pc = 0.6 for the 2-AFC and the duo-trio methods; $p_c = 0.4667$ for the 3-AFC and the triangle methods. For this reason another model based on the Thurstonian scaling has been introduced.

5.6   Thurstonian Model and *d'*

Human behavior has a complexity in sensory assessment that is not properly represented by the guessing model. A more elaborate model based on the Thurstonian scaling has been developed (Thurstone, L.L., 1927) that considers two assumptions:

- sensory perception probability follows a normal probability rule;
- assessors can faithfully execute the decision rule associated with the sensory task they are performing.

The basic idea behind this model is that sensory perceptions vary each time an assessor performs a sample evaluation, which happens both because of psychological effects and of lack of homogeneity in the samples. The Thurstonian model is an improvement with respect to the guessing model since it accounts for the difference in inherent variability. Stimuli variations are based on normal probability distributions that are represented on a sensory magnitude continuum. Each sample distribution has a different average magnitude, which means that they are displaced over the sensory axes. The judgment of assessors is related to the distance of the mean values: if two samples have very different average sensory magnitude, their distributions will not overlap and assessors will clearly perceive a difference. However, assessors may confuse the samples in case their distribution overlap, thus reflecting a small difference between them.

The fundamental measure of sensory difference in this model is δ, which is defined as the difference between the means of the intensity distributions for two samples measured in perceptual standard deviations. When an experiment is performed, only an estimation of the population difference in terms of δ is obtained: this estimate is called *d'*. Conceptually, the estimate corresponds to the difference between an intensity value from one distribution and an intensity value from the other distribution. The more data are collected, the more likely are the values to be closer to the actual mean of each distribution (Bi et al., 1997). An important aspect to be mentioned is that different tests may have the same guessing probability level, but some protocols are more difficult than others, which means that a bigger sensory difference is required to obtain the same number of correct

judges. For instance, both the triangular method and 3-AFC method require choices among three samples.
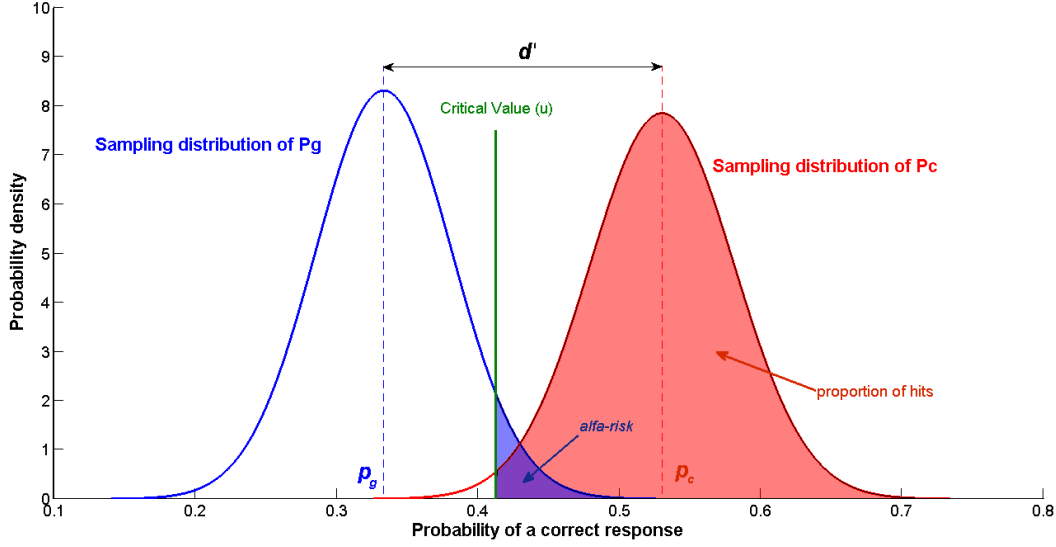
Figure 5.3 - Normal approximation to the distribution of the probability of guessing p_g (left) and of a correct response p_c (right). The difference between the means under the null and alternative hypotheses is represented by d'. The blue curve has been calculated for n=96, p_g =1/3 and d'=0 while the red curve is relative to n=96, p_c =0.53 and d'=1.62. The critical value u is the cutoff value for the upper 5% of the tail of the p_g distribution.

A signal strength of *d'*=2 means that the respective sampling distribution p_c increases the input level to the brain by an amount that is twice the standard deviation of the variation in the sampling distribution of pg. If one refers to the principal concept behind signal detection theory, which is that the sensory system has a variable background noise that is perturbed by a signal sent from the sensory organs, it can be concluded that *d'* is a signal to noise ratio respect to the brain (O'Mahoney, 1992).

The relation between the probability of a correct response pc and *d'* is given by the psychometric function, which varies for each discrimination protocol. For the triangular method, this mapping is given by (David, H. A. et al., 1962):

$$p_c = f_{ps}(d') = 2 \cdot \int_0^\infty \left\{ \Phi\left[-z\sqrt{3} + d'\sqrt{2/3}\right] + \Phi\left[-z\sqrt{3} + d'\sqrt{2/3}\right]\right\} \cdot \phi(z)\, dz \qquad (5.8)$$

where ϕ is the standard normal probability density function and Φ is the standard normal cumulative distribution function. The solutions to this equation can be found in (Ennis, 1993), where a table reporting the relationship between pc and d' is given.

Since the evaluation of *d'* is not enough to obtain inference in discrimination test, other parameters need to be calculated, such as variance of *d'*, confidence intervals, critical point and power. An overview about the estimation of these values based on (Ellis, 1993) and (Bi et al., 1997) follows.

5.6.1 Variance and Standard Deviation of *d'*

The standard error of *d'* can be calculated as follows (Christensen, 2013):

$$se(d') = \frac{se(p_c)}{f'_{ps}(d')} = \frac{\sqrt{p_c(1-p_c)/n}}{f'_{ps}(d')} \tag{5.9}$$

where $f'_{ps}(d')$ is the derivative of the psychometric function with respect to *d'*. The variance is obtained by my means of the *B*-value, which is a transformed Z-value for the calculation of conditional power. *B* values for the triangular test are given by (Bi et al., 1997) together with the following equation to evaluate the variance of *d'*:

$$d^{\#}_{var} = \frac{B}{N} \tag{5.10}$$

Thus the variance gets smaller as the sample size increases.

5.6.2 Confidence Intervals

Confidence intervals are used in difference and similarity testing in order to accept or reject the alternative hypothesis. Similarly to the case of guessing model, here we have:

$$C^{lower}_{\alpha} : d' - z_{\alpha} \cdot se(d') \qquad C^{upper}_{\beta} : d' - z_{\beta} \cdot se(d') \tag{5.11}$$

where C^{upper}_{β} is the upper confidence limit with a z_{β} confidence interval and C^{lower}_{α} is the lower confidence limit with a z_{α} confidence interval on the proportion of correct answer.

5.6.3 Critical Point

The critical point is that point above which the area under the normal distribution of sample p_c with mean $1/m$ and standard deviation $s_d = \sqrt{m-1}/(m\sqrt{n})$ is α ($m = 3$ for a triangular test). By using the inverse of the cumulative distribution function Φ^{-1}, the critical point can be obtained as follows:

$$u = \frac{1}{m} + \Phi^{-1}\left[\frac{(1-\alpha)\sqrt{m-1}}{m \cdot \sqrt{n}}\right] \tag{5.12}$$

The critical point can be the critical value is the smallest number of correct answers that renders the test significant.

5.6.4 Power

(Ellis, 1993) defines power as the probability that the null hypothesis will be rejected when the null hypothesis is false and a particular sample size and type-I

error probability (α) has been specified. With reference to the sampling distribution of pc values and the case of a triangular test, power is the probability that a p_c value from this distribution will exceed the critical value u, that is:

$$power = 1 - \Phi\left[\frac{\sqrt{n} \cdot u - \sqrt{n} \cdot f(\delta)}{\sqrt{f(\delta)[1 - f(\delta)]}}\right] \tag{5.13}$$

where $f(\delta)$ is the psychometric function.

5.7 On the Choice of the Triangular Test for In-situ Scattering Coefficient

Triangular testing is a demanding and difficult discrimination technique mainly because judges are not informed about the nature of the differences between stimuli. It was found that just by giving a few hints about the typology of the differences involved (thus switching from a triangle to a 3-AFC protocol) performances improved significantly. This phenomenon, first noticed by (Byer et al., 1953) and later called the paradox of discriminatory nondiscriminators (Gridgeman, 1970), was explained by (Frijters, 1979) by means of the Thurstonian model: Frijters showed that rather than a paradox, the differences in performance was due to the diverse cognitive strategies for the triangle and 3-AFC test. These strategies, namely the *comparison of distances* and the *skimming strategy*, go under the name *decision rules* and are very well explained in (O'Mahoney, 1995). An example for the decision rule for a triangle test is shown in the next figure: the assessor selects the b sample because perceptually it farther from both of the a samples than the a samples are from each other: the answer is correct. In a second trial, he selects a_1 because it is farther from the a_2 and b sample than the a_2 sample and the b samples are from each other: the answer is incorrect.
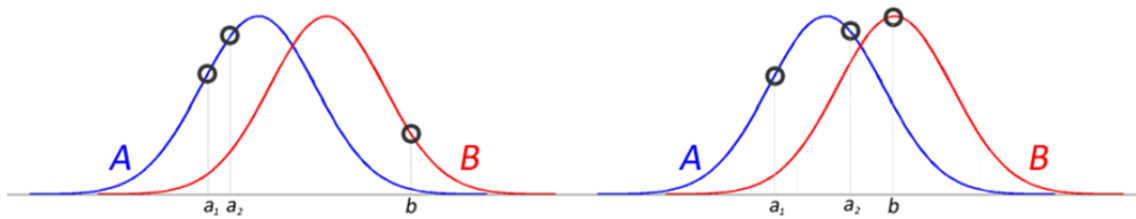
Figure 5.4 - Decision rule in a triangular test: (left) assessor select b because is the farther away, hence he answers correctly; (right) assessor select a_1 because is the farther away, hence he answers incorrectly.

The decision rule for a triangle test can be written in terms of probability of correct answers as follows (Meilgaard et al., 2007):

$$P_c = P\left(\left|a_1 - a_2\right| < \left|a_1 - b\right| \ and \ \left|a_1 - a_2\right| < \left|a_2 - b\right|\right) \tag{5.14}$$

It was also shown that triangular testing requires a pretty high number of subjects in order to assess a significance difference, that is many assessors are needed in order to increase the power of the test (Ennis, 1993). For these reasons, the triangular method should actually only be used when differences are obvious.

In the in situ scattering coefficient investigation carried out in this work, this was not case. A pre-analysis phase of the auralized binaural impulse responses from ESPRO at IRCAM surprisingly revealed that the perceptible differences between different configurations were very little. Even comparisons between the two most distant cases, which is reverberant walls against the scattering walls (Par.7.4), showed a high degree of similarity. This circumstance confirmed that the choice of a triangular testing method would have been risky because, given the difficulty of the task, results might have been compromised.

However, the main goal of this listening test was specifically to understand if common listeners, without any kind of hint or advice, would have been able to detect a perceivable difference in the samples. Moreover, even though previous listening test in simulated circumstances identified coloration as a possible affected quantity (Torres et al., 2000), it was not sure that, in real measurements, coloration was the same or only magnitude to be involved. In other words, considering both (a) the consciousness that the psychoacoustic quantities affected by scattering coefficient in situ are not known and (b) the potential consequence that listeners could have been informed with inexact details, lead to the choice of a triangular protocol.

In order to minimize this error, four repetitions for each configuration comparison were introduced, so that the number of trials increased to a number that would have guaranteed a higher testing power. In particular, a total number of trials of 96 were obtained (26 participants x four repetitions), thus achieving a 90% of power at $\alpha = 0.05$ for estimating a $d' > 1.3$ (see Table 6 in Ellis, 1993). It follows that one would be 90% sure to detect a difference in d' higher than 1.3 at a level of confidence of 95%, which is equivalent to state that for $d'=1.3$ a judge is most likely to get 90% of the triangular test correct. This can be considered as a fair and reasonable compromise.

5.8 Physiological Response to Scattering Coefficient

One of the main aims of psychophysics, and consequently of psychoacoustics, is to detect the physiological response to a physical stimulus. For instance, loudness is the sensory perception related to intensity, pitch is the sensory perception related to frequency. What is the sensory perception related to scattering coefficient? This is a difficult question to answer because there is not an obvious cause-effect phenomenon. If sound intensity is increased, then an increase in the loudness is perceived; if the frequency increases, then the pitch gets higher. If the scattering

coefficient increases, none of these happens. A change in scattering coefficient affects primarily the frequency spectrum of sounds in a way that changes according to the specific texture of the surface (see Par.6.2.1).

Two surfaces might have an identical scattering coefficient, but their way to affect the sound might be different. We can think of it as the case of two musical instruments, which are built with exactly the same materials, by the same manufacturer, under the same conditions. Even though they would sound very similar, a professional musician would most probably be able to detect a difference in their "character". Previous studies have shown that, among the possible perceptual correlates, the scattering coefficient might be related to *spaciousness* and *coloration* (Torres et al., 2000; Vitale et al., 2011). This makes sense if one considers the physical meaning of scattering, which ultimately spreads or redirects reflections of a sound field. The question would be whether the spatial component (time domain) has a stronger effect than the spectral one (frequency domain) on a sensory level. In this concern, it has been shown that a variation in scattering coefficient affects the spectral components, hence the coloration, more than the spaciousness (Torres et al., 2000; Vitale et al., 2011). It can be argued that a higher scattering "soften" the sound, it blurs most of the frequency components, particularly the mid-high range. Two terms from the visual domain could be borrowed to affirm that the lower the scattering, the sharper the sound, whereas the higher the scattering, the more blurry the sound. There is not an absolute better in *sharpness* or *blurriness*; they are two tendencies of sound that might be more appropriate to some music repertoires rather than others. However, it must be stressed that these effects are really fine and subtle: only a very trained and competent listener would be able to detect a difference.

The next chapters will show how these conclusions have been gathered by a detailed psychoacoustic investigation both of a simulated and a real concert hall.

6 Perception of Scattering in Auralized Concert Halls

The first studies on subjective impression of listeners in concert halls have appeared in the early 60s; since then, they have constantly increased. It is not surprising that the interest of researchers strongly moved towards the understanding of relations between objective and subjective parameters. A common reason for that is the need to support architects and engineers during the planning stages of new concert halls, where a clear statement between acoustic measurements and human perception is necessary. Unfortunately, it was already shown that it is very difficult to find a direct connection between architectural planning criteria, objective acoustical descriptors and subjective response from listeners.

The perception of diffusion is an aspect, which has been rarely analyzed. A relevant study on diffusion and perception was performed by (Torres et al., 2000), who auralized a few samples with binaural impulse responses, as obtained from a simulated concert hall. In this study, the sidewalls were characterized with a frequency dependent scattering coefficient by means of a step function going from 10% to 60% of scattering, which was used for three different frequency ranges. Results showed that perceived differences were strongly depending on the input signals. Moreover, the differences were described by the listener as related to the coloration and the spaciousness of the perceived sound.

A more recent study by (Jeong et al., 2013) investigated the subjective effect of the scattering coefficient on the audience using a scale model of a small performance hall, where simple periodic diffusers were considered. It was found that the presence of sidewall diffusers had an influence over the perceived loudness, spaciousness and reverberance. Further contributions in the same direction have recently been provided by (Shtrepi et al., 2013; Shtrepi et al., 2014), who also investigated the relationship between scattering coefficient and acoustical objective parameters.

It has been shown how computer software for room acoustic simulation have implemented sound scattering for improving the accuracy of results (see Ch.4). Sound scattering is controlled in terms of scattering coefficient, which quantifies the amount of the sound field scattered in all directions expect for the specular one. Although the enhancement of the simulation performances due to the implementation of scattering has been proven, no information is available about

the influence of scattering variations on auditory perception. In other words, if the scattering coefficient in the computer simulation assumes different values, would listeners be available to detect any difference? If so, is there a difference limen for scattering coefficient?

This chapter aims to contribute to the understanding of the relations between human perception and objective parameters by investigating the perception of scattering coefficient (s). In particular, difference limens for various scattering coefficients associated to lateral walls of simulated enclosed spaces will be investigated. In order to answer to the previous questions, listening tests were conducted as follows. Several acoustical simulations of two rooms, namely a shoebox-shaped room and the Konzerthaus Dortmund, have been performed with different configurations of scattering surfaces and scattering values. The scattering coefficient has been constantly changed with the respect to frequency; it assumed five different values: 0.1, 0.3, 0.5, 0.6, 0.7 and 0.9. For each value of scattering coefficient, a computer simulation has been performed, so that a binaural impulse response in relevant sampling positions (side and center) could be obtained. Afterwards, each binaural impulse response has been convolved with three different anechoic music samples (choir, piano and orchestra). The auralized signals have been processed and included in the listening tests. Subjects were presented with several series of three samples, two of which being identical. They were asked to detect the different sample and possibly to explain what the difference was consisting of, with particular reference to coloration and spaciousness. Results in terms of psychometric functions will be presented and discussed.

6.1   Effects of Surface Scattering

Let us suppose, to be in a concert hall where a listener is sitting close to a sidewall; a sound source is present on the stage, be it a musical instrument or an instrumental ensemble (Fig.6.1). If the scattering coefficient of the sidewall would suddenly change, will the listener be able to perceive any difference in the performed music?

Room acoustic simulation could help to answer to this question. In order to conceptually illustrate the effects of surface scattering, a shoebox-shaped room model has been developed and simulated (Fig.6.1). A source has been placed on the stage and a receiver in the stalls. All the surfaces have been set as absorbing (absorption coefficient of 0.99 and scattering coefficient of 0.01) except for a sidewall slice, for which two different setups have been created: a *reverberant* surface ($\alpha = 0.01$, $s = 0.01$) and a *scattering* surface ($\alpha = 0.01$, s equal to the scattering curve in Fig.7.12). A simulation has been performed for each situation;

consequently, monaural impulse responses have been collected at a listener position close to the sidewall, namely to the variable surface.
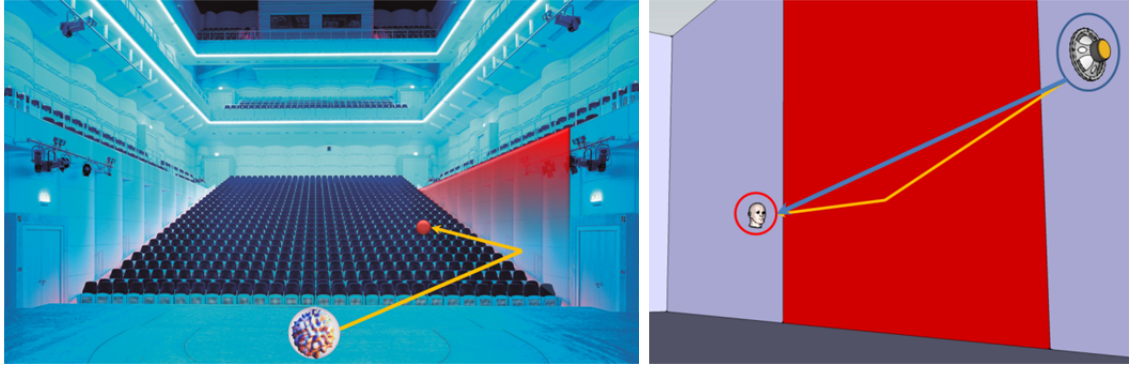
Figure 6.1 – (left) A sound field propagates from the stage to the audience through a direct sound and wall reflections; this situation can be simulated with several values of scattering coefficient for the sidewall as schematically represented to the right.

The effect of a scattering surface as compared to a reverberant surface can be observed by looking at the frequency responses (Fig.6.2). A totally reverberant surface does not the diffuse the sound field; it rather behaves as a specular surface, which radiates a single pulse towards the listener that is delayed with respect to the direct sound. Hence, the frequency response has a comb-shaped spectrum. On the contrary, a scattering surface diffuses the sound field in many different components, which propagate in several directions depending on the surface roughness. This behavior results in a more chaotic frequency spectrum that might be named *colored* spectrum, because it differently "equalizes" the original sound. This effect might also have an impact over the perception in terms of spaciousness, because reflections from a wall are scattered in multiple directions, thus the resulting multiple paths reach a listener with different time delays. Therefore, if these observations are translated into the psychoacoustic domain, it can be argued that the effects of a scattering coefficient change on the perception might happen in terms of coloration or spaciousness.
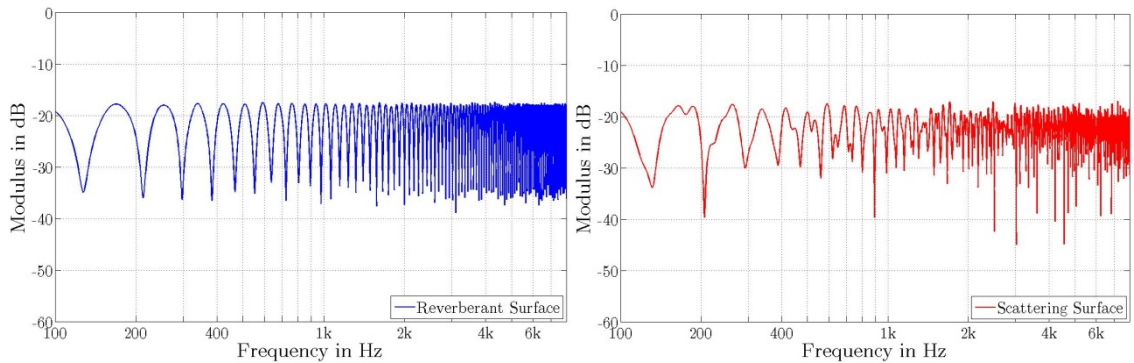
Figure 6.2 – Monaural impulse responses obtained for a shobeox-shaped concert hall for a reverberant (left) and a scattering (right) variable sidewall surface.

6.2   Case Study: Shoebox-shaped Room

A first approach for studying the influence of the scattering coefficient will be hereafter presented with the analysis of a simple configuration: one shoebox-shaped room with one receiver located next to a sidewall and one source located in the position where a music ensemble is supposed to be. This approach allows to isolate the influence due to the scattering coefficient in an easier way as compared to a concert hall, which is a more complex environment containing a wide amount of surfaces that might be responsible for other side effects.

6.2.1 Room Acoustic Computer Simulation

The simulation model is based on a shoebox-shaped room with a volume of 384 m^3 and a total surface of 240 m^2; a source and a receiver have been placed at a distance of 10 m, being the receiver 2 m away from the sidewall (Fig.6.3). The acoustical model consisted of 6 polygons, 2nd order image source and ten thousand ray tracing particles for each frequency band. Acoustic simulations have been executed with the hybrid room acoustics simulation software RAVEN, which uses a hybrid method that combines deterministic image sources to ensure an exact localization of sound sources with a stochastic ray tracing algorithm for determining the late reverberant sound field (see Par.4.3.1).
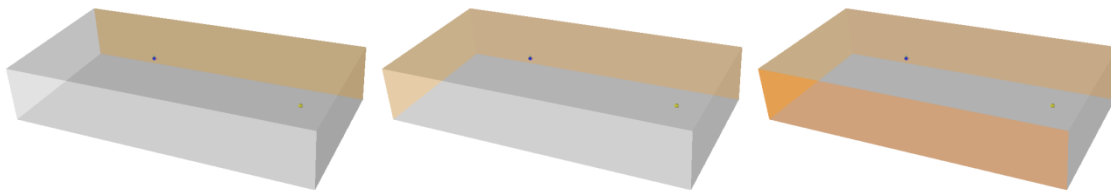
Figure 6.3 - Room configurations under investigation: orange surfaces are scattering, grey surfaces are absorbing. The source-receiver distance is 10 m, the receiver-sidewall distance is 2 m.

The approach of this simulation is based on the idea that only one, two or three walls respectively are scattering (orange surfaces), whereas the remaining surfaces are completely absorbing (grey surfaces, with $\alpha = 0.01$). In particular, a frequency constant scattering coefficient for the diffusing surfaces has been selected with values of 0.1, 0.3, 0.6, 0.7, 0.8, and 0.9 respectively; the absorption coefficient for these surfaces is 0.01.

It has to be considered that room acoustic computer simulations, which utilizes Lambert-modeled scattering (such as in RAVEN), are essentially simulations with stochastic and random mechanisms. In those simulations, differences may sometimes be audible between responses with the same scattering coefficient; therefore, it may be difficult to compare responses with different scattering coefficients. In RAVEN, the late part of the RIR is synthesized by means of a noise process based on a Poisson distribution (Schröder et al., 2007). In order to

avoid possible influences on perception given by this random process, the Poisson sequence has been maintained constant by means of a constant sequence number.

As for the modeling of diffusion, RAVEN implemented an algorithm, which does the following: the occurring reflections are either specular, that is the incident angle is equal to the angle of reflection, or diffuse (scattered), that is in random direction. This is decided by comparing a random number between [0,1] with the material and frequency dependent scattering coefficient of the hit object. The scattered energy is usually assumed to be distributed according to Lambert's cosine law, that is the intensity of a reflected particle on an ideal diffuse scattering wall is independent of the angle of incident but proportional to the cosine of the angle of reflection (see Par.4.1.2). As it follows from the definition of the scattering coefficient, the factor s has to be taken into account for the energy attenuation of each particle. Therefore, the energy of the particle is weighted with s if the reflection is diffuse and with $(1 - s)$ if the reflection is specular.

The binaural room impulse responses obtained from the software simulation for three different wall configurations are shown in Fig.6.4. It can be observed that if the scattering surface increases, diffuse reflections in the late tail of the impulse response increase accordingly. However, because of the presence of completely absorbing walls, the reverberation time remains relatively low.
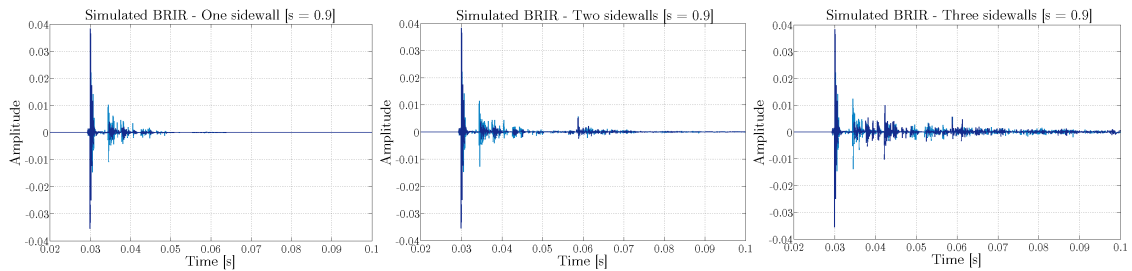
Figure 6.4 – Binaural room impulse responses obtained from acoustic simulation for a room with one (left), two (middle) and three (right) scattering surfaces respectively.

Besides monaural impulse responses, also binaural room impulse responses for each scattering value have been determined. These signals have been used for generating auralized samples to be used in listening tests.

6.2.2 Music Samples

For the purpose of this study, three music samples of anechoic music recordings have been selected, that could be enough representative for classical music played in concert halls and different in terms of style, tempo and spectral content. The samples included a choral recording ("Alleluia"- Randall Thompson, St. Olaf Cantorei, Anechoic Choral Recordings, Wenger), a piano solo ("Ètude Op. 10 no. 4" - Frédéric Chopin, Renzo Vitale, Digital Recording) and an orchestra track ("Water Music Suite" - Handel/Harty, Osaka Philarmonic Orchestra, Anechoic Orchestral Music Recordings, Denon). Scores of the excerpts are shown in Fig.6.5.

Figure 6.5 - Scores of the music excerpts selected for the listening tests: (left) orchestra sample, (top right) piano smple, (bottom right) choir sample.

The spectral content of each music sample is shown in Fig.6.6. The samples offer substantial signal energy in the frequency range from the 63 Hz to 4 kHz octave bands. The piano sample is a fast, articulated and forte music excerpt. It was digitally recorded with a Roland RD-700NX using a Grand Piano patch without any added effect, so that an anechoic sound could be obtained. The frequency spectrum of this sample shows a relevant contribution at low-middle frequencies. The choir sample is a slow, sustained, and mezzo piano music excerpt, which was recorded in an anechoic chamber by the St Olaf choir. The frequency spectrum of this sample shows a harmonic structure with a relevant contribution at low-middle frequencies. The third sample is an orchestra excerpt from the "Water music suite" composed by Handel. It is an allegro with a chordal structure, partially staccato and forte music sample, which was recorded in an anechoic chamber by the Osaka Philharmonic Orchestra. The frequency spectrum of this sample is richer than the previous samples and shows a significant spectral content also at higher frequencies.
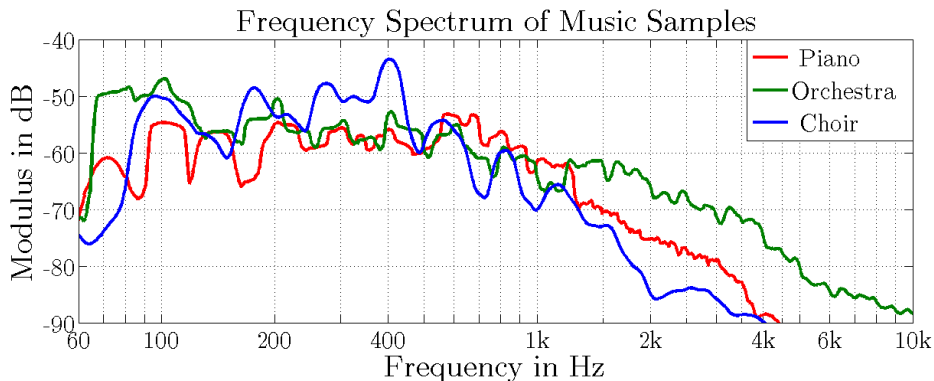
Figure 6.6 - Frequency spctrum of the music samples used in the listening test.

The length of the audio samples was chosen in order to provide a complete musical prhase, which was long enough to represent the acoustical sensation and at the same time short enough to allow multiple comparisons. This length was in

between 5-6 s. Once the music samples have been convolved with the simulated binaural impulse responses, it has been possible to perform the listening tests.

6.2.3 Listening Test Design and Procedure

A 3-Alternative Forced Choice test was chosen, in which the participants were asked to choose the music sample which was di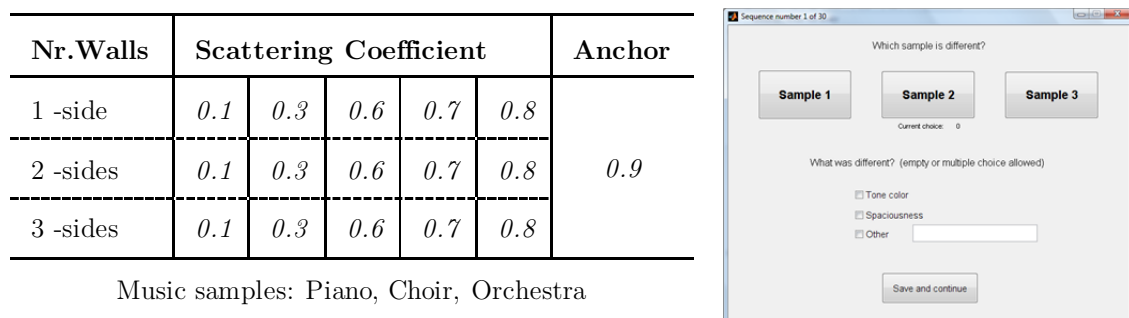fferent among a sequence of three. The test was attended by twenty people, who were mainly students and research assistants aged from 22 to 35 from the Institute of Technical Acoustics, RWTH Aachen. In reference to the definition of assessor in norm ISO 8586-2, three categories were represented. Half of the assessors could be considered as expert because of their knowledge and experience in the field of acoustics. A fourth of the assessors could be considered as initiated assessors, because they had already participated in a sensory test; a remaining fourth of the listeners could be considered as naïve assessors, as they did not meet any particular criterion. Most of the subjects were already familiar with the triangular test. It was ascertained that all the listeners had normal hearing.

The test structure is summed up in Fig.6.7. A binaural impulse response corresponding to six different values of scattering coefficient has been generated. The value 0.9 has been adopted as reference (or *anchor*) value. It means that, for each room configuration, every impulse response associated to a certain value has been compared with the value 0.9. For each value of scattering coefficient, a computer simulation has been performed, so that a binaural impulse response in the sampling position could be obtained. Each BRIR has been subsequently convolved with the selected music samples (choir, piano and orchestra). The auralized signals have been presented to the listeners with fifteen series of three samples, two of which being identical.

Nr.Walls	Scattering Coefficient					Anchor
1 -side	*0.1*	*0.3*	*0.6*	*0.7*	*0.8*	
2 -sides	*0.1*	*0.3*	*0.6*	*0.7*	*0.8*	*0.9*
3 -sides	*0.1*	*0.3*	*0.6*	*0.7*	*0.8*	

Music samples: Piano, Choir, Orchestra

Figure 6.7 - (left) Listening test design: a BRIR is generated for each value of scattering coefficient and for each room configuration; this signal is subsequently convolved with three different music samples. During each triad of the listening test, a comparison between one sample and the anchor value sample is proposed to the assessor by means of a selective mask (right).

A MATLAB script has been programmed so that, for each trial, a triad of three samples was randomly prepared among six possible combinations (ABB, BAA, AAB, BBA, ABA and BAB). The three samples of each triad have been

simultaneously presented to the assessors in the form of a pop-up window as shown in Fig.6.7. Listeners were asked to detect the different sample and possibly to explain what the difference was consisting of, with particular reference to coloration and spaciousness. Before the test started, assessors were presented a short introduction that included two triads of samples played consecutively, one with noise samples and another with orchestra samples. The listening test started soon after the introductive session with the appearance of a selective mask.

The test was a 3-AFC without repetitions, which means that the assessors were not allowed to replay samples after they had been reproduced. Moreover, listeners were not allowed to take a break during the test (which lasted 15 to 20 minutes), and they were instructed that, if no difference could be detected in a triad, they were allowed to randomly select one sample. Assessors could also optionally describe the nature of the difference either by clicking on one of the radio-button with two proposed subjective quality (coloration and spaciousness) or by specifying another aspect in a dedicated text field. Coloration was described as any variation, which would affect the timbre, quality, clarity or equalization of the sample; spaciousness was described as any difference in the feeling of being enveloped in the music, that is how wide and large the sound source appeared to be.

The listening tests were set up at the Virtual Reality Laboratory at the Institute of Technical Acoustics, RWTH Aachen. The equipment consisted of one computer, a sound card (RME Multiface II) and open headphones (Sennheiser HD-600). The background-noise level of the listening test environment was estimated over a period of time of 20 min and resulted to be lower than 30 dB. No replay of sounds was allowed. Participants could optionally specify which kind of differences they detected, if it was in coloration, spaciousness or something else.

6.2.4 Methodology of Data Analysis

Results from listening tests allowed the determination of psychometric functions, which is a curve that relates an observer's ability to detect a stimulus (or differences between two or more stimuli) to the intensity of the stimulus (or to the size of the difference). Its range is a probability measure, namely the probability with which the listener can correctly identify the target stimulus in comparison with others (for more details see Par.5.3.1). Psychometric functions were fitted using *psignifit*, a software package that implements the maximum-likelihood method described by (Wichmann et al., 2001a-b).

There are two parameters of the psychometric function that are of interest. One is the stimulus intensity at which the observer achieves a certain prescribed probability of detection: this is often called a sensory "threshold", and it effectively specifies the location of the curve along the stimulus axis. The other

parameter is the slope of the function, the rate at which performance increases with increasing stimulus intensity. A psychometric function can be read as follows: the x-axis represents the stimulus magnitude, which is the scattering coefficient. The y-axis represents the probability of a correct answer.

Results will be hereafter interpreted by means of the graphical solution approach as follows (Lawless et al., 2010). At the end of the 3-AFC the group percent correct has been calculated and the number of correct choices has been expressed as the proportion correct. As the stimulus difference increases from the anchor value, this proportion should go from near the chance level (1/3) to nearly 100% correct, which often forms an S-curve. The threshold is defined as the level at which performance is 50% correct, after having adjusted the data for chance, which can be done by means of Abbott's equation (Eq.5.5). This equation can be rewritten in a slightly different form, which is:

$$p_{req} = \frac{p_{corr} - p_g}{1 - p_g} \tag{6.1}$$

where p_g is the guessing probability (1/3 for 3-AFC), p_{corr} is the chance-corrected probability and p_{req} is the observed proportion that is required in order to achieve a certain chance corrected level of performance. Therefore, in order to get a chance corrected proportion of 0.5 in a 3-AFC test (that is a 50% detection threshold), the chance corrected probability would be:

$$p_{corr} = p_{req} \cdot (1 - p_g) + p_g = \frac{1}{2} \cdot \left(1 - \frac{1}{3}\right) + \frac{1}{3} = \frac{2}{3} \ (66.7\%) \tag{6.2}$$

Thus, the difference threshold results as the difference between the x-axis value for a probability of 66.7% and the anchor value, which in the current case has been set to 0.9. Once the curve if fitted to the data, the value of scattering coefficient at which the assessors would achieve 66.7% correct can be simply interpolated by eye (or numerically solved). Formally this can expressed as:

$$JND = s_{anchor} - s_{66.7\%} \tag{6.3}$$

This value represents a differential threshold for the perception of the scattering coefficient over a 0 to 1 range for the given anchor value. Other choices of the anchor value (e.g. 0, 0.1 or 1) would also have been reasonable. However, the value 0.9 was chosen because it was able to provide a valid variation range of the stimulus, without potentially generating any singularity in the acoustic computer simulation, such as for $s = 0$.

A clarification should be done for the terminology that will be used hereafter. In Par.5.3 it was affirmed that the difference threshold is called *just noticeable difference* (JND) if it is determined by changing the variable stimulus by small amounts above and below the standard until the assessor notices a difference, otherwise it would be simply named as difference threshold (or limen). However,

despite the difference of the experimental methodology, which should be used for determining a JND, namely an ascending (or adaptive) 3-AFC of limits, the two terms have been often interchanged in many applied fields of research for addressing difference limits detection. For this reason, the term JND will be from now on used for describing the difference limen detected in the listening test.

6.2.5 Listening Test Results

Results from listening tests were processed and psychometric functions were detected for each music sample and for each room configuration (Fig.6.8).
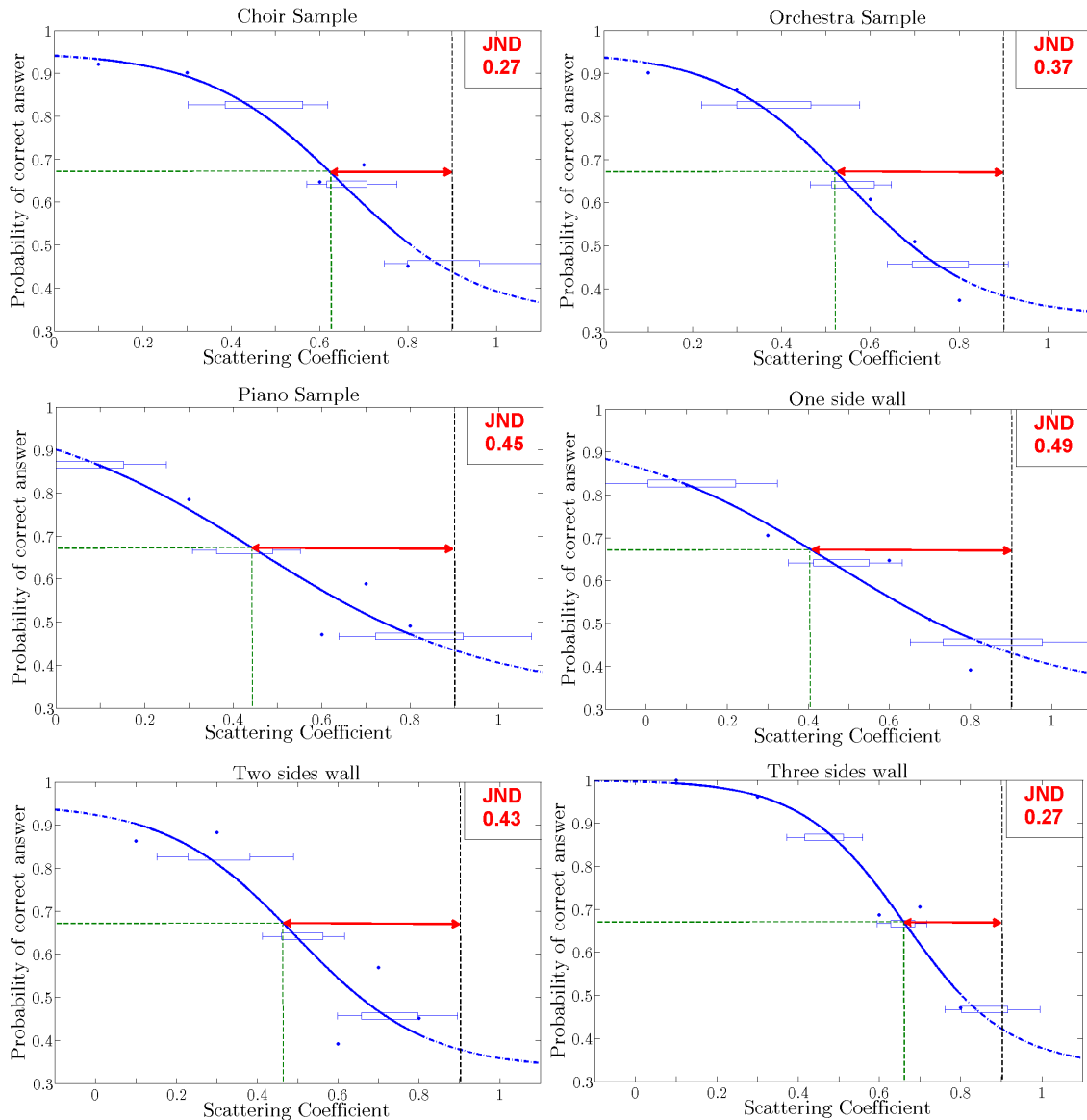
Figure 6.8 - Psychometric functions for each music sample and for each room configuration.

For the choir sample a JND of 0.27 was detected. It means that the scattering coefficient needed to be lowered at least of 0.27 in order that a difference could be heard by the listeners. For the orchestra sample a JND of 0.37 was detected, whereas for the piano sample a JND of 0.45 was detected. A difference between different piano samples appeared to be particularly difficult, as suggested from

the psychometric function slope. The reason may be found in the nature of the piano music signal, which was fast, articulate and with a high note density. The complexity of the sample decreased the ability of the listeners in detecting the differences.

In order to understand how the variations of scattering are influencing the JND, psychometric functions have been obtained also for different room configurations. It seems that it would be very difficult for the listeners to perceive differences if only one wall is scattering (a JND of 0.49 was detected). If two walls are scattering, the slope of the psychometric function increases; the JND in this case has been found to be 0.42, that is a consistent variation of the scattering coefficient was necessary in order that a difference could be heard. A clear improvement in the ability of detecting a difference in the musical samples by the listeners has been achieved in the room configuration with three scattering walls: the variance of data decreased and the measured JND is 0.27.

	Choir	Piano	Orchestra	1 side	2 sides	3 sides
JND	0.27	0.45	0.37	0.49	0.43	0.27

Table 6.2 - JND values for each musica sample and room configuration.

Results about the nature of differences have also been collected during listening tests. Fig.6.9 shows that differences in spaciousness were more audible than differences in coloration, independently from music samples and room configurations. Other aspects were also described by listeners, such as differences in loudness or reverberation. Results slightly diverges from (Torres et al., 2000), where for a static organ chord more differences in coloration where detected. However, as soon as the music content is more articulated, such as in the string quartet sample used by Torres or in the samples used in this study, spaciousness seems to play a major role.
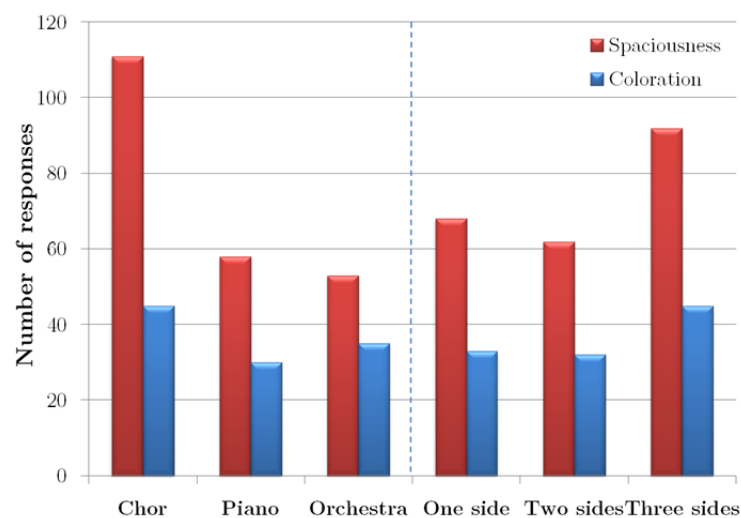
Figure 6.9 - Subjective qualities as perceived by the listeners.

6.3   Case Study: Konzerthaus Dortmund

The investigation carried out with a shoebox-shaped room provided interesting insights about the influence of scattering coefficient on auditory perception. This analysis will hereafter expand to a more complex scenario of a concert hall, namely the *Konzerthaus Dortmund* in Germany (Fig.6.10).

After several years of planning and construction, this concert hall was officially opened in September 2002. Designed by the architect Schröder Schulte-Ladbeck, the building consists of two parts: a rectangular part, which hosts the concert hall in the center, and a small foyer area. The outer shell is cast in reinforced concrete and opens to the foyers through a rough, dark texture. As a requirement of the acoustical design, the 1550 spectators have been divided into four areas: 800 people in the stalls (which presents a distinct slope), the other on the three balconies, where two rows of seats are located on both longitudinal sides up to the front wall.

Figure 6.10 - Konzerthaus Dortmund, Germany (photo rights by Konzerthaus Dortmund).

The Konzerthaus Dortmund has a volume of almost 19.000 m^3 (24 m x 43 m x 19 m). In order to improve the acoustic conditions, maple parquet and rounded diffusers on the sidewalls have been used. The hall can be divided by means of a curtain located almost in the middle of the room, so that the volume is reduced and smaller events, such as chamber concerts, can take place, which host up to 900 people. A large concert organ has been built over the stage, which can be adjusted hydraulically through lifting devices. There are many architectural aspects suggesting that the design has been clearly inspired by the Vienna Musikverein. Instead of the mid-high frequency diffusing elements present on the side of the Viennese auditorium, the Konzerthaus present rounded plaster elements with some sort of frieze boxes. The protection from external noise is favored by 40 cm thick concrete walls.

6.3.1 Room Acoustic Computer Simulation

A model of the Kozerthaus Dortmund was developed in a CAD software starting from the original plans. This model was later imported in three room acoustic simulation software, so that further analysis could be performed. The software used are RAVEN, CATT-Acoustic and ODEON (see Par.4.3 for details).

The original CAD version plan was very detailed, but it had the drawback of including too many surfaces that would have compromised the simulation. For this reason, a compromise between level of details and correctness of the simulation has been found, which allowed a simplification for the simulation in terms of number of polygons. This has been possible by applying a Level-of-Details approach, which introduces an auralization engine which is based on geometrical acoustics and which uses a set of models of the same room but with graduated level of details (Pelzer et al., 2010).
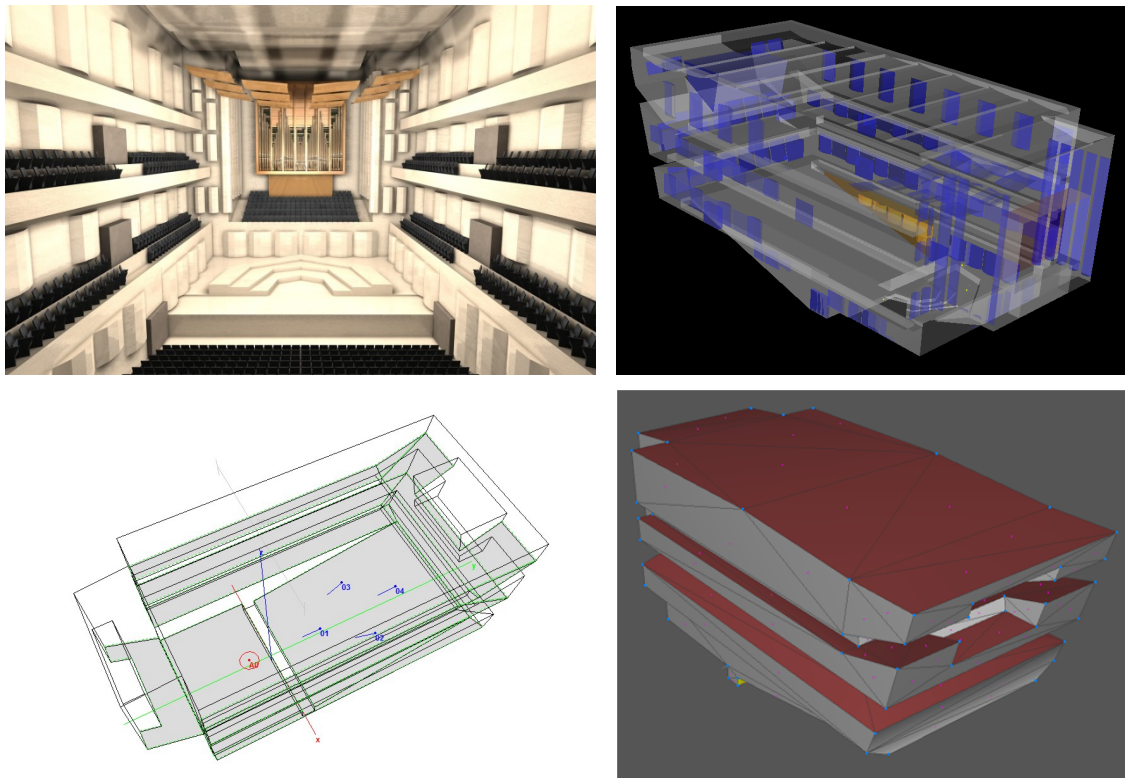
Figure 6.11 - (top left) CAD model of Konzerthaus Dortmund and its implementation in RAVEN (top right), CATT-Acoustic (bottom left) and ODEON (bottom right).

One source has been placed on stage whereas four receivers have been located on the stalls; however, only two receiver positions were used in the listening tests, namely a sidewall and a middle-rear position (S03 and S04 respectively in Fig.6.11-bottom left). The distance between the source and the sidewall is circa 20 m, while the middle position is over 28 m away from the source. The acoustical model consisted of 6 polygons, 2nd order image source and ten thousand ray tracing particles for each frequency band.

The values of the scattering coefficient refer to the scattering contribution from surface roughness only; other contributions, such as scattering due to the limited size of the surface and edge diffraction, are handled automatically by each type of software.

The way of specifying scattering coefficient differs for every software: RAVEN allows to enter absorption and scattering coefficients for each one-third octave band; CATT limits the entering to octave bands, whereas in ODEON only a single value at 707 Hz can be specified, which is later expanded over all the frequencies by selected frequency functions.

Acoustic simulations have been performed for each type of software, varying the scattering coefficient values of the ceiling, and of the side and rear walls, as shown in Fig.6.12. In RAVEN and CATT, simulations were run with frequency-independent scattering coefficients, as it was possible to select input data for the 125 Hz to 16 kHz octave bands; in ODEON, the same values were assumed at the mid-frequency of 707 Hz.

Position	Scattering Coefficient					Anchor
Sidewall	0.1	0.3	0.5	0.6	0.7	0.9
Center	0.1	0.3	0.5	0.6	0.7	

Music samples: Piano, Choir, Orchestra

Figure 6.12 - Simulation and listening test structure: a BRIR is generated for each value of scattering coefficient and for each position; this signal is subsequently convolved with three different music samples. During each triad of the listening test, a comparison between one sample and the anchor value sample is proposed to the assessor.

As for the other surfaces, values of scattering coefficient of 0.7 and 0.1 were assigned for the audience area and the remaining surfaces respectively. Same values for absorption coefficients, air temperature and relative humidity, were considered for all the simulations in order to enable a comparison of the alternatives; moreover, the same settings (transition order, number of rays), type and positions of the source and receivers were maintained.

It is important to observe that the analysis hereafter proposed, is not about which software performs better. Each type of software has implemented surface scattering in a different way, which contributes to model room acoustics with results that, in many cases, are more or less representative or real situations. The question here is instead, whether a change in the scattering coefficient affects the auralization results in a way that is perceivable by listeners. Nothing can be affirmed about differences, which are maybe happening in real situations. This could be done only by comparing results of listening tests based on BRIRs, as obtained for a specific room in a simulated and real environment, where changes

in scattering coefficient happened in the exact same way. These aspects need to be investigated in the future.

6.3.2 Listening Test Design and Procedure

The listening test design for the Konzerthaus Dortmund was the same as for the shoebox-shaped room, except for the number of participants and the location. Three different groups of twenty people each were selected: one in Granada (Spain), one in New York City (USA) and one in Turin (Italy). The first group performed the listening test based on BRIRs obtained in CATT-Acoustic, the second group was based on RAVEN outcomes and the third used auralizations from ODEON.

A 3-Alternative Forced Choice test was chosen, in which the participants were asked to choose the music sample which was different among a sequence of three. People were mainly students and research assistants aged from 18 to 34. In reference to the definition of assessor in norm ISO 8586-2, three categories were represented. Half of the assessors could be considered as expert because of their knowledge and experience in the field of acoustics. A fourth of the assessors could be considered as initiated assessors, because they had already participated in a sensory test; a remaining fourth of the listeners could be considered as naïve assessors, as they did not meet any particular criterion. Most of the subjects were already familiar with the triangular test. It was ascertained that all the listeners had normal hearing.

Similarly to the shoebox-shaped investigation (Par.6.2.3), a binaural impulse response corresponding to six different values of scattering coefficient has been generated. The value 0.9 has been adopted as anchor value. For each value of scattering coefficient, a computer simulation has been performed, so that a binaural impulse response in the sampling positions could be obtained. Each BRIR has been subsequently convolved with the music samples describe in Par.6.2.2. The auralized signals have been presented to the listeners with forty-eight series of three samples, two of which being identical.

6.3.3 Results

Results from listening tests have been expressed for each music sample (choir, piano and orchestra) and each position (sidewall and middle-rear) in terms of psychometric functions (Fig.6.13), which were fitted using *psignifit*, a software package that implements the maximum-likelihood method described by (Wichmann et al., 2001a-b). JNDs have also been evaluated for each situation according to Eq.6.3; results are shown in Tab.6.2.
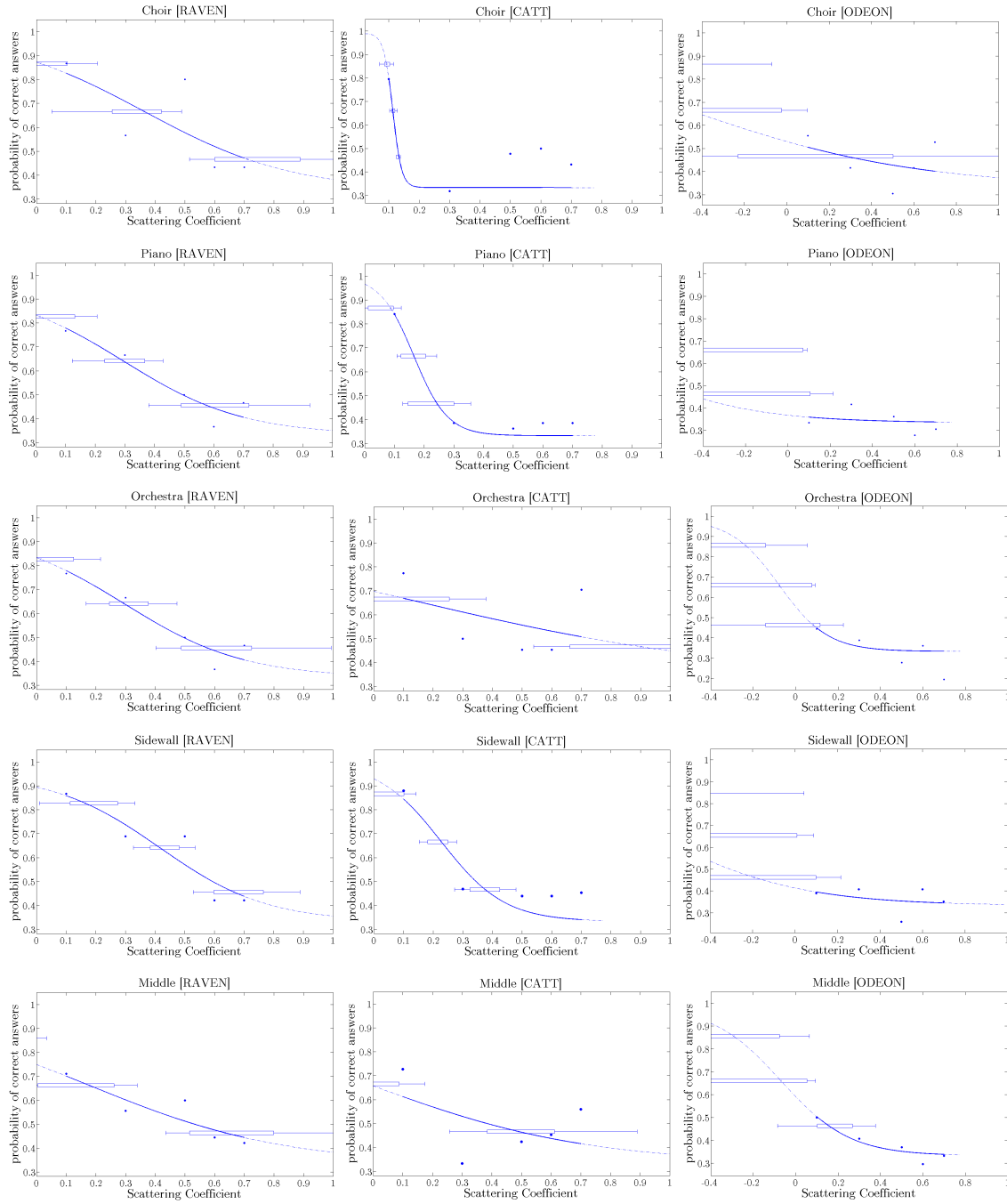
Figure 6.13 - Psychometric functions relative to RAVEN (left), CATT-Acoustic (middle) and ODEON (right). Each row represents (top to bottom): choir, piano, orchestra, sidewall and middle-rear position.

A first evident result is that it was not possible to detect any JND for the software ODEON. Results collected from listening tests related to this software showed that no statistically significant difference had been found (n.s.s.). When this is the case, it is not possible to make any statement about the perceivable quantities. However, it could be argued that differences between samples were very difficult to detect (i.e. the samples were very similar), so that most of the listeners have just guessed.

Results from CATT-Acoustics showed that scattering coefficient has to be changed at least by 0.7 in order for the listener to hear a difference between samples. There is a slight difference between each music sample, but this is not too evident. As for the room position, differences were detected for a scattering variation of 0.68 in the case of the middle position, but no conclusion can be drawn for the side position.

JND	RAVEN	CATT	ODEON
Choir	*0.54*	*0.78*	*n.s.s.*
Piano	*0.61*	*0.74*	*n.s.s.*
Orchestra	*0.65*	*0.79*	*n.s.s.*
Sidewall	*0.49*	*0.68*	*n.s.s.*
Middle	*0.72*	*n.s.s.*	*n.s.s.*

Table 6.3 - JND values for each music sample, position and type of software.

Results from RAVEN showed that a different scenario, where a JND was determined for each situation. A slight difference can be noted between music samples, however an average value of 0.6 could be considered as a variation needed for the listeners to perceive a difference. This software also allowed to determine a JND for two different positions. It seems that for a listener closer to a side wall is easier to detect differences than for a listener in the middle-rear of the stalls.

Results about the nature of differences have also been collected during listening tests. Fig.6.14 shows that, for RAVEN and CATT-Acoustics, differences in coloration were more audible than differences in spaciousness, almost independently from music samples and room configurations. In ODEON an opposite trend was detected, even though it has to be noted that the number of responses about subjective qualities was much lower respect to the other software. Other aspects were also described by listeners, such as differences in loudness or reverberation. Differently from the shoebox-shaped room, results resembles those from (Torres et al., 2000), where for a static organ chord more differences in coloration where detected.
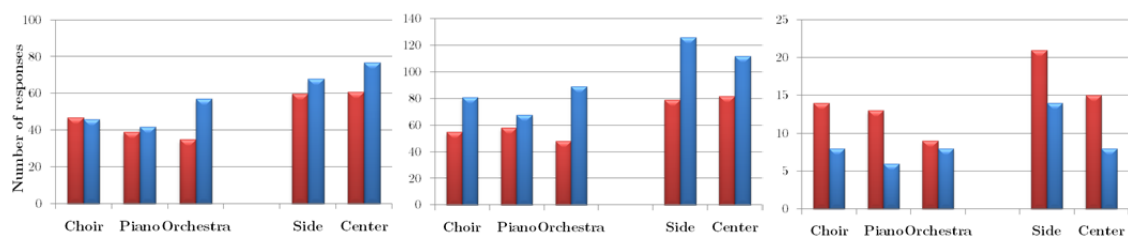
Figure 6.14 - Subjective qualities as perceived by the listeners for RAVEN (left), CATT-Acoustic (middle) and ODEON (right). The color blu represents coloration while red represents spaciousness.

At the end of each session, the listeners were asked to comment on their experience. Some listener affirmed that the perceived differences seem to depend on the input signals. The piano sample was considered to be to most difficult to

detect, followed by the choir and the orchestra sample. Only a few mentioned differences in reverberation.

It is important to observe that this investigation is not about which software performs better, but rather if there is homogeneity in the auralized outputs related to the scattering coefficient. For instance, the fact that it was not possible to determine any statistical significant difference in ODEON for the investigated configuration, it does not mean that results from auralization are not correct or valid. It just means that BRIRs, as obtained for different values of the scattering coefficient, may not generate perceivable differences if auralized with different music samples. Therefore, these specific investigations about scattering coefficient, which involve three different kind of software, do not constitute any objective validation or ranking of each type of software.

However, it can be affirmed that the different algorithms for controlling the diffuse part of the sound field have apparently an influence over the auralized outputs, in a way that differs between the software. Moreover, it can be concluded that it is very difficult for listeners to detect differences in auralized samples in relation to variation of the scattering coefficient. In other words, small variations of scattering coefficients are inaudible.

7 Perception of Scattering in Real Concert Halls

Room acoustic simulation allows to investigate several aspects related to the sound field propagation in enclosed spaces. Moreover, the opportunity of evaluating binaural impulse responses and performing auralization, with any kind of anechoic samples, extends the range of analysis toward the psychoacoustic domain. The previous chapter presented subjective results from listening tests based on binaural impulse responses obtained from two different room geometries, which made it possible to draw conclusions about difference limens for scattering coefficient. As much as the results from computer simulation may be close to the reality, it is always recommended to perform a comparison study in real environments.

There have been several thoughts on how to make subjective evaluation of scattering coefficient in real concert halls possible. The only potential solution would have been to artificially create several surfaces with different (increasing) scattering coefficients, to mount them on the sidewalls of a selected concert hall and performing acoustic measurements in certain positions. However, it is easy to imagine how complex and costly it would have been to realize this approach in actuality. There are practical, timing and uncertainty issues involved in this methodology that are immediately evident, and that could compromise the quality of results.

There has been a long search for the perfect room for this purpose, which ended when the authorization for conducting acoustical measurements at the *Espace de Projection* at IRCAM (Paris) has been granted. This performance space is one of the most advanced and peculiar hall that has been realized so far, which allows to entirely modify the physical characteristics of the sidewalls and ceiling within a few seconds through an automated and computer based system. Detailed information about this room and the measurements therein performed will be given hereafter.

This chapter explores the perception of scattering by means of in-situ acoustical measurements performed at IRCAM, which allowed to collect binaural impulse responses in two locations under different room configurations (hence scattering conditions). These BRIRs have been auralized with music and noise samples, so that listening tests were performed in the form of triangular tests, thus allowing the determination of difference and similarity thresholds.

7.1 *Espace de Projection* at IRCAM

It was 1969 when the project number 493 by architects Renzo Piano and Richard Rogers won the competition (for the first time in France to be open to foreigners) announced by President Pompidou for the planning of a new cultural institution in Plateau Beaubourg, right in the middle of Paris. This center was going to host four institutions: a modern art museum (MNAM), a huge public library (BPI), a design center (CCI) and an institute for contemporary music (IRCAM). The latter was placed under the direction of composer Pierre Boulez, who planned the IRCAM to be an institute where scientific research should have been at the disposal of composers and musicians "in order to envision the distant future".

The IRCAM building is completely underground and hosts, over an area of three thousand square meters, several studios, laboratories, offices, a small anechoic room, control rooms and a main auditorium called *Espace de Projection* (ESPRO). This space (Fig. 7.1) was conceived in a way to possess the utmost regarding spatial and acoustical flexibility, achieved through the possibility of changing both the volume and the height, as well as to vary the reverberation by keeping the spatial dimensions constant (Peutz, 1978).

Figure 7.1 - Espace de Projection at IRCAM (photo by Olivier Panier des Touches, 2005).

The acoustic design of this auditorium was curated by Victor Peutz, who was able to realize a remarkable and unique system aligned with the ideas of Boulez. This was mainly accomplished by the introduction of a single element, which was then replicated as a pattern all over the walls and the ceiling: a squared case containing three rotatable prisms, also called *periactes* (Fig. 7.2). Each side of the

prism has a specific acoustical behavior: *absorbing, reverberant* (plane-specular reflecting) and *diffusing.*
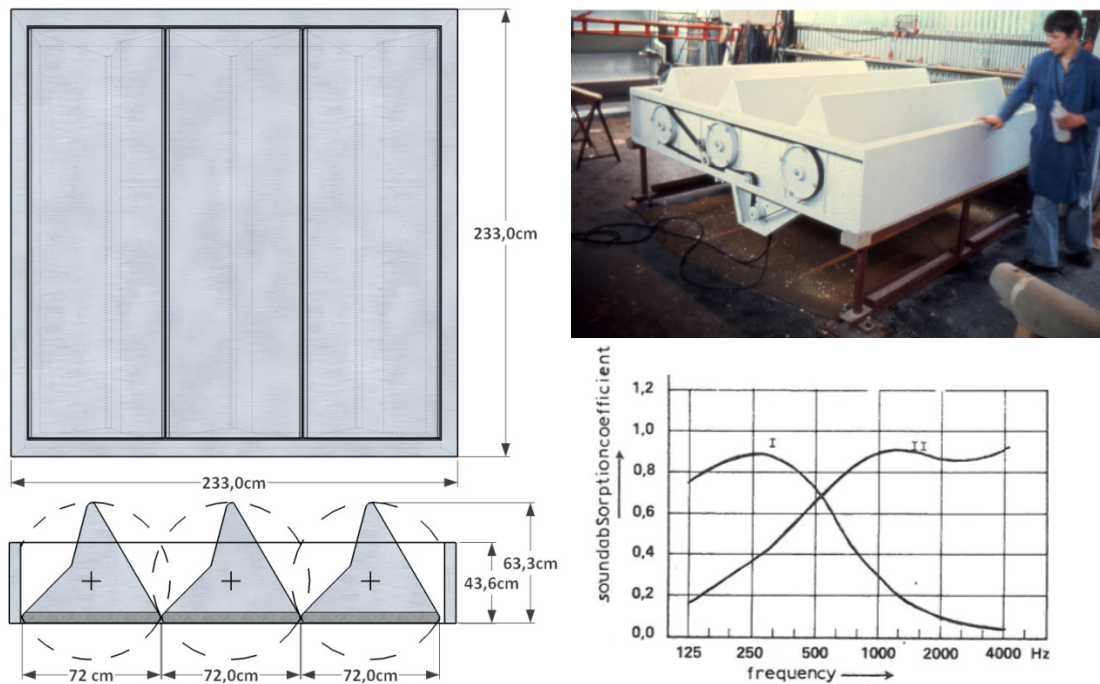
Figure 7.2 - (left) plain view and horizontal section of the main element consisting of three rotatable prisms; (top right) mechanical rotation system of periactes (photo by IRCAM); (bottom right) absorption coefficient of rotatable prisms: half of the panels relate to curve I while the other half relate to curve II (Peutz, 1978);.

There are two sets of elements in terms of absorption: the first is filled with chiefly low frequency absorbing material whereas the second has a chiefly high frequency absorbing side. The two different elements are equally spread all over the room in order to homogeneously distribute the sound absorption. However, there are no indications about their exact location. The sound absorbing properties as given by (Peutz, 1980) are also shown in Fig.7.2.

The volume of the hall can be changed in the range of 24 x 15.5 x (0.8 – 10.5) *m³*. The ceiling consists of three mobile parts, each of which can be raised or lowered independently; it takes almost thirty minutes to change the height of the ceiling. The hall can be bisected or trisected by means of roller curtains that run through a slit, thus allowing also a few scenographic alternatives. Moreover, the hall is provided with three wide scaffoldings, which serve as dislocation area for the lighting system. The hall is usually empty, but it can be filled up with chairs, platforms and stage modules so that, according to the type of concert, the interpretrs and the public, a wide range of configurations are allowed. All changes and movements of the wall elements are controlled by a computer located in the control room. The control system is based on a Max Msp patch, which shows every element of the four walls and the ceiling (Fig.7.3).
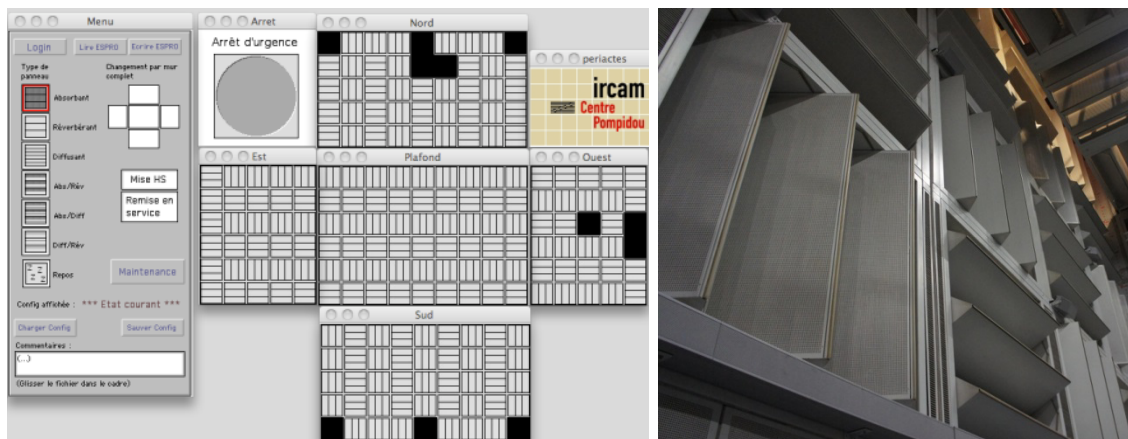
Figure 7.3 - (left) MaxMsp patch for controlling the movements of periactes; (right) prospective view of a sidewall at ESPRO.

The operator can select and move every single element: the prisms of a particular element, in fact, can be rotated independently of those of the other elements. It approximately takes from twenty seconds to one minute to switch from one configuration to another. Besides the three main acoustical behaviors (absorbing, reverberant and diffusing), three other mixed combinations can be obtained if the prisms are rotated with steps of sixty degrees: *absorbing/reverberant*, *absorbing/diffusing* and *reverberant/diffusing*.

The remarkable acoustical flexibility of this concert hall has recently been further expanded through the installation of a surrounding 350-loudspeakers array system, which aims at the physically correct synthesis of acoustical wave fields applying the wave field synthesis (WFS) and high-order Ambisonics (HOA) (Noisternig et al., 2012). These recent developments transformed the ESPRO in one of the most advanced, wide-ranging and complete concert hall in the world.

7.2   Acoustical Measurements

An extensive acoustical measurement campaign was conducted at the ESPRO at IRCAM (Paris) in November 2013. The hall was entirely emptied and later occupied by only the measurement equipment, which consisted of 32 Sennheiser KE-4 electret condenser microphones, two 3-way ITA loudspeaker systems, two ITA dummy-heads, one B&K omnidirectional microphone, a loudspeaker pre-amplifier, one RME Multiface, three RME Octamic, four Behringer ADA8000 and a computer. All the microphones and loudspeakers were located inside the hall, whereas the other devices were hosted inside an adjacent control room located on the northern wall. Inside the hall, several temperature and humidity sensors were also displaced in order to track the variations during the entire campaign. Microphones were displaced in an asymmetrical manner, both in the vertical and in the horizontal direction (Fig.7.4). The height of the microphones was ranging between 3.1 and 4.5 meters. The choice of having set them so high was due to the

fact that, for security reasons, the entire first level of periactes (which was set on absorbing) could have not been changed during the whole measurements because it had to remain on a fixed configuration.
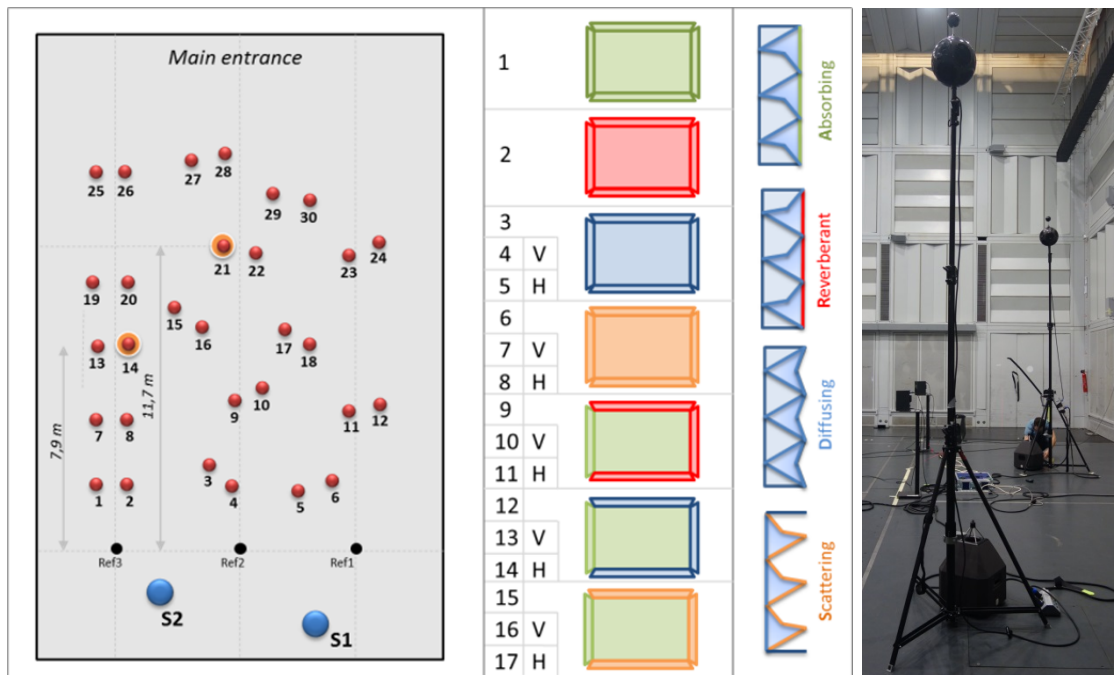
Figure 7.4 - (left) Plain view of the location of microphones (red), dummy-heads (yellow) and sound sources (blu); (center) typology of configurations under investigation and details of wall profiles; (right) 3-way loudspeaker setup: the mid- and high-frequency drives have been placed at an average height of 2.9 and 3.5 m, while the subwoofer remained on the floor.

Measurements of room impulse responses were made according to the ISO 3382 Standard and were performed by means of the ITA Toolbox (Dietrich et al., 2013). The PC-based measurement setup was based on 24 bit, 44.1 kHz audio interfaces for data acquisition.
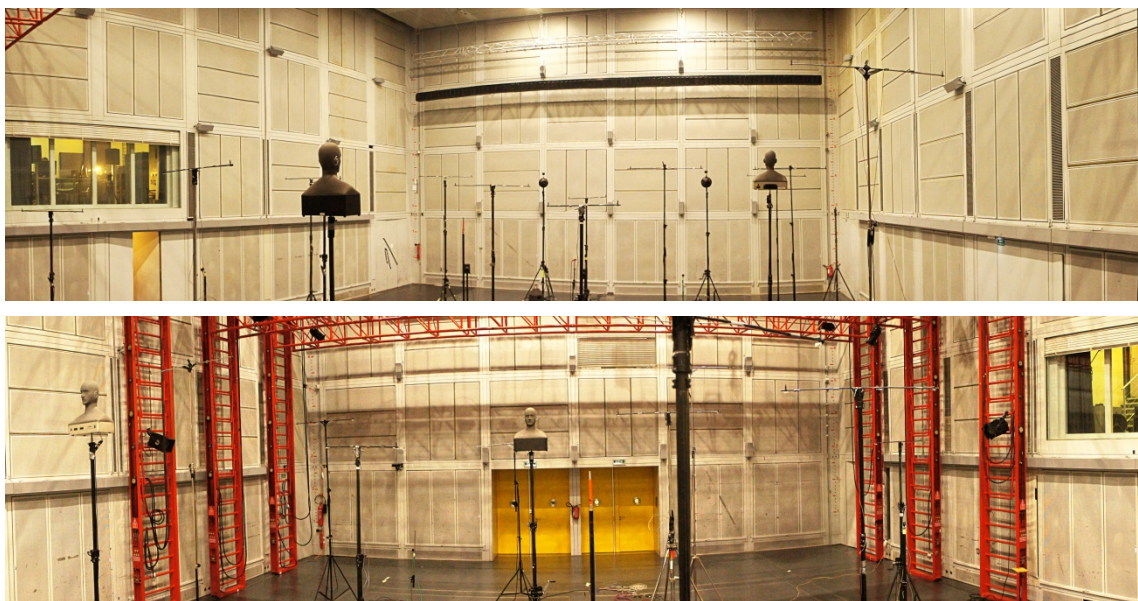
Figure 7.5 - Measurement setup as viewed from the rear (above) and front position (below).

The two 3-way loudspeaker systems were capable of reproducing the audible frequency range with a good concordance with the omnidirectional radiation pattern. Since the 3-way loudspeaker system was designed for the measurement of impulse responses for auralization purposes, the impulse response was later equalized in the post processing with an inverse filtering compensation, in order to account for the frequency and phase response of the sound source, resulting in a flat frequency response.

Figure 7.6 - Measurement setup inside the ESPRO during the measurement of configuration 15 (view from the control room); the 3-way loudspeakers and the two dummy-heads are highlighted in blue and orange respectively (from left to right: S1, S2, Pos. 14, Pos. 21).

Monaural and binaural room impulse responses were measured for a total of seventeen different configurations (Fig.7.7). Two main set were first selected according to the following principles:

- Elements change throughout the hall (1 to 8);
- Elements change only over the sidewalls and the rear wall (9 to 17).

The elements are displaced according to a chessboard-like layout: given an element, whose periactes axis is horizontal, his four neighbor elements will be displaced on a vertical axis. For this reason, further subsets were created so that, for configurations 3 to 17, three distinct situations were investigated:

- Elements are homogeneously selected (only reverberant, absorbing, ...);
- Elements aligned on their vertical axis are selected, while the others are set on reverberant;
- Elements aligned on their horizontal axis are selected, while the others are set on reverberant.

Aim of this secondary selection was to evaluate whether a change of the panel orientation, namely the direction of sound scattering, would have affected the auditory perception of listeners.
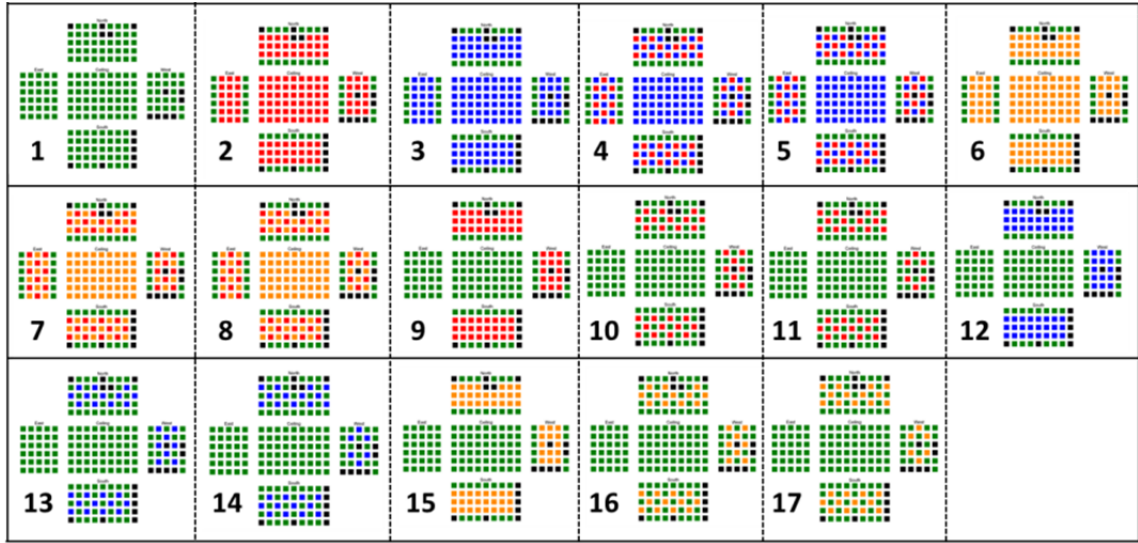
Figure 7.7 - Configurations under investigation. Colors stand for absorbing (green), reverberant (red), diffusing (blue) and scattering (orange). Black squares represent spots where doors or windows are located, as well as surfaces which are not usable.

7.2.1 Measurement Results

A large amount of data was collected at the end of the measurements, which provided 30 RIRs and 2 BRIRs for each of the seventeen configurations and for each of the two sound sources. Although these data would allow a wide range of room acoustics investigations, only two measurement positions will be hereafter analyzed: with reference to Fig.7.4, one position close to the sidewall (number 14) and one position in the middle of the hall (number 21) have been selected. In these two positions were located two dummy heads as well, so that measured BRIRs could be used for auralization purposes within the listing tests (see Par. 7.5). The monaural and binaural room impulse responses were collected in two separate sessions: first, the RIRs were measured for all the seventeen configurations; soon after, the KE-4 microphones placed in positions 14 and 21 were replaced with two dummy heads and eventually the BRIRs were measured for every single configuration. The distances between the sound source S1 and each of the microphones were 11.76 m (position 14) and 14.13 m (position 21) respectively. Results in terms of objective acoustical parameters (T30, EDT, C80, D80) for the side and middle position, with a source signal coming from loudspeaker S1, are shown in Fig. 7.8. The plots illustrate that there are slight differences for most of the parameters as a consequence of a configuration change. Variations are present both closer to the sidewall and in the middle position. In particular, it is observed that variations higher than the JND for C80 (1dB) and for EDT (5%) occur.
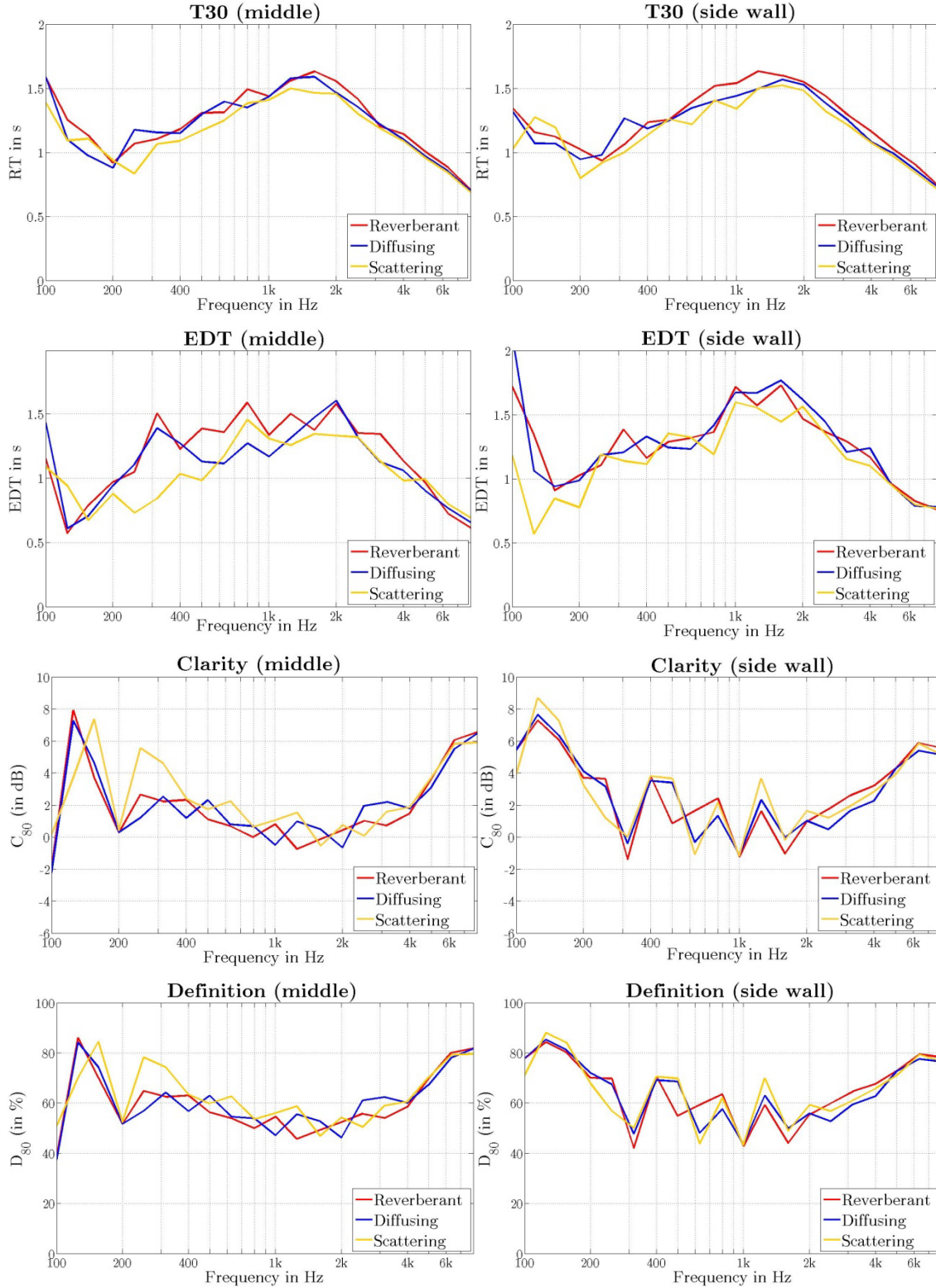
Figure 7.8 - Variations of acoustical parameters (T30, EDT, C80, D80) for two different microphone positions: (left) in the middle of the hall - position 21, (right) closer to the sidewall - position 14.

As for T30, the reverberant and diffusing configurations are more similar respect to the scattering one, which differs more with respect to the reverberant configuration. Differences are even more evident in the case of EDTs, where for instance variations between the scattering and the reverberant configuration cover

a range of 0.1-0.6 s (Fig.7.9). Differences are higher for the low frequencies and decrease at higher frequencies. As for clarity, results are slightly more homogeneous, except for major variations in the scattering configuration: clarity increases for all frequency values multiple of approximately 150 Hz. Even though at a first sight this might appear unusual, a deeper analysis reveals the following: the main element of the ESPRO has a squared shape with a lateral dimension of 2.33 m and shows geometrical patterns at distances of 0.72, 1.44 and 2.33 m (Fig.7.2), which corresponds to approximately 147, 238 and 476 Hz. This provokes an increase of clarity around those frequencies. However, this effect is more evident further away than closer to the side walls. Similar comments can be extended to sound definition.
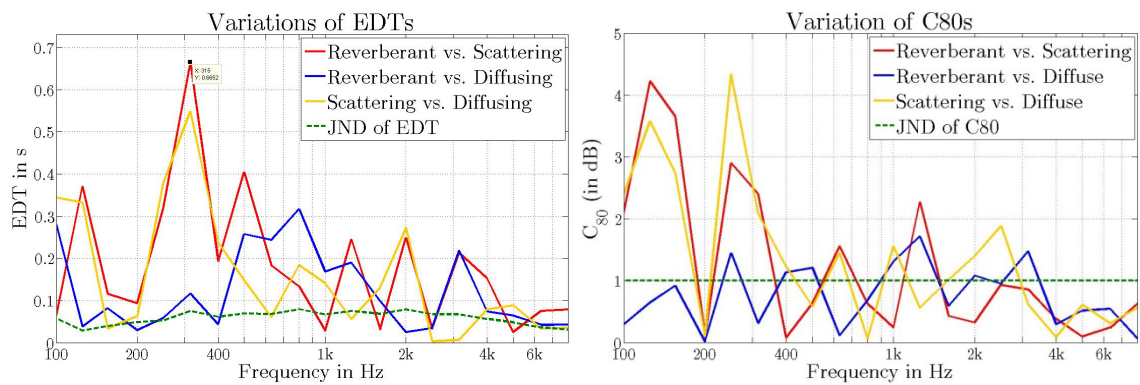
Figure 7.9 - Variations of EDTs and C80s in a cross-coomparison between different configurations with respect to the JND.

7.3   Scale Model Measurement of Scattering Coefficient

The knowledge of the scattering coefficient of the sidewalls for the different configurations is essential for the evaluation and understanding of results from listening tests. Since no information has ever been given about the scattering properties of the sidewalls of IRCAM, a new scale model of the variable geometrical element of the sidewalls was built, so that measurement of scattering coefficient could be performed. Based on the architectural sketches reported in (Peutz, 1980), a 1:10 model of the main element was made (Fig.7.10).
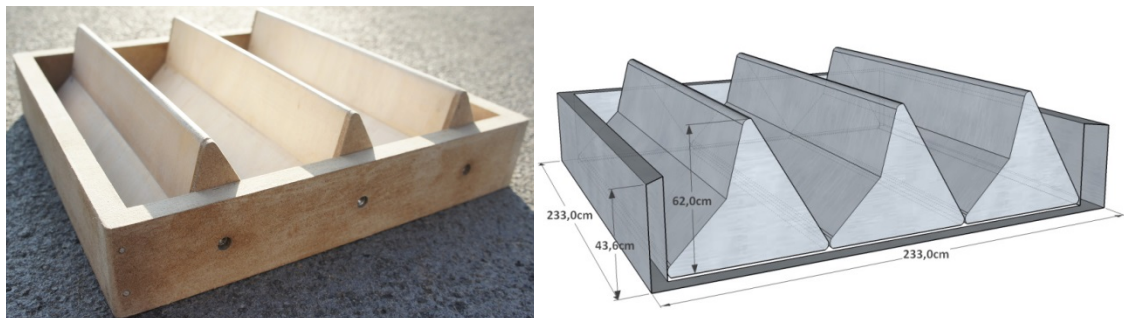
Figure 7.10 - A perspective view of the main element that constitutes walls and ceiling of the ESPRO in two versions: (left) a wooden model with 1:10 scale; (right) a CAD version showing the orginal dimensions.

Three periactes were assembled with wood and then attached on a squared frame by means of three aluminum bars. In a similar way to the real element, periactes could be rotated and differently positioned to obtain various configurations.

Measurements of scattering coefficient were performed in the scale model reverberation chamber at the Institute of Technical Acoustics in Aachen. Given the circular form and the diameter constrains of the turntable (90 cm), a circular wooden frame with a rectangular recess was built in order to avoid edge effects. The inner recess (71.9 x 49.6 cm) was hosting six replicas of the main element, so that a total of 18 periactes could be accommodated. This arrangement was necessary to comply with the ISO 17497-1 and with the prescription that at least 11 periods (periactes in this case) should be present (Vorländer et al., 2011). Besides, the limited surface of the turntable, this was also the reason why a chessboard-like layout of the elements, as it is in the real room, could not be reproduced.
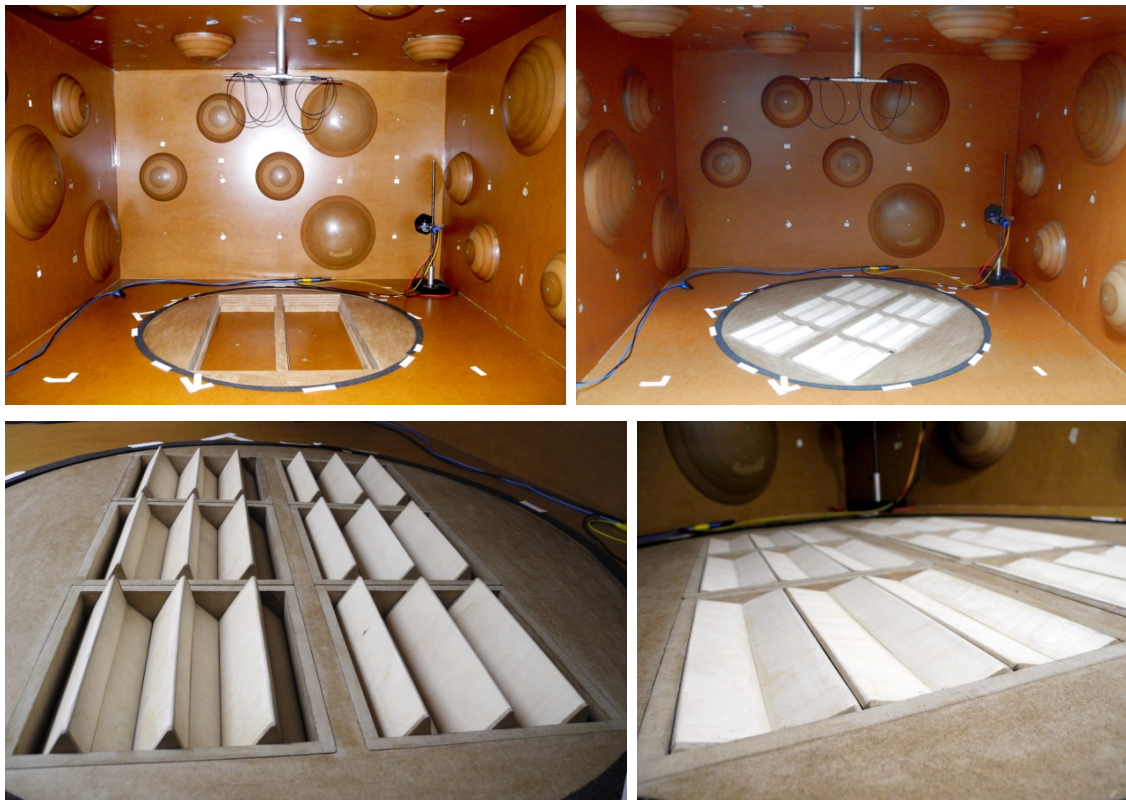
Figure 7.11 - Measurment set-up for determining the scattering coefficient of the main element. (Top left) A rounded frame with a rectangular incess has been placed on the turntable; (top right) six replicas of the main element have been arranged within the frame; reverberant, scattering (bottom left) and diffusing (bottom right) configurations have been measured.

Measurements of scattering coefficients were performed for three different layouts: reverberant, diffusing and scattering. Results show that, as expecting, the reverberant configurations has a scattering coefficient that ranges between 0÷0.05 and a mean value of 0.03, which means that it has an almost specular reflecting behavior (Fig.7.12). The scattering coefficient for the diffusing configuration has a

mean value of 0.26; it increases with a constant slope from 400 Hz and reaches its peak of 0.76 around 5kHz. The scattering coefficient for the scattering configuration has a mean value of 0.5; it increases with a constant slope from 160 Hz and reaches its peak of 0.84 at 3.2 kHz.

Ff	Rev	Diff	Scatt
200	0,03	0,03	0,17
250	0,00	0,01	0,31
320	0,00	0,00	0,50
400	0,04	0,02	0,53
500	0,01	0,05	0,56
640	0,02	0,11	0,53
800	0,02	0,19	0,54
1000	0,01	0,25	0,51
1250	0,01	0,30	0,72
1600	0,01	0,39	0,70
2000	0,01	0,45	0,70
2500	0,02	0,52	0,81
3200	0,03	0,65	0,84
4000	0,05	0,74	0,68
5000	0,03	0,76	0,77
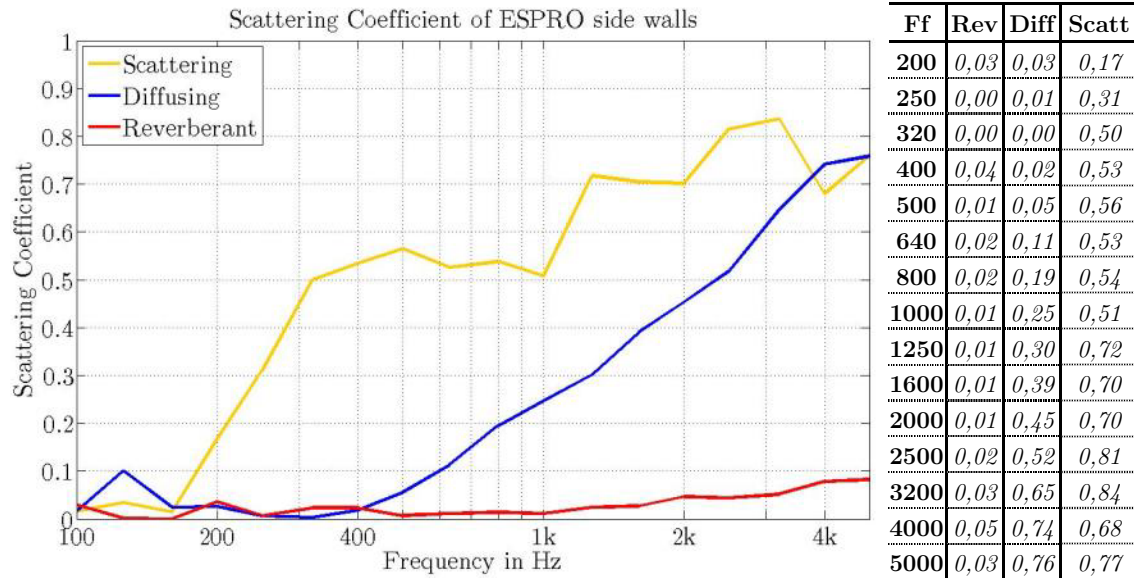
Figure 7.12 - Scattering coefficient plots and values for the reverberant, scattering and diffusing layout.

Results show that the ESPRO provides three distinct scattering layouts that can be named as *no-scattering* ($s = 0.03$), *low-scattering* ($s = 0.26$) and *mid-scattering* ($s = 0.5$). These terms have been used in reference to the mean values of each configuration. However, it is important to notice that if values above 1 kHz are considered, then the mean values of the scattering coefficient would become 0.02, 0.44 and 0.69 respectively. This means that in the frequency range of 1÷5 kHz, the diffusing layout can be considered as a mid-scattering configuration whereas the scattering layout can be considered as a high-scattering configuration.

7.4   Listening Test with IRCAM Measurements

The ESPRO at IRCAM offers a very unique opportunity, something that no other concert halls can offer: it allows to electro-mechanically modifying the geometrical and physical structure of five out of six entire walls within a few seconds (see Par.7.1).

The distinctive characteristics of this concert hall have provided the possibility of performing for the first time in situ acoustical measurements of three different geometrical layouts, corresponding to three different scattering coefficient levels. By switching from one configuration to another in fact the profile of the walls changes as well, thus representing three specific behaviors, which have been named as *reverberant* (no scattering), *diffusing* (low scattering) and *scattering* (high scattering).

7.4.1 Listening Test Design

Listening tests have been designed based on measurements carried out inside the ESPRO. The test objective was to determine whether people could perceive a difference in sound samples if they were to occur under different scattering properties of the sidewalls. In more general terms, if the scattering coefficient of surfaces in a concert hall changes, does this change affect the perception of people? Can listeners perceive a difference if the wall scattering (hence the scattering coefficient) varies?

In order to answer to these questions, a listening test was designed as shown in Fig.7.13. Two positions in the hall were under investigation, namely one close to the left side and another one in the middle. Both the monaural room impulse response (RIR) and the binaural room impulse response (BRIR) in those positions were obtained from acoustical measurements for three different configurations: reverberant, diffusing and scattering (see Par.7.2). The BRIRs were convolved with two sound files: (1) a noise signal made up of two 350 ms pink noise bursts separated by 150ms of silence, (2) a 2.8 s music sample from Handel ("Water Music Suite" - Handel/Harty, Osaka Philarmonic Orchestra, Anechoic Orchestral Music Recordings, Denon).
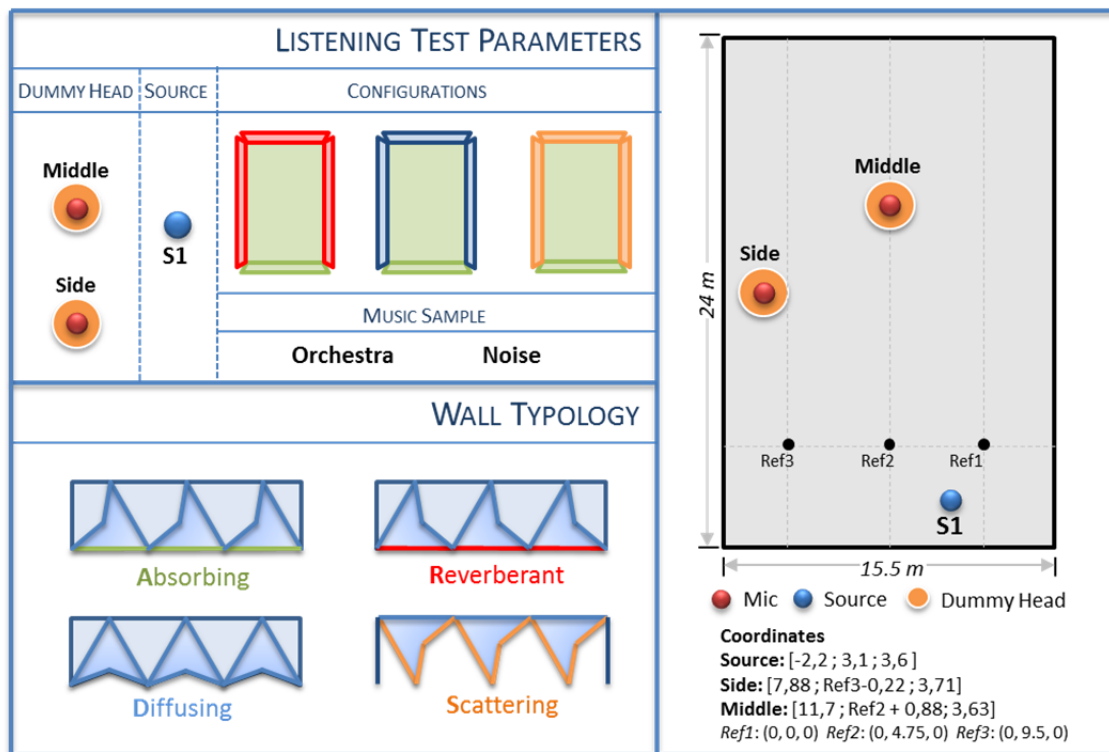
Figure 7.13 - Listening test design: BRIRs measured in two positions (side and middle) for three different configurations are eventually auralized with a music and a noise sample respectively.

The periactes on the rear and on the sidewalls were modified for each configuration, whereas the ceiling and the front wall (or the stage wall - the one

behind the sound source) remained in the absorbing configuration throughout the session. This setup resembles much more a scenario of a common concert hall, where the side and rear walls might have similar characteristics as compared to the rest of the hall. The total variable surface (2 sidewalls plus rear wall) is significant: it covers more than 900 m², which corresponds to 49% of the total surface of the hall. As for the sound source, it was placed in an asymmetrical position, specifically on the lower right corner of the front wall (plan view).

7.4.2 Test Subjects

Twenty-four subjects were selected for the listening test, thus representing an appropriate amount that satisfies the requirements by the norm ISO-4120 for a difference test. The listeners were mainly students and research assistants aged from 22 to 35 from the Institute of Technical Acoustics, RWTH Aachen. In reference to the definition of assessor in norm ISO 8586-2, three categories were represented. Half of the assessors could be considered as *expert* because of their knowledge and experience in the field of acoustics. A fourth of the assessors could be considered as *initiated* assessors, because they had already participated in a sensory test; a remaining fourth of the listeners could be considered as *naïve* assessors, as they did not meet any particular criterion. Most of the subjects were already familiar with the triangular test. It was ascertained that all the listeners had normal hearing.

7.4.3 Test Procedure

The test is a triangle test designed with a unified approach to difference and similarity testing (Meilgaard et al., 2007). Samples have been prepared according to the test parameters shown in Fig.7.13, so that a set of 12 combinations has been obtained. As one can see in Tab.7.1, there are three configuration comparisons for each audio sample in two different positions. Each 12-combinations set has been repeated four times overall, so that each assessor has been presented with a total of 48 triads. The use of repetitions addressed two main targets: controlling the variance and stability of results over time and increasing the number of trials, so that also similarity could have been verified. For a similarity test, in fact, at least 50 - 100 trials are required. If only a single test instance is considered, i.e. the number 1 in Tab.7.1, one obtain a total of 24 users x 4 repetitions = 96 trials for each configuration. Under these design conditions, a similarity test is also possible.

Sample	Position	#	Configuration	Sample	Position	#	Configuration
Orchestra	Middle	1	Scattering Vs Reverberant	Noise	Middle	7	Scattering Vs Reverberant
		2	Diffuse Vs Reverberant			8	Diffuse Vs Reverberant
		3	Scattering Vs Diffuse			9	Scattering Vs Diffuse
	Side	4	Scattering Vs Reverberant		Side	10	Scattering Vs Reverberant
		5	Diffuse Vs Reverberant			11	Diffuse Vs Reverberant
		6	Scattering Vs Diffuse			12	Scattering Vs Diffuse

Table 7.4 - Overview of the test subset, which is made up of 12 combinations: each set is repeated 4 times.

A MATLAB script has been programmed so that, for each trial, a triad of three samples was randomly prepared among six possible combinations (ABB, BAA, AAB, BBA, ABA and BAB). The three samples of each triad have been simultaneously presented to the assessors in the form of a pop-up window as shown in the following pictures.
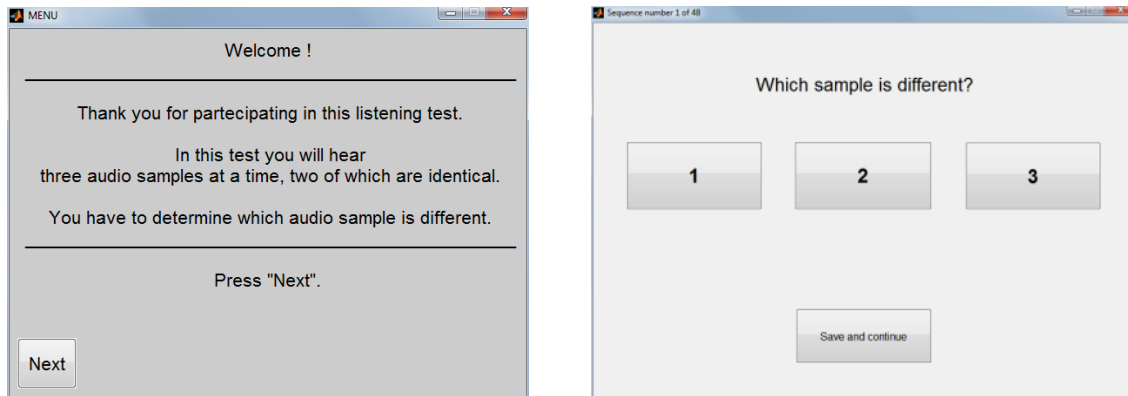
Figure 7.14 - Pop up windows of the listening test: introduction (left) and main selective mask (right).

Before the test started, assessors were presented a short introduction that included two triads of samples played consecutively, one with noise samples and another with orchestra samples. The listening test started soon after the introductive session with the appearance of a selective mask. The assessor could play each sample several times until a choice was made. Samples could have also been stopped during their reproduction so that a faster and more dynamic comparison was possible. The listeners were not allowed to take a break during the test, which lasted 15 to 20 minutes. Assessors were instructed that, if no difference could be detected in a triad, they were allowed to randomly select one sample.

The listening tests were set up at the Virtual Reality Laboratory at the Institute of Technical Acoustics, Aachen. The equipment consisted of one computer, a sound card (RME Multiface II) and open headphones (Sennheiser HD-600). The background-noise level of the listening test environment was estimated over a period of time of 20 min and resulted to be lower than 30 dB.

7.5   Analysis and Interpretation of Results

Listening tests were considered to be difficult from most of the assessors. They reported that it was not easy to detect the odd sample. A general agreement was on the fact that differences were easier to detect for noise samples, which has been confirmed by the results. Moreover, only few people could describe the nature of differences, which were considered to be found in the spectral components of the sound, hence the coloration.

Results from the listening tests will be hereafter presented according to two analysis protocols: the guessing model (see Par.5.5) and the Thurstonian model (see Par.5.6). For each section, results have been evaluated both in terms of difference and similarity testing.

7.5.1 Difference and Similarity with the Guessing Model

In order to perform a difference and similarity analysis according to the guessing model, several values were collected and evaluated after the listening test, such as (Tab.7.2): the number of correct responses (x), the proportion of correct responses (p_c), the proportion of discriminators (p_d), the standard deviation of p_d (s_d), the lower (C-) and upper ($C+$) one-sided confidence limit.

Sample	Position	Configuration	n	x	Pc	Pd	Sd	CI -	CI +
Orchestra	Middle	Scattering Vs Reverberant	96	51	0,53	0,30	0,051	0,45	0,62
		Diffuse Vs Reverberant	96	46	0,48	0,22	0,051	0,40	0,56
		Scattering Vs Diffuse	96	46	0,48	0,22	0,051	0,40	0,56
	Side	Scattering Vs Reverberant	96	43	0,45	0,17	0,051	0,36	0,53
		Diffuse Vs Reverberant	96	40	0,42	0,13	0,050	0,33	0,50
		Scattering Vs Diffuse	96	39	0,41	0,11	0,050	0,32	0,49
Noise	Middle	Scattering Vs Reverberant	96	48	0,50	0,25	0,051	0,42	0,58
		Diffuse Vs Reverberant	96	64	0,67	0,50	0,048	0,59	0,75
		Scattering Vs Diffuse	96	48	0,50	0,25	0,051	0,42	0,58
	Side	Scattering Vs Reverberant	96	66	0,69	0,53	0,047	0,61	0,77
		Diffuse Vs Reverberant	96	66	0,69	0,53	0,047	0,61	0,77
		Scattering Vs Diffuse	96	43	0,45	0,17	0,051	0,36	0,53

Table 7.5 - Results from the listening test evaluated according to the guessing model. Variables: n (nr. Trials), x (nr. of correct answers), Pc (proportion of correct), Pd (Proportion of discriminators), Sd (standard deviation of Pd), CI- (one-sided lower confidence limit), CI+ (one-sided upper confidence limit).

For a sensory difference test using a forced-choice method, the null and alternative hypothesis in reference to p_c can be written as (Christensen, 2013):

$$H_0 : p_d \geq p_{d0} \quad versus \quad H_a : p_d > p_{d0} \qquad (7.1)$$

where p_{c0} is the minimum number of correct responses required for significance at a stated α-risk level for a corresponding number of assessors. This value can be obtained from Tab.1 in ISO-4120. If the null hypothesis is rejected, it can be concluded that a perceivable difference exists between the samples.

Results have been analyzed according to the guessing model as follows. Let us consider the first case in Tab.7.2: the comparison between scattering versus reverberant surfaces resulted in 51/96 paired comparisons, that is the probability of correct answers was 53%. The proportion of discriminators p_d was calculated by means of Abbott's formula (set reference) and resulted to be 0.30. In order to protect from falsely concluding that a difference exists, a α-risk level of 0.05 has been selected for this test. From Tab.3 in ISO-4120, it can be stated that having 96 trials for each configuration also ensures that the test has a 99% chance [i.e.$100 \cdot (1 - \beta)$ %] of detecting the case in which 30% of the assessors can detect a difference between the samples in the test (the actual entry in Tab. A3 for α (0.05) = 0.01 and p_d = 30% is = 98). From Tab. 2 in ISO-4120, in the row corresponding to α = 0.05 a value of 41 is reported; hence, since we obtained 51 correct responses, we can conclude that the two samples are perceptibly different. The same analysis process has been applied to every single configuration. Results from the sensory difference tests have been gathered together and shown in the following figure.
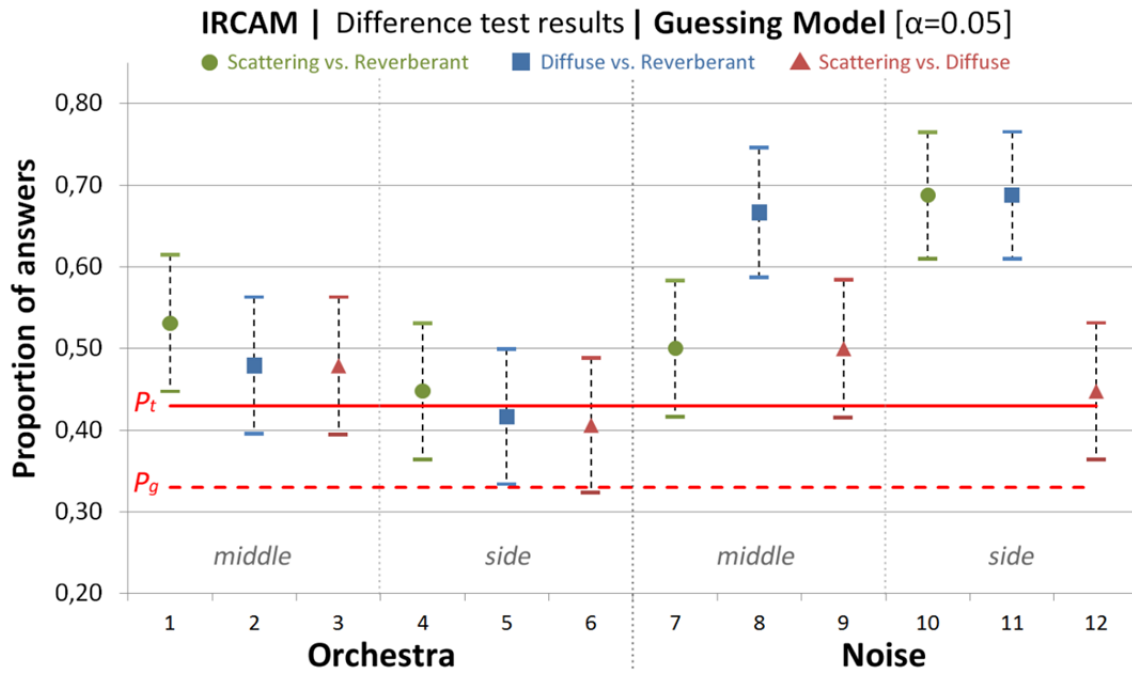
Figure 7.15 - Results from sensory difference tests with 95% confidence. Outcomes 1 to 6 are related to an orchestra sample, whereas outcomes 7 to 12 are related to a pink noise bursts sample. Each configuration comparison is represented by different colors and symbols. Pg is guessing probability (0.33), Pt is the minimum number of correct responses needed to conclude that a perceptible difference exists between the two samples, i.e. two configurations.

From a statistical point of view, it has to be considered that all the outcomes whose lower confidence interval falls below the guessing probability threshold (p_g) are not statistically significant. This is the case only for outcome 6. Moreover, for all the outcomes whose probability of correct answers (p_c) falls above the minimum number of correct responses (p_t) a perceptible difference can be

assessed. However, if the lower confidence interval goes partially below p_t, the difference is considered to be weak.

In acoustical terms, the figure shows that: (1) sensory differences due to scattering coefficient variations are much more difficult to detect for a music sample as opposed to a noise sample, for which perceptible differences are more evident; (2) a listener located in the middle of the hall might have slightly more chances to detect differences as compared to a listener located closer to the sidewall; (3) in the presence of a music sample, it can be affirmed that the higher the difference in scattering coefficient between the configurations, the easier will be to perceive a difference; (4) a variation from a condition of no scattering (reverberant) to a condition of scattering (whether diffusing or scattering) is more evident than a variation between two conditions of scattering.

For a sensory similarity test using a forced-choice method, the null and alternative hypothesis in reference to p_d can be written as (Christensen, 2013):

$$H_0 : p_c \leq p_{c0} \quad versus \quad H_a : p_c > p_{c0} \tag{7.2}$$

where p_{d0} is the maximum allowable proportion of discriminators. In order to draw conclusions about similarity, a comparison of p_{d0} to a confidence interval around the proportion correct needs to be done. This implies that an upper limit on the proportion of acceptable discriminators is required. This choice is not always straightforward; in fact, it usually involves professional judgment based on previously observed trends of the same sensory magnitude: this value is not found in any statistics book (Lawless et al., 2010). However, considering the nature of the samples, the actual perceivable effect and the previous experience with listening tests of computer simulated BRIRs with various scattering coefficients (see Ch.6.) a maximum allowable proportion of discriminators has been set to 30%. For determining similarity, the upper bound of the confidence interval is required; however, it is worth to calculate also the lower bound as it gives more information about the population of discriminators. The one-sided upper and lower confidence intervals on the proportion of the population, which can perceive a difference between the samples in the configuration nr.1, can be calculated according to Eq.5.7 as follows:

$$CI : p_d \pm z \cdot s_d = [1.5 \cdot 0.53 - 0.5] \pm 1.64 \cdot \sqrt{\frac{0.53(1-0.53)}{96}} = 0.297 \pm 0.084 \tag{7.3}$$

Since the maximum allowable proportion of discriminators has been set to 30%, there is evidence that 95% of the time we would fall over this acceptable level. In fact, we would have up to 38% discriminating, given the observed percent correct of 53% which gives us the calculated best estimate of discriminators at 30%. Hence, it is possible to conclude with 95% confidence that the true proportion of the population that can distinguish the samples is no greater than 38% and may

be as low as 21%. This means that at least 21% of the population can perceive a difference between the samples, that the samples cannot be considered similar and they cannot be used interchangeably. Results from the sensory similarity tests have been gathered together and shown in the following figure.
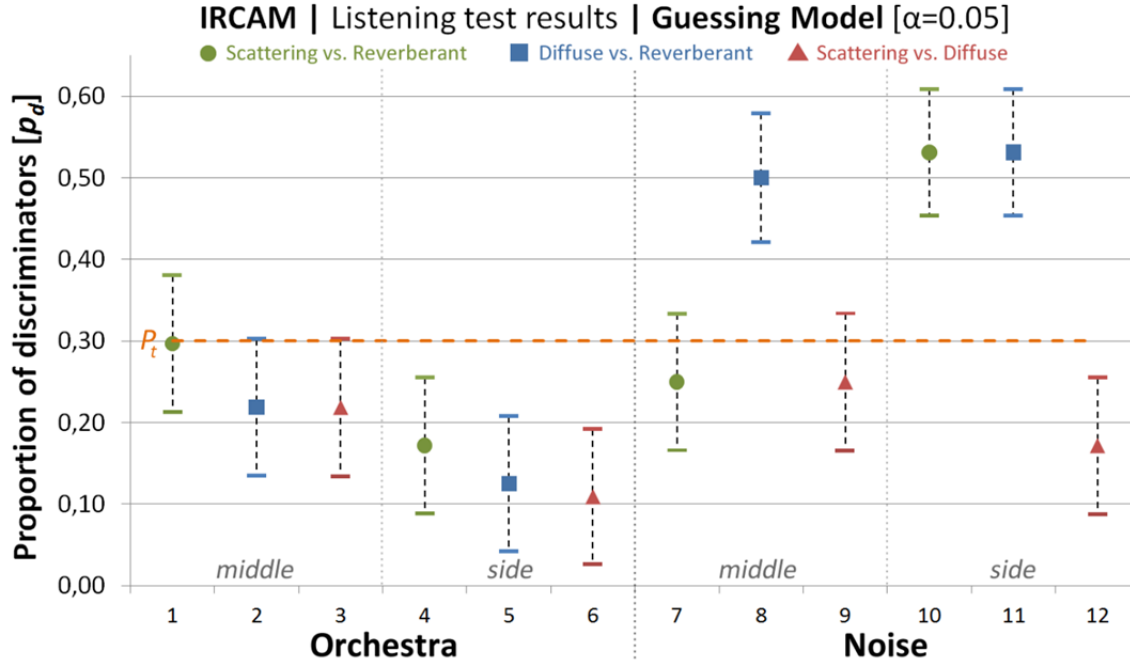
Figure 7.16 - Results from sensory similarity tests with 95% confidence. Outcomes 1 to 6 are related to an orchestra sample, whereas outcomes 7 to 12 are related to a pink noise bursts sample. Each configuration comparison is represented by different colors and symbols. Pt is the maximum allowable proportion of discriminators needed to conclude that a perceptible similarity exists between the two samples, i.e. two configurations.

In acoustical terms, the Fig.7.16 shows that: (1) sensory similarity related to scattering coefficient variations is very strong in the presence of a music sample as opposed to a noise sample, for which similarity can only be partially noted; (2) sensory similarity is much more sample dependent than position dependent; (3) in the presence of a music sample, it can be stated that, if no major variations of scattering coefficient occur, than listeners will not be able to detect any perceptible change if the sidewalls were to be exchanged.

7.5.2 Difference and Similarity with the Thurstonian Model

In order to perform a difference and similarity analysis according to the Thurstonian model, several values were collected and evaluated after the listening test, such as (Tab.7.3): the number of correct responses (x), the proportion of correct responses (p_c), the sensitivity (d'), the B-value (B), the standard deviation (s_d') and variance of d'(v_d'), the lower (CI-) and upper (CI-) one-sided confidence limit and the power of the test.

Sample	Position	Configuration	n	x	Pc	d'	B	vd	sd	CI -	CI +	Power
Orchestra	Middle	Scattering Vs Reverberant	96	51	0,53	1,62	6,50	0,07	0,26	1,11	2,13	0,990
		Diffuse Vs Reverberant	96	46	0,48	1,36	7,27	0,08	0,28	0,82	1,90	0,905
		Scattering Vs Diffuse	96	46	0,48	1,36	7,27	0,08	0,28	0,82	1,90	0,905
	Side	Scattering Vs Reverberant	96	43	0,45	1,19	8,21	0,09	0,29	0,62	1,76	0,758
		Diffuse Vs Reverberant	96	40	0,42	1,01	9,88	0,10	0,32	0,38	1,64	0,533
		Scattering Vs Diffuse	96	39	0,41	0,95	10,68	0,11	0,33	0,30	1,60	0,451
Noise	Middle	Scattering Vs Reverberant	96	48	0,50	1,47	6,87	0,07	0,27	0,95	1,99	0,957
		Diffuse Vs Reverberant	96	64	0,67	2,34	6,38	0,07	0,26	1,83	2,85	1,000
		Scattering Vs Diffuse	96	48	0,50	1,47	6,87	0,07	0,27	0,95	1,99	0,957
	Side	Scattering Vs Reverberant	96	66	0,69	2,45	6,52	0,07	0,26	1,94	2,96	1,000
		Diffuse Vs Reverberant	96	66	0,69	2,45	6,52	0,07	0,26	1,94	2,96	1,000
		Scattering Vs Diffuse	96	43	0,45	1,19	8,21	0,09	0,29	0,62	1,76	0,758

Table 7.6 - Results from the listening test evaluated according to the Thurstonian model. Variables: n (nr. Trials), x (nr. of correct answers), Pc (proportion of correct), d' (sensitivity), B (B-value), vd (variance of d'), sd (standard deviation of d'), CI- (one-sided lower confidence limit), CI+ (one-sided upper confidence limit), Power (power of the test).

According to the Thurstonian modeling (see Par.5.6), sensory differences can also be measured in terms of d' instead of p_d. For a difference test using a forced-choice method, the null and alternative hypothesis can be written as:

$$H_0 : d' \leq d_0' \; versus \; H_a : d' > d_0' \tag{7.4}$$

where d_0' is the difference limit. This is equivalent to testing if the probability of correct responses p_c in a test using a forced-choice method is smaller than a specified value p_{c0}. If the null hypothesis is rejected, it can be concluded that a perceivable difference exists between the samples.

Results from listening tests have been analyzed according to the Thursotnian model as follows. Let us consider the first case: the comparison between the scattering versus the reverberant surfaces resulted in 51/96 paired comparison, that is the probability of correct answers was 53%. The experimental estimate of was found to be $d'=1.62$ (Ennis, 1993). A value of 95% for the confidence intervals has been selected, which means that the real δ has a 95% chance of falling within a certain range of the experimental estimate d'. A value of $B = 6,499$ has been gathered from Tab.3 in (Bi, Ennis, O'Mahoney, 1997), hence a variance $v'_d = 6,499/96 = 0.07$ and a standard deviation of $s'_d = 0.26$ have been calculated with reference to the normal distribution assumption. Under these conditions, a confidence interval of 1.96 x 0.26 = 0.51 was obtained. Thus, we can conclude that the value δ has a 95% chance of falling within the range 1.26 ± 0.51, that is within 1.11 and 2.13. The 95% confidence interval is [1.11, 2.13].

How to select threshold values for d', in order to asses a difference between two samples? A common orientation in psychophysics is to consider a d' of 1 as a threshold value in difference tests (O'Mahoney et al., 2002). The corresponding correct response probability value can be obtained from Tab.3 in (Ennis, 1993) as follows: if a value of 95% for the confidence interval is selected ($\alpha = 0.05$), then a

critical value $u = 0.412$ is obtained, which corresponds to $d' = 1$. For $d' = 1$ a judge is most likely to get 41,2% correct responses for the triangular test, which also means that if this judge were to perform 10 tests, he would be most likely to get 4 triangle test correct. If d' for a difference test is greater than 1, then it can be concluded that the two samples are perceptibly different. If the lower confidence interval falls below this threshold but the mean value falls above, a difference can still be assessed, however it would be defined as a slight or weak difference.

What about sensory similarity? According to the Thurstonian modeling, sensory similarity can also be measured in terms of d' instead of p_d. For a similarity test using a forced-choice method, the null and alternative hypothesis can be written as:

$$H_0 : d' \geq d_0^{'} \quad versus \quad H_a : d' < d_0^{'} \tag{7.5}$$

Where $d_0^{'}$ is the similarity (or equivalent) limit, i.e. an allowed difference. If the null hypothesis is rejected, similarity can be concluded. This is equivalent to testing if the probability of correct responses p_c in a test using a forced-choice method is smaller than a specified value p_{c0}.

How to select a threshold value for $d_0^{'}$ in order to assess similarity between two samples? Such a value is in fact needed for any similarity or equivalence test, in order to specify an allowed difference. The similarity limit is usually specified from practitioners, rather than statisticians, but this is not an easy task. A few recommendations about this topic are given by (Bi, J., 2011), where the following specification can be found: the similarity limit $d_0^{'}$ can be chosen as 0.2, 0.4 and 1.0, which represent, respectively, a strict, a common and a liberal criterion. However, this recommendation is based on the fact that these values correspond, respectively, to a probability of $P(X < Y) = 0.56$, 0.61 and 0.76 in comparison of two products (X and Y) in a yes-no method.

There is unfortunately a limiting factor of using d' as a criterion: the variance of d' is calculated as B/N (see Eq.5.10). The B factor is not regularly distributed, which makes it difficult, from any practical perspective, to find a significance difference between some upper limit threshold for d' and a lower level found experimentally (Lawless et al., 2010). For the ordinary size of testing panels ($N = 50$-100), it might not be efficient to test an obtained d' against a d' limit less than 1.5 as well as it is difficult to demonstrate a d' lower than 1.0. For these reasons, conclusions about similarity using d' is based on simple rules of thumb due to experience.

Nevertheless, a few considerations would help to find proper thresholds for the actual case. Tab.6 in (Ennis, 1993) shows that with $N = 96$ a test power of 80% at α-level of 0.05 allows to detect significant differences between stimuli over $d' =$

1.20. Hence, this value will be selected in the present work as the threshold for the different test: $d'_t = 1.20$. As for the similarity test, we can reformulate the recommendation from (Bi, 2011) for a common criterion ($d' = 0.4$) in reference to the threshold for difference, that is we can set his common criterion over the difference threshold. Thus, we would get a threshold for the similarity of $d'_s = 1.20 = (1.2 + 0.4) = 1.6$. This value appears to be very appropriate if compared with the choice taken for the guessing method ($p_d = 30\%$ - $p_c = 53\%$). From Tab.3 in (Ennis, 1993) we obtain, in fact, that $d' = 1.6$ corresponds to 52.58%.

Results from the sensory difference and similarity tests for the Thurstonian model have been gathered together and shown in the following figure.
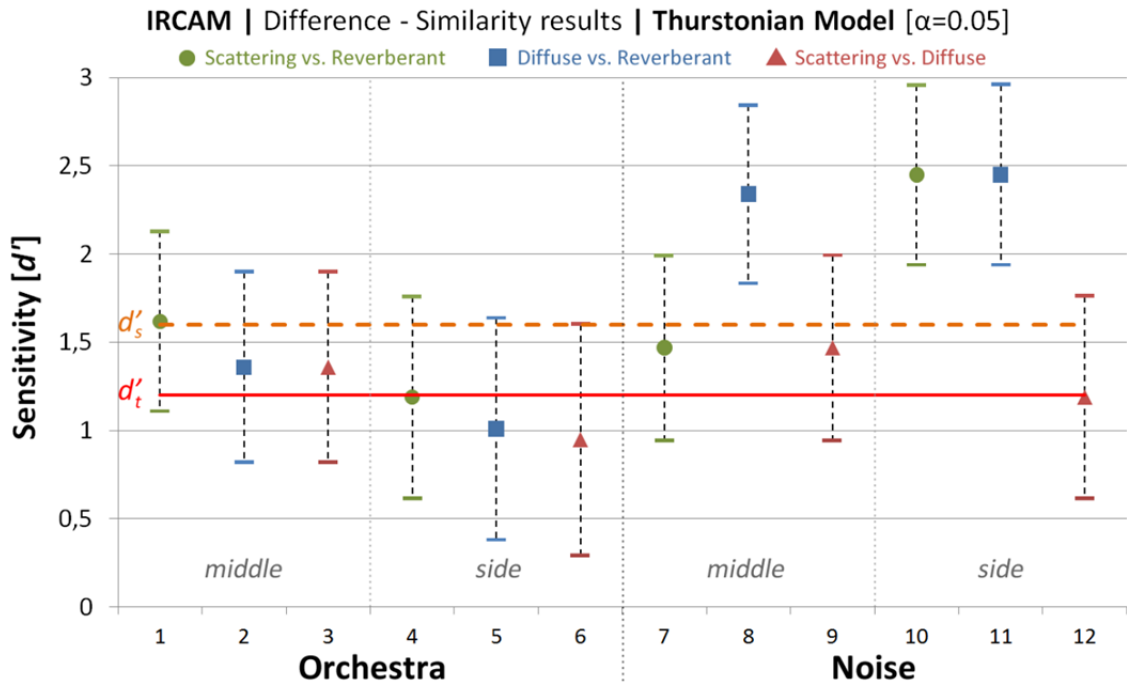
Figure 7.17 - Results from sensory difference and similarity tests with 95% confidence. Outcomes 1 to 6 are related to an orchestra sample, whereas outcomes 7 to 12 are related to a pink noise bursts sample. Each configuration comparison is represented by different colors and symbols. Pt is the threshold for difference (d'), Ps is the threshold for similarity.

As for sensory difference, from a statistical point of view we can affirm that all the outcomes, whose discriminal distance (d') falls below the threshold for difference (d'_t), cannot be considered as different. This is the case for outcomes 4, 5, 6 and 12; however, outcomes 4 and 12 are right below the threshold (0.01) so a liberal approach might include them among the different cases. For all the outcomes whose lower confidence interval falls below this threshold, a difference can still be assessed; however, it would be defined as a slight or weak difference. In terms of sensory similarity, we can affirm the outcomes can be considered as perceptibly similar, hence interchangeable, if their upper confidence interval falls entirely or partially below the threshold for the similarity (d'_s). This is the case for outcomes 2, 3, 4, 5, 6, 7, 9 and 12.

In acoustical terms, we can draw analogous conclusions as those mentioned for the guessing models: (1) sensory differences due to scattering coefficient variations are much more difficult to detect for a music sample as opposed to a noise sample, for which perceptible differences are more evident; (2) a listener located in the middle of the hall might have slightly more chances to detect differences as compared to a listener located closer to the sidewall; (3) in the presence of a music sample, it can be affirmed that the higher the difference in scattering coefficient between the configurations, the easier will be to perceive a difference; (4) a variation from a condition of no scattering (reverberant) to a condition of scattering (whether diffusing or scattering) is more evident than a variation between two conditions of scattering. As for similarity, we can conclude that: (1) sensory similarity related to scattering coefficient variations is very strong in the presence of a music sample as opposed to a noise sample, for which similarity can only be partially noted; (2) sensory similarity is much more sample dependent than position dependent; (3) in the presence of a music sample, it can be stated that, if no major variations of scattering coefficient occur, than listeners will not be able to detect any perceptible change if the sidewalls were to be exchanged.

Results from both statistical models have been gathered together and summed up in the Tab.7.4. Situations with a clear result have been indicated with "No" and "Yes", whereas situations with overlapping confidence intervals have been indicated with "Weak". Non statistically significant results have been indicated with "n.s.s.".

Sample	Position	Configuration	#	Guessing Model		Thurstonian Model	
				Different	Not Similar	Different	Not Similar
Orchestra	Middle	Scattering Vs Reverberant	1	Yes	Yes	Yes	Yes
		Diffuse Vs Reverberant	2	Weak	No	Weak	Weak
		Scattering Vs Diffuse	3	Weak	No	Weak	Weak
	Side	Scattering Vs Reverberant	4	Weak	No	No	Weak
		Diffuse Vs Reverberant	5	No	No	No	No
		Scattering Vs Diffuse	6	n.s.s.	n.s.s.	No	No
Noise	Middle	Scattering Vs Reverberant	7	Weak	Weak	Weak	Weak
		Diffuse Vs Reverberant	8	Yes	Yes	Yes	Yes
		Scattering Vs Diffuse	9	Weak	Weak	Weak	Weak
	Side	Scattering Vs Reverberant	10	Yes	Yes	Yes	Yes
		Diffuse Vs Reverberant	11	Yes	Yes	Yes	Yes
		Scattering Vs Diffuse	12	Weak	No	Weak	Weak

Table 7.7 - Results from the guessing model and the Thurstonian model. There are four possible situations: "Yes" and "No" mean that the results are evident and that the confidence intervals do not overlap any threshold; "Weak" means that the result are partially evident as either the upper or lower confidence interval is crossing a threshold; "n.s.s." means no statistical significance, which happens when the lower confidence interval crosses the guessing probability.

A comparison between the Guessing Model and the Thurstonian Model reveals that results presented a strong overall agreement. There are four situations (1, 8, 10, 11) where the change in scattering coefficient (the configuration switch), was

clear. In those cases, listeners were able to easily detect the different sample. In particular, differences were so evident that configurations were not considered as similar. There are two outcomes (5, 6) where the configuration switch could not be perceived at all. For two other outcomes (7, 9), a "Weak" response was overall assessed, which speaks for both a slight difference and similarity. In the remaining cases (2, 3, 4, 12) the overall result was not identical: in particular, for outcomes 2, 3 and 12, we can conclude that both a weak difference and a similarity can be assessed.

8 Conclusion and Outlook

The main objective of this work was to expand the understanding of sound scattering in architectural spaces and the comprehension of its influence on the auditory perception in concert halls. In order to achieve these goals, a specific methodology has been developed, which consisted of a systematic use of scale model measurements, room acoustic computer simulations, in situ measurements and listening tests.

1. **Measurement of scattering coefficient and improved room acoustic computer simulations**

After a brief excursus about the sound field in enclosed spaces and its diffusion on architectural surfaces, acoustic measurements of scattering and diffusion coefficient have been presented. Since the lack of scattering coefficient data limited the practical application of room acoustic computer simulation so far, acoustic measurements of the scattering coefficient of common objects, such as desks, chairs and tables have been performed in a common scaled reverberation chamber. The measurement process highlighted several limitations of the chamber itself. Therefore, in order to improve the quality of measurements, a revised model for the reverberation chamber has been developed and proposed, which relocated the turntable directly outside of the room. Moreover, a real-scale measurement of angle-dependent scattering coefficient, namely of directional diffusion coefficient, has been performed as a comparison, which showed that directional information about the sound field is lost by using the scattering coefficient. At the same time, it was shown that real scale measurements of directional diffusion coefficient are very complex, hence their execution is worth to consider only in special situations.

In a second part, principles of room acoustic computer simulations have been introduced with specific reference to the modeling and the implementation of scattering coefficient in three different type of software. The scattering influence of typical objects within rooms has been investigated through a specific case study of an ordinary classroom, which has been simulated by using measured values of common pieces of furniture, such as chairs and desks. In particular, it has been shown that room acoustic simulations could be enhanced if proper values of scattering coefficient are used.

2. **Perception of scattering coefficient in auralized concert halls**

In a third part, the perception of scattering coefficient in auralized concert halls has been investigated. Difference limens for scattering coefficients associated to several configurations of lateral walls of simulated enclosed spaces have been determined. Concepts behind sensory evaluation techniques as well as their statistical framework have been introduced, with specific reference to three methodological approaches, specifically the threshold, difference and similarity testing techniques.

Two different enclosed spaces, namely a shoebox-shaped room and the Konzerthaus Dortmund, have been acoustically simulated with different configurations of scattering surfaces and scattering values. In particular, the scattering coefficient has been constantly changed with respect to the frequency, thus assuming five different values: 0.1, 0.3, 0.5, 0.6, 0.7 and 0.9. For each value of scattering coefficient, a computer simulation has been performed, so that a binaural impulse response in relevant sampling positions, such as close to a sidewall and in the middle of the stalls, could be obtained. Afterwards, each binaural impulse response has been convolved with three different anechoic music samples (choir, piano and orchestra). The auralized signals have been presented to assessors in multiple 3-AFC listening tests, where subjects were presented with several series of three samples, two of which being identical. They were asked to detect the different sample and possibly to explain what the difference was consisting of, with particular reference to coloration and spaciousness. Results from listening tests have been eventually presented in terms of psychometric functions for each music sample, for each room configuration and for each case study.

As for the shoebox-shaped room, JNDs between 0.27 and 0.49 have been detected. In particular, JNDs of 0.27, 0.37 and 0.47 have been detected for a choir, an orchestra and a piano sample respectively. The slope of the psychometric functions suggested that a difference between piano samples due to a change in scattering is more difficult to detect than for choir and orchestra samples. It seemed that the textural complexity of the samples decreased the ability of the listeners in detecting the differences. In terms of room configurations, it has been shown that is very difficult for the listeners to perceive differences if only one sidewall is scattering (a JND of 0.49 has been detected). If two walls are scattering, the slope of the psychometric function increased and the JND has been found to be 0.42. A clear improvement in the ability of detecting a difference in the musical samples by the listeners has been observed for three scattering walls; in this case, the variance of data decreased and a JND of 0.27 has been measured. Results about the nature of differences have also been presented for the shoebox-shaped room, which suggested that differences in spaciousness are more audible

than differences in coloration, independently from music samples and room configurations.

As for the Konzerthaus Dortmund, an investigation on how variations of scattering coefficient affect the human perception has been performed with multiple comparisons between three types of room acoustic software, namely RAVEN, CATT-Acoustic and ODEON.

Results from RAVEN showed that, although a slight difference in JNDs could be noted between music samples, an average value of 0.6 could be considered as a variation needed for the listeners to perceive a difference. In terms of listener position, it seemed that for a listener closer to a sidewall is easier to detect differences than for a listener located in the middle-rear of the stalls.

Results from CATT-Acoustic showed that scattering coefficient had to be changed at least by 0.7 in order for the listeners to hear a difference between samples. As for the room position, differences have been observed for scattering variations of 0.68 in the case of the middle position, but no conclusions could be drawn for the position close to the sidewall.

Results collected from listening tests related to the software ODEON where found to be statistically not significant.

Results about the nature of differences were also collected during the listening tests. They showed that, for RAVEN and CATT-Acoustics, differences in coloration were more audible than differences in spaciousness, almost independently from music samples and room configuration. An opposite trend was detected in ODEON, even though the number of responses about subjective qualities was much lower with respect to the other software.

At the end of each session, listeners reported that it was difficult to determine differences between the samples. Some listeners affirmed that the perceived differences seemed to depend on the input signals. The piano sample was considered to be to most difficult to detect, followed by the choir and the orchestra sample. Only a few mentioned differences in reverberation.

Finally, it has been shown that the different algorithms for controlling the diffuse part of the sound field have apparently an influence over the auralized outputs, in a way that differs between the software. However, it can be concluded that it is very difficult for listeners to detect differences in auralized samples in relation to variation of the scattering coefficient. In other words, variations of scattering coefficient up to 0.5 are inaudible in auralized concert halls.

3. **Perception of scattering coefficient in real concert halls**

Listening tests for assessing the perception of scattering coefficient in concert halls have been conducted based on in situ BRIRs from ESPRO at IRCAM (Paris). Three different geometrical configurations of walls, corresponding to three different scattering coefficient values (average of 0.01, 0.25 and 0.56) were measured in two different audience positions (close to the sidewall and in the middle of the hall). A total of 12 auralized samples for all configurations and positions were obtained by means of a convolution with both an orchestra excerpt and pink noise bursts. These samples were simultaneously presented to assessors by means of a triangular test in a four trials session, during which panelists were asked to detect which sample was different. The results from the listening tests have been analyzed with two different statistical models, namely the Guessing Model and the Thurstonian Model. In particular, a parallel analysis both on the difference and on the similarity of the samples was conducted with a unified approach.

It was found that sensory differences due to scattering coefficient variations are very difficult, if not impossible, to detect in the presence of music as opposed to pink noise bursts, for which perceptible differences are more evident. It might be easier for listeners located in the middle of the hall to detect differences as compared to those located closer to the sidewalls. In the presence of music, a clear perceptible difference might be heard only as a consequence of strong variations in scattering coefficient ($s > 0.5$). Variations from a condition of no scattering (reverberant) to a condition of scattering (whether diffusing or scattering) are more evident than variations between two conditions of scattering.

It was also found that sensory similarity related to scattering coefficient variations is very strong in the presence of a music sample as opposed to a noise sample, for which similarity can only be partially noted. Moreover, sensory similarity is much more sample dependent than position dependent. Finally, if no major variations of scattering coefficient occur in the presence of music, than listeners would not be able to detect any perceptible change if the sidewalls were to be exchanged.

These results are rather unexpected if one considers that the existence of a perceptible difference does not necessarily imply that the surfaces are not interchangeable. A test for difference is a procedure for determining whether a perceptible sensory difference exists, whereas a test for similarity is a procedure for determining whether similarity exists between two samples: if it exists, than samples (i.e. configurations) can be interchanged without generating a perceivable difference. In fact, a few outcomes (see 2, 3, 4 and 12 in Tab.7.7) showed that, even though listeners could perceive a weak difference between the configurations, a similarity could be assessed with certainty, which means that surfaces could be

interchanged without provoking any perceivable difference. Hence, the majority of the audience would not perceive any difference as a consequence of a variation in the scattering coefficient.

This is a major and surprising result, which becomes even stronger if one considers that sensory similarity was assessed for all the musical outcomes but one (scattering versus reverberant in the middle of the hall). This means that, in the normal conditions of use of concert halls, which is with a classical, neo-classical or even contemporary repertoire, a change of scattering coefficient up to 0.6-0.7 on the side and rear walls, with respect to a reverberant condition, may not produce any perceivable difference.

A consequence of these results is that the influence of scattering coefficient, i.e. of the geometric profile of surfaces, is less evident than it would be expected. These results may have a relevant impact on the architectural and interior design of concert halls. In fact, the perceptual response of people to changes in scattering coefficient showed that, in the case of a musical repertoire, they are not sensitive to major variations in the geometrical wall texture and structure. It follows that architects and designers might have much more freedom to design patterns and textures that have a specific appearance and personality. New esthetical elements can be introduced in concert halls, without necessarily affecting the auditory perception.

It is important to observe, that a new potential design must not introduce any acoustical problem or artefact. Configurations such as parallel walls and concave geometries have to be avoided because they are responsible for acoustical artefacts, such as flutter echo and focusing effects. Nevertheless, scattering surfaces can be a constructive solution against these types of artefact, since they allow to diffuse the sound field, thus avoiding focusing and flattering. In this concern, an accurate surface testing should be carried out not only in terms of scattering coefficient but also in terms of diffusion coefficient. A BEM analysis of patterns as well as the determination of three-dimensional polar balloons for different angles of incidence is therefore suggested.
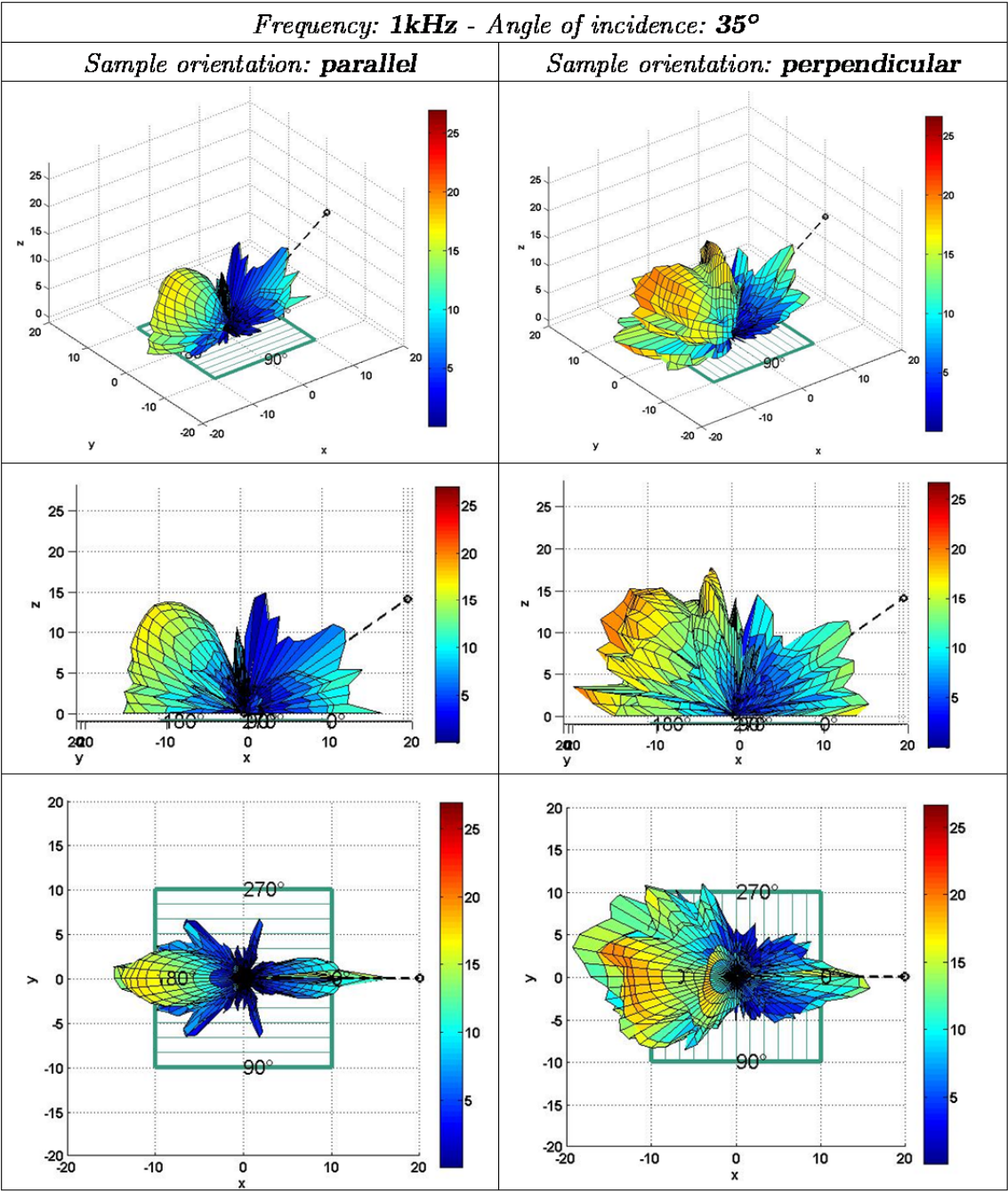
8.1 Outlook

Although results showed that the influence of variations of scattering coefficient on human perception is not as evident as one might expect, there certainly are other aspects that might be investigated. For instance, listening tests with a head and torso simulator whose orientation can be controlled in multiple degrees of freedom could be performed. In this way, it could be observed if head movements contribute to a decrease of JNDs for scattering coefficient.
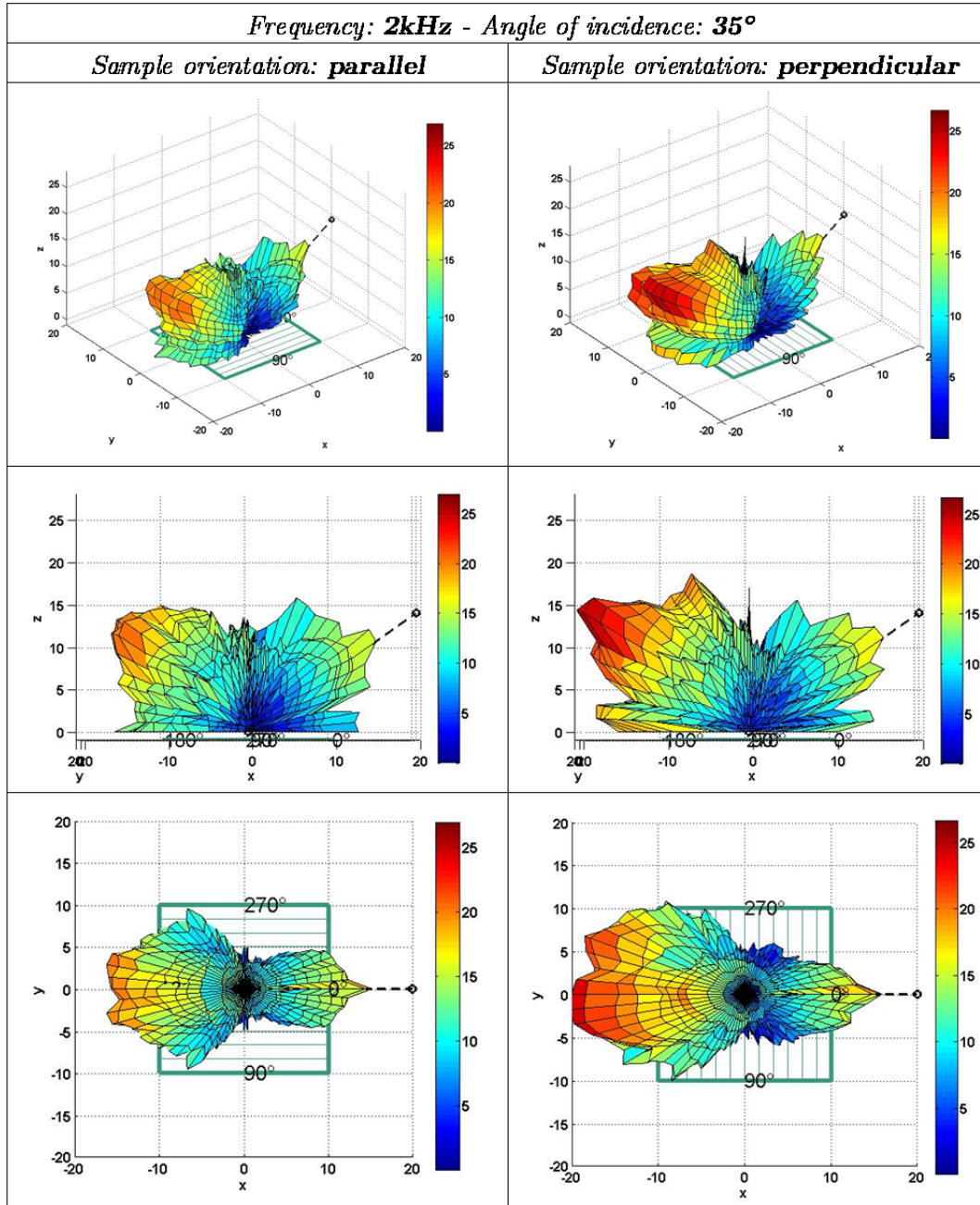
Another possibility would be to perform simulation with binaural hearing model in order to better understand the sensory perception related to scattering coefficient. The human perception presents limits to process a multiple amount of information; therefore, a multi-modal analysis that includes visual elements could also be carried out. Since the visual domain affects our auditory perception by weaken it, it might turn out that very detailed and peculiar influences, such as those of scattering coefficient over perception, have even a stronger effect on perception.
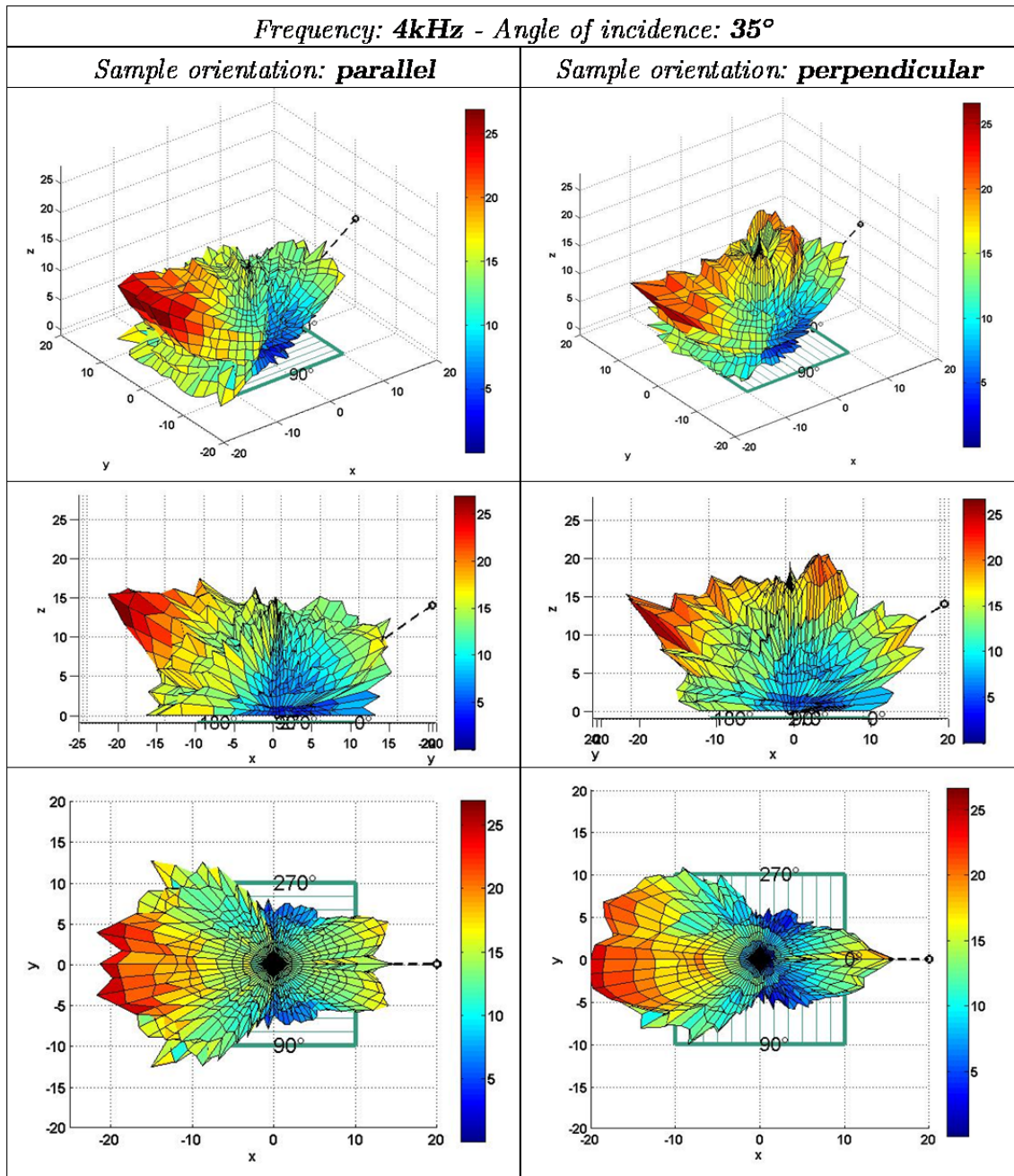
The listening tests in auralized concert halls have been performed with constant frequency variations and only for a single anchor value. Hence, a wider listening test campaign might be carried out to better define JNDs for a wider set of situations. Finally, listening tests with angle dependent scattering coefficient or directional diffusion coefficient should be carried out for a variety of surfaces, in order to understand whether peculiar textures and patterns might have a different influence over the human perception.

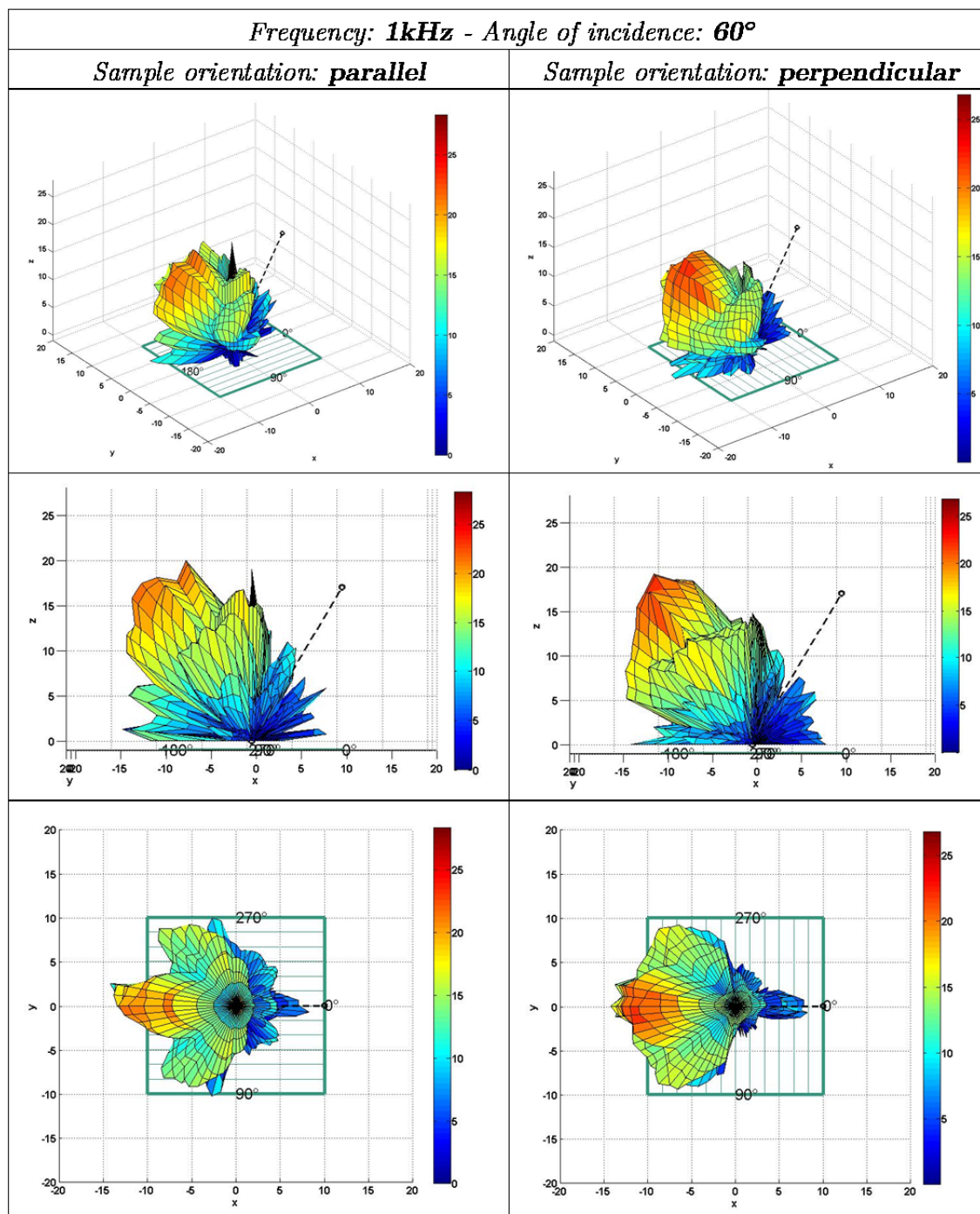# Appendix A: Random Incidence Diffusion Coefficient Measurements

Three-dimensional polar balloons measured for a side wall diffuser made up of a metal grid and wooden laths with triangular sections laid in parallel alignment. Original panel dimensions: 2.68 m x 2.68 m; extracted sample: 90 cm x 85 cm. Measurements details and comment are described in paragraph 3.4.
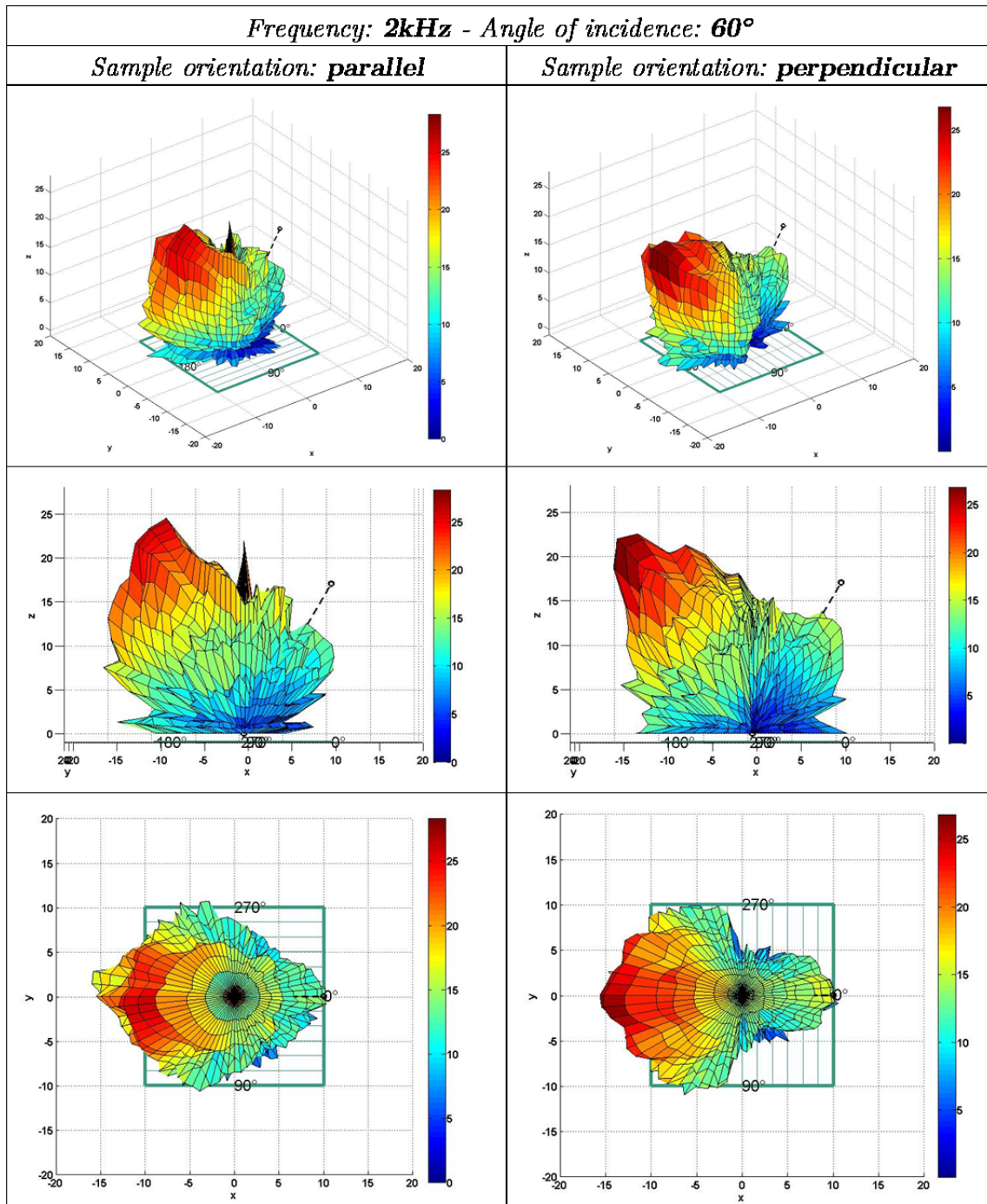

Frequency: **1kHz** - Angle of incidence: **35°**
Sample orientation: **parallel** — Sample orientation: **perpendicular**

Frequency: **2kHz** - Angle of incidence: **35°**

Frequency: **4kHz** - Angle of incidence: **35°**

Frequency: **1kHz** - Angle of incidence: **60°**

Sample orientation: **parallel** — Sample orientation: **perpendicular**

Frequency: **2kHz** - Angle of incidence: **60°**

Frequency: **4kHz** - Angle of incidence: **60°**

Frequency: **1kHz** - Angle of incidence: **80°**

| Sample orientation: **parallel** | Sample orientation: **perpendicular** |

Frequency: **2kHz** - Angle of incidence: **80°**

Frequency: **4kHz** - Angle of incidence: **80°**

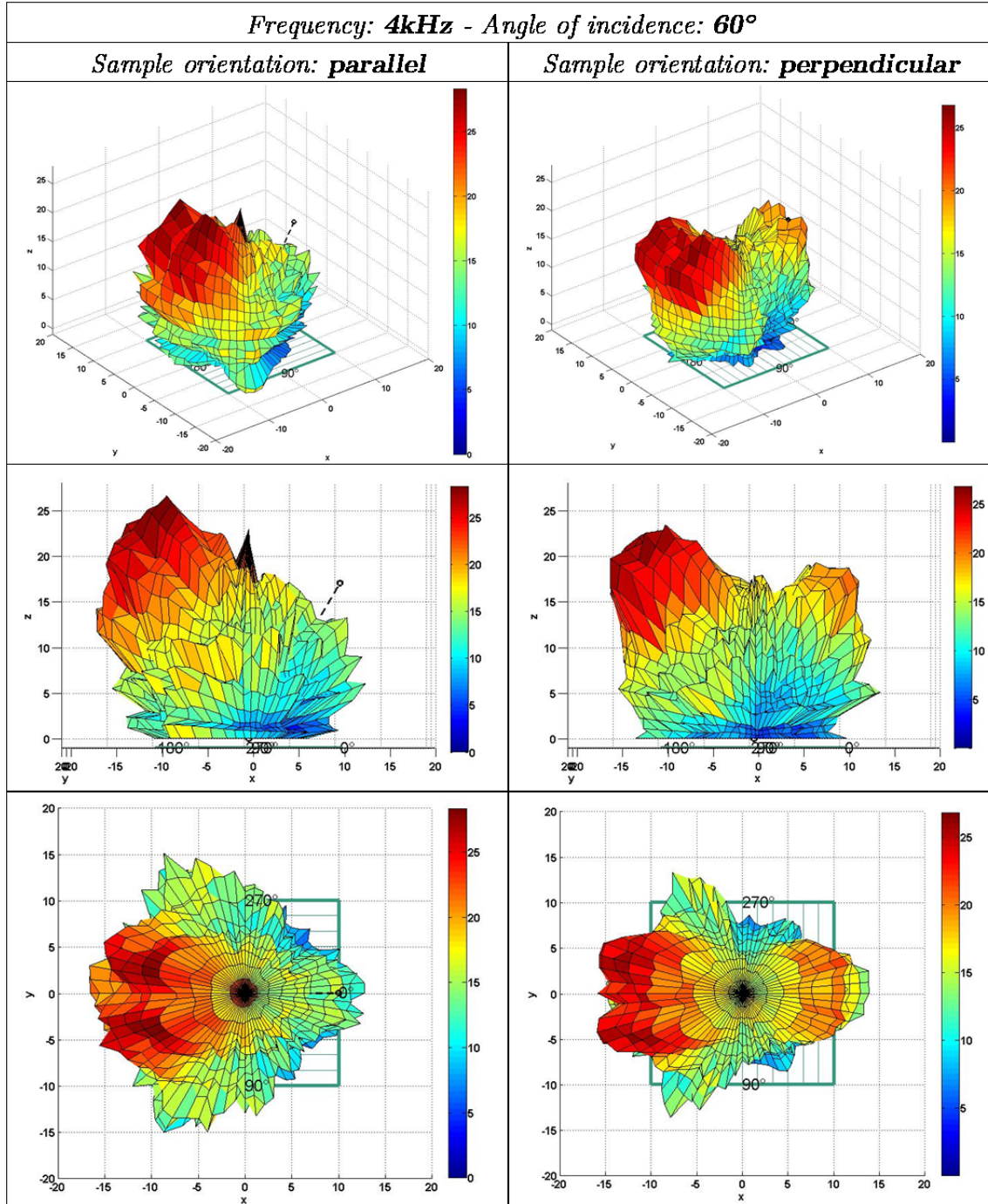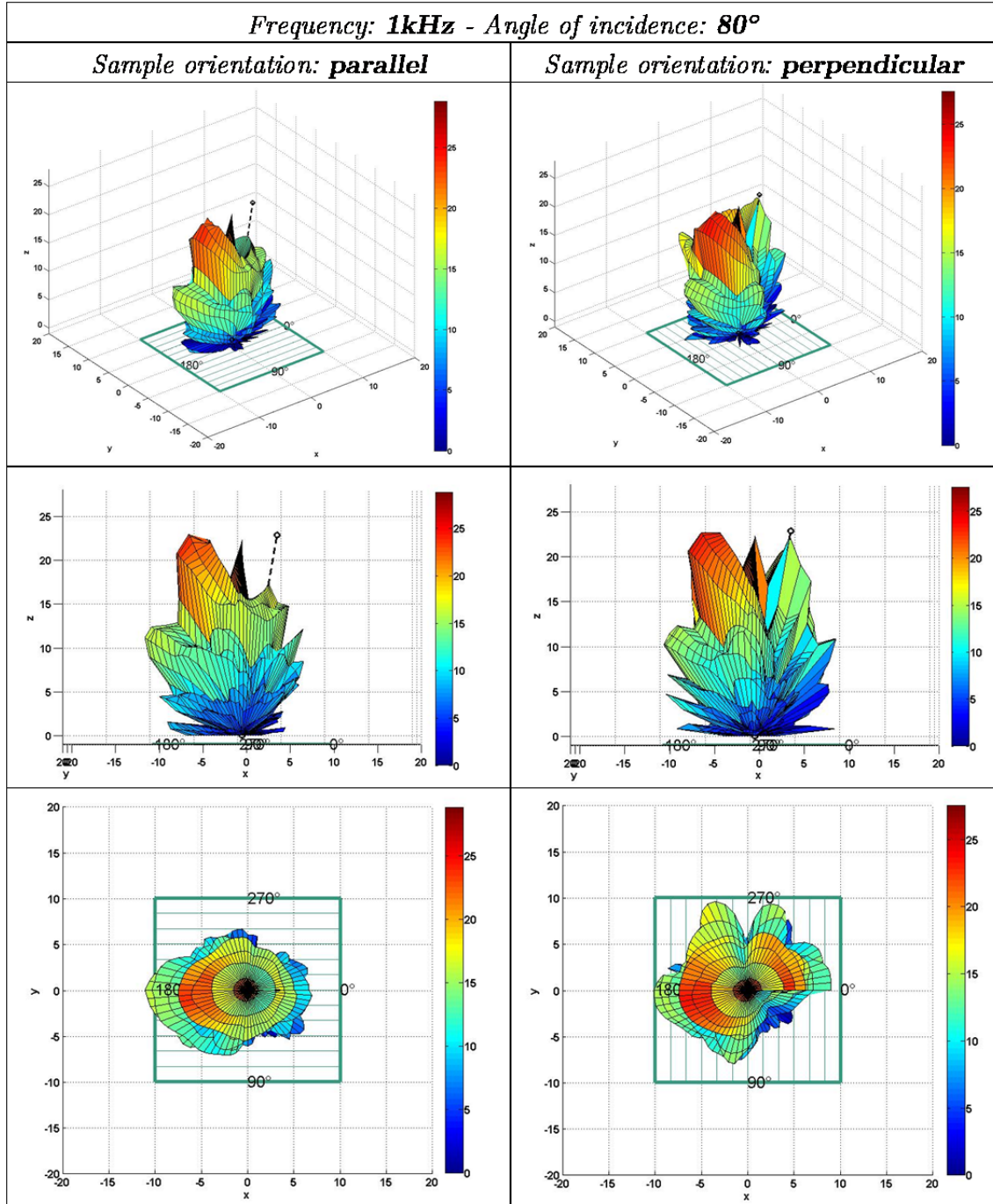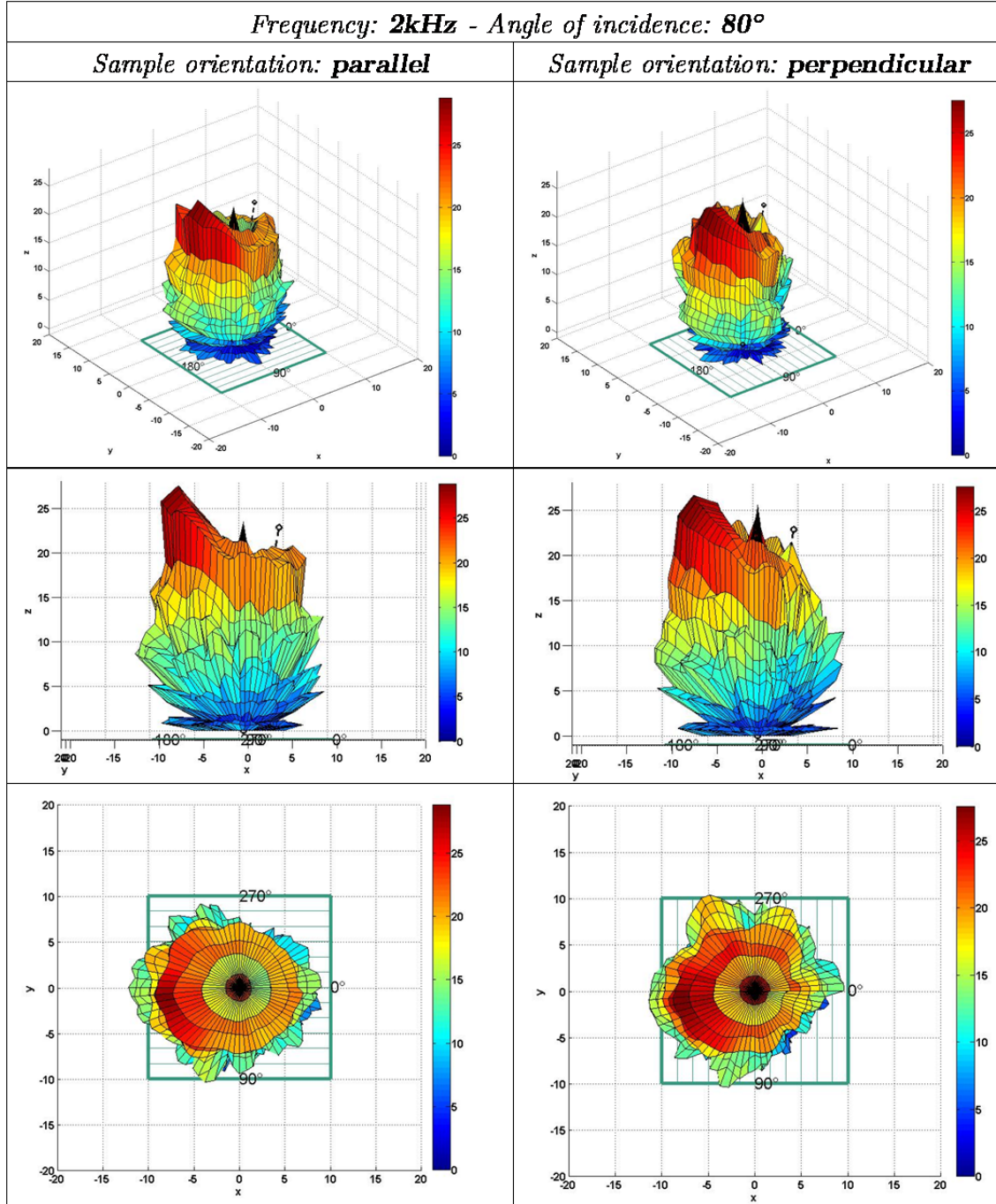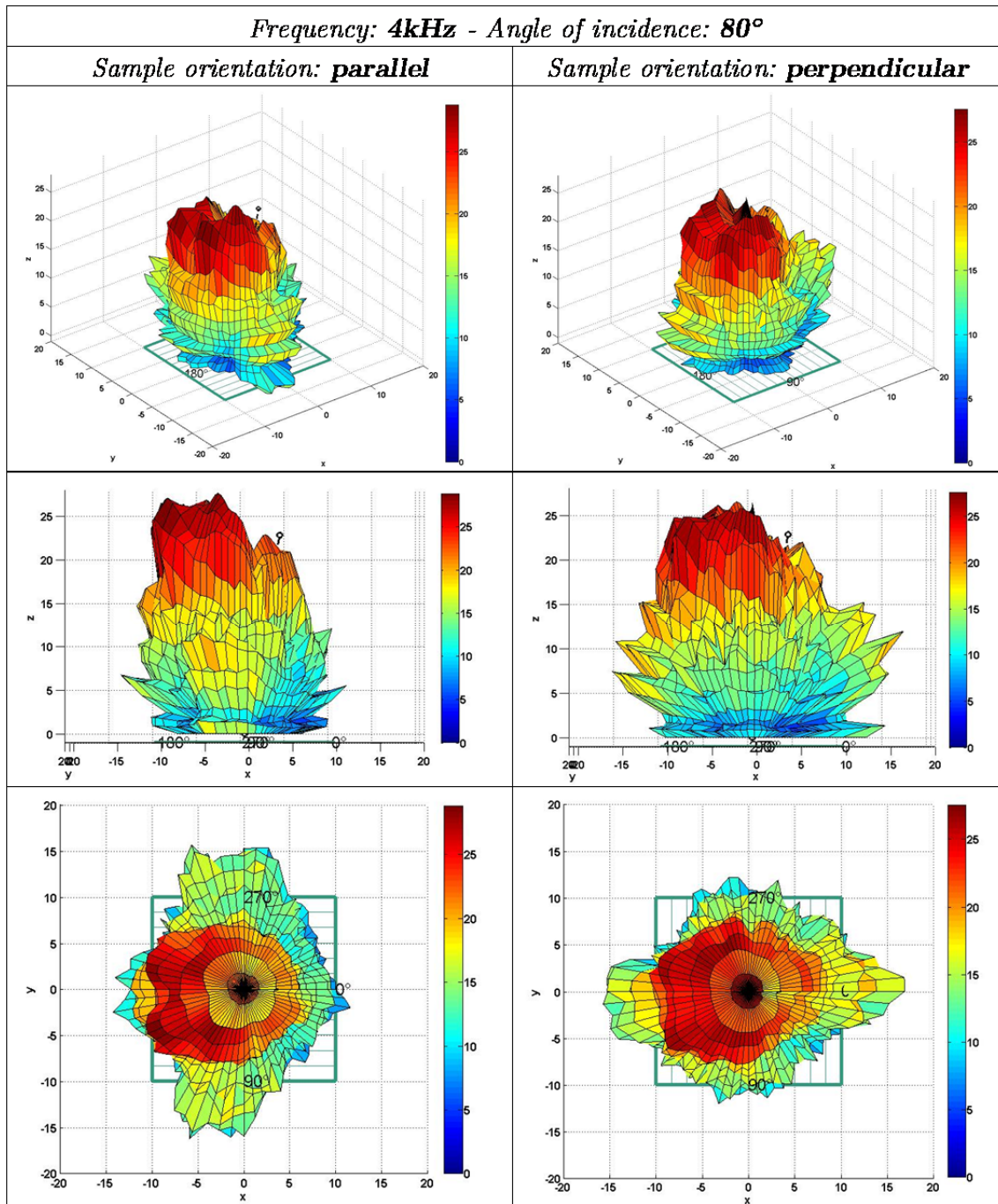| Sample orientation: **parallel** | Sample orientation: **perpendicular** |

Bibliography

ALERTZ, C., Asselineau, M., (2007), *Acoustics By Peutz - Theatres and concert halls*, Ed. Daidalos Peutz.

ARETZ, M., DIETRICH, P., VORLÄNDER, M., (2014), *Application of the mirror source Method for low frequency sound prediction in rectangular rooms, Acta Acustica united with Acustica*, Vol. 100, pp. 306-319.

BAINES, N.C., (1983), *An investigation of the factors which control non diffuse sound fields in rooms*, Ph.D. Thesis, Univeristy of Southampton.

BERANEK, L., (1996), *Concert and opera halls: how they sound*, Woodbury, Acoust. Soc. Am., New York.

BI, J., (2011), *Similarity tests using forced-choice methods in terms of Thurstonian discriminal distance, d'*, Journal of Sensory Studies, Vol.26, pp. 151-157.

BI, J., ENNIS, D.M., O'MAHONEY, M., (1997), *How to estimate and use the variance of d' from difference test*, Journal of sensory studies, Vol. 12, pp. 87-104.

BISTAFA, S. R., BRADLEY, J. S., (2001), *Predicting speech metrics in a simulated classroom with varied sound absorption*, J. Acoust. Soc. Amer. 109, pp. 1474-1482.

BLAUERT, J. (1996), *Spatial Hearing – The Psychophysics of Human Sound Localization*, revised edition. MIT Press.

BLESSER, B., SALTE, L.R. (2007), *Spaces Speak, Are You Listening? – Experiencing Aural Architecture*, MIT Press.

BORK,I., A, (2000), *Comparison of room simulation software – The 2nd round robin on room acoustical computer simulation*, Acustica united with Acta Acustica 86 (2000) 943-956.

BORISH, J., (1984), *Extension of the image model to arbitrary polyhedral*, J. Acoust. Soc. Am., Nr. 75, pp.1827-1836.

BRADLEY, D.T., MÜLLER-TRAPET, M., ADELGREN, J., VORLÄNDER, M. (2014), *Effect of boundary diffusers in a reverberation chamber: Standardized diffuse field quantifiers*, J. Acoust. Soc. Am., 135 (4).

BREE, H.E., LEUSSINK, P., KORTHORST, L., JANSEN, H., LAMMERINK, T.S.J., ELWENSPOEK, M., (1996), *The l-flown: A novel device for measuring acoustic flows*, Sens. Actuators, A 54(1–3), 552–557.

BYER, A.J., ABRAMS, D. (1953), *A comparison of the triangular and two-sample taste-test methods*, Food Technology, Vol. 9, pp. 23-26.

CARR, B.T. (1995), *Confidence intervals in the analysis of sensory discrimination tests - the integration of similarity and difference testing*, Proceeding of the 4th AgroStat, Djion

CHRISTENSEN, R.H.B. (2013), *Statistical methodology for sensory discrimination tests and its implementation in sesnR.*

CHRISTIANSEN, C.L., RINDEL, J.H., (2005), *Predicting acoustics in Class Rooms*, Internoise, Rio, 2005.

CHRISTIANSEN, C.L., (2009), *Odeon Room Acoustics Program - User Manual Version 10.1*, Denmark.

CHU W. T., (1995), *Time-variance effect on the application of the m-sequence correlation method for room acoustical measurements*, Proceedings 15th ICA, Vol.IV, p.25-28.

CIVILLE, G.V., SELTSAM, J. (2003), *Sensory evaluation methods applied to sound quality*, Noise Control Eng. Journal, 51 (4).

COX, T. J., DAVIES, B., LAM, Y.W. (1993), *The sensitivity of listeners to early sound field changes in auditoria*, Acustica, 79, 27-41.

COX, T.J., D'ANTONIO, P., (2004), *Acoustic Absorbers and Diffusers: Theory, Design and Application*, 2nd ed., Spon, New York.

DALENBÄCK, B.I.L., (1995), *A New Model for Room Acoustic Prediction and Auralization*, PhD thesis, Chalmers University if Technology, Gothenburg, Sweden.

DALENBÄCK, B.I.L., (1996), *Room acoustic prediction based on a unified treatment of diffuse and specular reflection*, J. Acoust. Soc. Am., 100:899.

DAMMERUD, J.J., BARRON, M. (2008), *Concert hall stage acoustics from the perspective of the performers and physical reality*, Auditorium Acoustics, Oslo.

DAVID, H.A. AND TRIVEDI, M.C. (1962), *Pair, triangle and duo-trio tests* (Technical Report 55), Virginia Polytechnic Institute, Department of Statistics, Blacksburg, VA.

DE AVELAR GOMES, M., VORLÄNDER, M., GERGES SAMIR, N.Y., (2002), *Aspects of the sample geometry in the measurement of the random-incidence scattering coefficient*, Forum Acusticum, Sevilla.

DE GEETERE, L., (2004) *Analysis and improvement of the experimental techniques to assess the acoustical reflection properties of boundary surfaces*, PhD Thesis, University of Leuven.

DIETRICH P., GUSKI M., KLEIN J., MÜLLER-TRAPET M., POLLOW M., SCHARRER R. AND VORLÄNDER M. (2013), *Measurements and Room Acoustic Analysis with the ITA-Toolbox for MATLAB*, AIA-DAGA 2013, Meran.

EMBRECHTS, J.J., DE GEETERE, L., VERMEIR, G., VORLÄNDER, M., SAKUMA, T., (2006) *Calculation of the random-incidence Scattering Coefficients of a Sine-Shaped Surface*, Acustica united with Acta Acustica 92, 593-603.

ENNIS, D.M. (1993), *The power of sensory discrimination methods*, Journal of sensory studies, Vol. 12, pp. 353-370.

FASTL., H., ZWICKER, E., (2007), *Psychoacoustics - Facts and Models*, Springer.

FELS, J. SCHRÖDER, D., VORLÄNDER, M., (2007), *Room acoustics simulations using head-related transfer functions of children and adults*, ISRA, Sevilla.

FRIJTERS, J.E.R., (1979), *The paradox of discriminatory nondiscriminators resolved*, Chim. Senses, Vol. 4, pp. 355-358.

GADE, A.C. (2007), *Acoustics in Halls for Speech and Music*, in Springer Hanbook of Acoustics, Springer.

GARAI, M. (2001), *Acustica geometrica e modelli di simulazione, in "Manuale di acustica,* edited by Spagnolo, ed. UTET, Ch.6.

GELFAND, S.A. (2010), *Hearing: An introduction to Psychological and Physiological Acoustics*, Informa Heltcare, 5th Ed.

GRIDGEMAN, N.T. (1956), *Group size in taste sorting trials*, Food Research, Vol. 21, pp. 534-539.

GREEN, D.M., SWETS, J.A. (1966), *Signal Detection-theory and Psychopysics*, John Wiley, New York.

HAAN, C.H., FRICKE, F. R., (1997), *An evaluation of the importance of surface diffusivity in concert halls*, Appl. Acoust. 51, 53-69.

HANYU, T., (2013), *Analysis method for estimating diffuseness of sound fields by using decay-cancelled impulse response*, ISRA, Toronto.

HEINZ., R., (1993), *Binaural room simulation based on an image source model with addition of statistical methods to include the diffuse sound scattering of walls and to predict the reverberant tail*, Applied Acoustics, 38:145.

HEINZ., R., (1994), *Entwicklung und Beurteilung von computergestützten Methoden zur binauralen Raumsimulation*, PhD thesis, RWTH Aachen University, Aachen, Germany.

ISO 354 (2003), Acoustics - *Measurement of sound absorption in a reverberation room*, International Organizations for Standard.

ISO 3382 (2009), Acoustics - *Measurement of room acoustic parameters - Part 1: Performance spaces*, International Organizations for Standard.

ISO 17497-1, (2004), *Acoustics – Measurement of the sound scattering properties of surfaces – Part 1: Measurement of the random-incidence scattering coefficient in a reverberation room*, International Organizations for Standard.

ISO 17497-2, (2012), *Acoustics – Measurement of the sound scattering properties of surfaces – Part 1: Measurement of the directional diffusion coefficient in a free field*, International Organizations for Standard.

ISO 4120 (2004), *Sensory analysis - Methodology - Triangle test, International Organizations for Standard*, International Organizations for Standard.

ISO 8586-2 (1994), *Sensory analysis - General guidance for the selection, training and monitoring of assessors - Part 2: Experts*, International Organizations for Standard.

ISO 18233 (2006), *Acoustics - Application of new measurement methods in building and room acoustics*, International Organizations for Standard.

JEON, J.Y., LEE, S.C., VORLÄNDER, M. (2004), *Development of scattering surfaces for concert halls*, Applied Acoustics 65, 341-355.

JEONG, D., CHOI, Y.J., (2013), *The subjective effect of random-incidence scattering coefficients*, ISRA 2013, Toronto.

JOYCE, W.B., (1978), *Effect of surface roughness on the reverberation time of a uniformly absorbing spherical enclosure*, J. Acoust. Soc. Am., Nr. 64., pp.1429-1436.

JORDAN, V.L. (1981) *A group of objective acoustical criteria for concert halls*, Applied Acoustics, Vol. 14.

KOSAKA, Y., SAKUMA, T., (2005), *Numerical examination on scattering coefficients of architectural surfaces using the boundary elements method*, Acoust., Sci. & Tech. 26, 2.

KREUTNER, U., (1995), *Messung des Diffusitätsgrades strukturierter Flächen im Hallraum*, Diplomarbeit at the Institute of Technical Acoustics, RWTH Aachen.

KROKSTAD, A., STROM, A., SØRSDAL, S., (1968), *Calculating the acoustical room response by the use of a ray tracing technique*, Journal of Sound and Vibration, Elsevier.

KULOWSKI, A., (1985), *Algorithmic representation of the Ray-Tracing Technique*, Applied Acoustics, Nr. 18, pp. 449-469.

KUTTRUFF H., (1995), *A simple iteration scheme for computation of decay constants in enclosures with diffusely reflecting boundaries*, J. Acoust. Soc. Am., Nr. 98, pp.288-293.

KUTTRUFF H., (2000), *Room acoustics*, 4th Ed., Taylor&Francis.

KUTTRUFF H., (1976), *Reverberation and Effective Absorption in Rooms with Diffuse Wall Reflexions, Acustica*, Vol. 35, Nr. 3.

LAM, Y.W., (1996), *A comparison of three diffuse reflection modelling methods used in room acoustics computer models*, J. Acoust. Soc. Amer. 100 (1996) 2181-2192.

LAWLESS, H.T., HEWMANN, H. (2010), *Sensory Evaluation of Food*, 2nd Ed., Springer, 2010.

LOKKI, T., (2013), *Throw away that standard and listen: your two ears work better*, ISRA, Canada.

LOKKI, T., SAVIOJA, L., (2008), *State-of-the-art in auralization of concert hall models – what is still missing?*, Joint Baltic-Nordic Acoustics Meeting, Rejkjavik.

MacRAE, A.W. (1995), *Confidence intervals for the triangle test can give assurance that products are similar*, Food Quality and Preference, 6.

MAKRINENKO, L.I., (1994), *Acoustics of auditoriums in public buildings*, edited by John Bradley, J. Acoust. Soc. Am..

MEILGAARD, M.C., CIVILLE, G.V., CARR, B.T. (2007), *Sensory Evaluation Techniques*, 4th edition, CRC Press.

MOMMERTZ E., VORLÄNDER M., (1995), *Measurement of scattering coefficients of surfaces in the reverberation chamber and in the free field*, Proceedings 15th International Conference on Acoustics, Vol.II, p.577-580.

MÜLLER-TRAPET, M., VITALE, R., VORLÄNDER, M. (2010), *A revised scale model reverberation chamber for measurements of scattering coefficients*, J. Acoust. Soc. Am., 128(4):2465.

NAYOLR, G.M. (1996), *ODEON - another hybrid room acoustical model*, Appl. Acoutics, 38, 131.

NISHI, T. (1992), *Relation between objective criteria and subjective factors in a sound field, determined by multivariate analyses*, ACUSTICA, Vol. 76.

NOISTERNIG, M., CARPENTIER, T., WARUSFEL, O., (2012), *ESPRO 2.0 – Implementation of a surrounding 350-loudspeaker array for 3D sound field reproduction*, 25th AES UK Conference, York.

O'MAHONEY, M. (1992), *Understanding discrimination tests: a user-friendly treatment of response bias, rating and ranking R-Index tests and their relationship to signal detection*, Journal of sensory Studies, Vol. 7, pp. 1-47.

O'MAHONEY, M., ROUSSEAU, B., (2002), *Discrimination testing: a few ideas, old and new*, Food Quality and Preference, Vol. 14, pp. 157-164.

O'MAHONEY, M. (1995), *Who told you the triangle test was simple?*, Food quality and preference, Vol. 6, pp. 227-238.

OPPENHEIM, A.V., WILLSKY, A.S., YOUNG, I.T. (1983), *Signals and systems*, Prentice-Hall International.

ORAN BRIGHAM, E. (1988), *The fast Fourier transform and its applications.* 1988. Prentice-Hall International.

MÜLLER-TRAPET, M., DIETRICH, P., ARETZ, M., GEMMEREN, J. VORLÄNDER, M. (2013), *On the in situ impedance measurement with pu-probes—Simulation of the measurement setup*, J. Acoust. Soc. Am. 134, 1082.

PELZER, S., MAEMPEL, H.J., L., VORLÄNDER, (2010), *Room Modelling for Acoustic Simulation and Auralization Tasks: Resolution of Structural Details*, DAGA Berlin.

PELZER, S., ASPÖCK, L., VORLÄNDER, M., SCHRÖDER, D., (2013), Interactive real-time simulation and auralization for modifiable rooms, ISRA 2013 Toronto.

PERYAM, D.R. & SWARTZ (1950), *Measurement of sensory differences*, Food Technology, 4, pp. 390-395.

PEUTZ, V.M.A. (1978), *The Variable Acoustics of the Espace De Projection of IRCAM (Paris)* - 59th AES Convention, Hamburg.

PEUTZ, V.M.A. (1981), *Nouvelle examen des theories de reverberation*, Revue d'Acoustique 57, 99-109.

PEUTZ, V.M.A. and Bernfeld, B. (1980), *Variable acoustics of the IRCAM concert hall in Paris*, Proc. 10th ICA (Sidney), Abstract El.3.

SAKUMA, T., KOSAKA, Y., DE GEETERE, L., VORLÄNDER, M., (2009) *Relationship between the scattering coefficients determined with coherent averaging and with directivity correlation*, Acta Acustica united with Acustica 95, pp. 669-677.

SCHLICH, P., (1993), *Risk tables for discrimination tests*, Food quality and Preference, Vol. 4, pp. 141-151.

SCHRÖDER, D., (2011), *Physically based real-time auralization of interactive virtual environments*, PhD Thesis, RWTH Aachen University.

SCHRÖDER, D., VORLÄNDER, M., (2007), *Hybrid method for room acoustic simulation in real-time*, ICA, Madrid.

SCHRÖDER, D., DROSS, P., VORLÄNDER, M., (2007), *A Fast Reverberation Estimator for Virtual Environments*, AES 30TH International Conference, Saariselkä.

SCHROEDER, M., (1954), Die statistischen Parameter der Frequenkurven von grOßen Räume, Acustica, 4, 5943.

SCHROEDER, M., (1970), *Digital Simulation of Sound Transmission in reverberant spaces*, J. Acoust. Soc. Am., Nr. 47, pp.424-431.

SCHROEDER, M., ATAL, B.S., BIRD, C. (1972), *Digital computers in room acoustics*, Proc. 4th ICA, Copenhagen, M21.

SHTREPI, L., PELZER, S., VITALE, R., ASTOLFI, A., RYCHTARIKOVA, M., VORLÄNDER, M., (2013), *Subjective assessment of scattered sound in a virtual acoustical environment simulated with three different algorithms*, ISRA, Toronto.

SHTREPI, L., PELZER, S., VITALE, R., ASTOLFI, A., RYCHTARIKOVA, M. (2014), *Objective and perceptual assessment of the scattered sound field in a simulated concert hall*, J. Acoust. Soc. Am. (submitted).

SUH, J.S., NELSON, P.A. (1999), *Measurement of transient response of rooms and comparison with geometrical acoustic models*, J. Acoust. Soc. Am., 105:2304.

STEPHENSON, U.M., SVENSSON, U.P. (2007), *An improved energetic approach to diffraction based on the uncertainty principle*, in Proc. of the 19th ICA, Madrid, Spain.

SVENSSON, U.P., FRED, R.I., VANDERKOOY, J. (1999), *An analytic secondary source model of edge diffraction impulse responses,* J. Acoust. Soc. Am. 106, 2331.

THURSTONE, L.L. (1927), *A law of comparative judgement*, Psychol. Rev. 34.

TORRES, R., KLEINER, M., DALENBÄCK, B. I., (2000), *Audibility of diffusion in Room acoustics Auralization: an initial investigation*, Acta Acustica 86, 919-927.

URBAN, F.M. (1910), *The Method of Constant Stimuli and its Generalization, The Psychological Review*, Vol 17(4), 229-259.

VITALE, R., VORLÄNDER, M., (2010), *Investigation of the just noticeable difference of scattering coefficient in auralized concert halls*, J. Acoust. Soc. Am. 127, 1751.

VITALE, R., VORLÄNDER, M., ALCÁZAR, J. A. G., (2011), *Perception of scattering coefficient in auralized concert halls*, J. Acoust. Soc. Am. 129, 2502.

VORLÄNDER, M., (1989), *Simulation of the transient and steady-state sound propagation in rooms using a new combined ray-tracing/image-source algorithm,* Journal of the Acoustical Society of America, 86:172.

VORLÄNDER, M., BIETZ, H., (1994), *Comparison of methods for measuring reverberation time, ACUSTICA Vol. 80. Pags.205-215.*

VORLÄNDER, M., (1995), *International Round Robin on Room Acoustical Computer Simulations*, Proc. 15th International Congress on Acoustics, Trondheim, p. 689-692.

VORLÄNDER, M., (2008), *Auralization*, Ed. Springer, Berlin.

VORLÄNDER, M., EMBRECHTS, J.J., DE GEETERE, L., VERMEIR, G., GOMES, M., (2004) *Case studies in measurement of random incidence scattering coefficients*, Acta Acustica united with Acustica 90, pp. 858-867.

VORLÄNDER, M., MOMMERTZ, E., (2000), *Definition and measurement of random-incidence scattering coefficients*, Applied Acoustics 60, 187-199.

WICHMANN, F. A., HILL, N. J. (2001a), *The psychometric function: I. Fitting, sampling and goodness-of-fit*, Perception and Psychophysics 63(8), 1293-1313.

WICHMANN, F. A., HILL, N. J. (2001b), *The psychometric function: II. Bootstrap-based confidence intervals and sampling*, Perception and Psychophysics 63(8), 1314-1329.

XIANYANG, Z., (2006) Christiansen, C.L., Rindel, J.H., *Practical methods to define scattering coefficients in a room acoustics computer model*, Applied Acoustics 67, pp. 771-786.

Acknowledgments

Curriculum Vitae

PERSONAL DATA

	Renzo Vitale
22.04.1979	Born in Sora, Italy

EDUCATION

2008 – 2014	PhD Studies at the Institute of Technical Acoustics
	RWTH Aachen University, Germany
2004 – 2007	Master of Science in Electronic Engineering
	University of L'Aquila, Italy
2006	Erasmus Program
	KTH - Royal Institute of Technology, Stockholm, Sweden
2000 – 2004	Bachelor of Science in Electronic Engineering
	University of L'Aquila, Italy
2001	Master Course for Organist and Kapellmeister
	Conservatoire "A. Casella", L'Aquila, Italy
1994 – 2000	Diploma in Piano (eq. Master of Art in Piano Performance)
	Conservatoire "Santa Cecilia", Rome, Italy

POSITIONS AND APPOINTMENTS

2010 – 2012	Research Scholar at the School of Architecture
	Pratt Institute, New York City, USA
2008 – 2010	Research Assistant at the Institute of Technical Acoustics
	RWTH Aachen University, Germany
2008	Research Scholar at the Dept. of Speech, Music and Hearing
	KTH - Royal Institute of Technology, Stockholm, Sweden
2007	Visiting Scholar at the Institute of Technical Acoustics
	RWTH Aachen University, Germany
2006	Scientific Employee in the contest of aircraft surveillance
	Dept. of Electrical and Information Engineering, L'Aquila, Italy
2005	Web Developer and Graphic Designer
	Center of Excellence in embedded systems, L'Aquila, Italy
2003	Internship
	Pisani - Acoustic Engineering Studio, Torino, Italy
2002	Multimedia Lab Supervisor
	Faculty of Engineering - University of L'Aquila, Italy

Aachen, Germany, June 23, 2014.